1-1-2012

Bond Degradation and Residual Flexural Capacity of Corroded RC Beams

Hao Wu
Ryerson University

BOND DEGRADATION AND RESIDUAL FLEXURAL CAPACITY OF CORRODED RC BEAMS

by

Hao Wu

Bachelor of Engineering in Civil Engineering

Zhengzhou University, Zhengzhou, China, 2008

A thesis presented to Ryerson University

in partial fulfillment of the requirements

for the degree of Master of Applied Science

in the program of Civil Engineering

Toronto, Ontario, Canada, 2012

Author's Declaration

I hereby declare that I am the sole author of this thesis. This is a true copy of the thesis, including any required final revisions, as accepted by my examiners.

I authorize Ryerson University to lend this thesis to other institutions or individuals for the purpose of scholarly research.

Hao Wu

I further authorize Ryerson University to reproduce this thesis by photocopying or by other means, in total or in part, at the request of other institutions or individuals for the purpose of scholarly research.

Hao Wu

I understand that my thesis may be made electronically available to the public.

Bond Degradation and Residual Flexural Capacity of Corroded RC Beams

Hao Wu

MASc., Department of Civil Engineering, Ryerson University, 2012

Abstract

An analytical model is developed to predict the residual flexural capacity of corroded RC members. This was established by first developing an analytical model to calculate the residual bond strength at steel-concrete interface. The bond model is then implemented within the framework of the moment resistance method, and a new strain compatibility analysis was developed: to account the analysis of a corroded reinforced concrete beam, to incorporate dependence of the bond response on the stress strain and damage state of the concrete and steel. Method for calculating flexural capacity of corroded RC beams is then proposed, which is based on flexural analysis of RC beams that considers the effect of bond degradation. The predicted results of these models correlated very well with results observed in various experimental studies. This indicates that those developed analytical models tend to estimate conservatively the residual bond strength and flexural capacity of corroded RC beams.

.

Acknowledgment

First of all, I'd like to thank my supervisor Dr. Lamya Amleh who gave me worthy guidance and suggestions in choosing topic, composing, modifying and finalizing this thesis. Her encouragement is very helpful to me in completing this research.

I would also like to thank my family for supporting my graduate study.

Colleges and friends, Luaay, Muhammad, Jastej Gill, and Chan helped and encouraged me a lot in my study in Canada. I appreciate what all those people have done for me.

Table of Contents

List of Figures

List of Tables

List of Symbols

α = coefficient experimentally determined regarding stirrups geometry

α_1 = the ratio of stress of compression stress block to the compressive strength of concrete

α_i = load factor of ith specified variable load

β_1 = the ratio of depth of stress block and the actual depth of compression zone

μ = friction coefficient between steel and concrete

$\tau_{AD}(x)$ = bond strength contribution due to adhesion between corroded steel and cracked concrete

Φ_a = maximum size of aggregate

Φ_p = diameter of principle bar

Φ_{st} = diameter of stirrups

Δz = stirrups spacing

σ_r = radial stress at location r

$\sigma_\theta(r)$ = hoop stress at location r

σ_{rc} = residual tensile strength of cracked concrete

σ_{st} = stress in stirrups

$\varepsilon_r(r)$ = radial strain of concrete at location r

$\varepsilon_\theta(\mathrm{r})$ = hoop strain of concrete at location r

ε_{θ,R_i} = hoop strain at surface of the steel

ε_c = the strain of compressive extreme fiber

ε_{cx} = strain of compressive extreme fiber at corrosion depth x

ε_s^{ub} = the strain of the tensile steel over the unbonded RC beam

ε_s = the strain of tension reinforcing bars

ε_{sx} = the strain of tension reinforcing bars at corrosion depth x

κ = coefficient experimentally determined

ν = Poison' ratio

ν_1 = Poison's ratio in the radial directions

ν_2 = Poison's ratio in the tangential directions

τ_{avg} = average bond stress

$\tau_{bu,avg}$ = the average bond strength

τ_{bu} = ultimate bond strength of corroded reinforcing steel and concrete

a = depth of the equivalent rectangular compressive zone

a_0 = coefficient related to the ideal trilateral local bond-slip law of the stirrups

a_1 = coefficient related to the ideal trilateral local bond-slip law of the stirrups

a_2 = coefficient related to the ideal trilateral local bond-slip law of the stirrups

A = constant solving plain stress problem

A_p^* = area of principle bar in the splitting plane

A_{st}^* = global cross-section area

b = the width of the beam member

c = depth of compression zone

c_x = depth of compression zone at corrosion depth x

C = constant solving plain stress problem

c_x = depth of compression zone at corrosion depth x

d = effective depth of beam section

d_{bx} = diameter of rebar at corrosion depth x

d_b = diameter of rebar

E_0 = initial modulus of elasticity of concrete

E_θ = hoop stiffness of concrete

E_s = modulus of elasticity of steel

f_{ct0} = tensile strength when concrete begin to crack

$f_c^{'}$ = compressive strength of concrete

f_y = yielding strength of reinforcing bar

f_t = tensile strength of concrete

$g(x)$ = interpolating function of x

k = coefficient as a function of the rib properties and friction angle between steel and concrete

l = total length of tensile rebar

l_{eq} = the equivalent plastic length

M_f = the moment due to the factored loads

M_r = the factored moment resistance of the cross-section

M_{rx} = moment resistance at corrosion depth x

M_{r1} = the moment resistance provided by the imaginary beam

M_{r2} = the moment resistance provided by the coupling reinforcement

n = number of tensile rebar

n_p = number of longitudinal reinforcing steel (principle bar)

p_{corr} = corrosion pressure

p_c = the radial pressure on the crack front

$p_{c,c}(x)$ = the confinement by concrete

$p_{c,st}$ = the confinement by stirrups

p^{max} = maximum confining pressure at bond failure, including confinement of concrete and stirrups

r = location of analysis from the center of rebar

R = nominal resistance of a structural element

R_0 = the radius of concrete cover front

R_c = cracking front

R_i = the initial radius of reinforcing steel

S_i = ith specified variable load

t = rust layer thickness

T = tensile force of steel

u_r = radial displacement at location r

u_{R_i} = radial displacement at rebar surface

$v_{r/s}$ = the ratio between specific volumes of rust and steel

w = crack opening

x = corrosion depth (mm)

x_{cr} = corrosion depth associated with through concrete cracking

Chatper 1

INTRODUCTION

1.1 Background and Research Significance

Corrosion of reinforced concrete was first recognized early in the twentieth century, but it has become worse in recent years with the widespread use of de-icing salts on highways and bridge decks. The corrosion of steel reinforcement in concrete greatly reduces the loading carrying capacity, shortens the service life and increases the maintenance cost of the structure. According to a report (Highway, 1997), about 101,518 bridges of the 581,862 bridges in USA were rated as structurally deficient, and corrosion of the reinforcing steel is a significant contributor to the structural deficiencies. The average annual cost, through year 2011, for just maintaining the overall bridge conditions in US is estimated to be $5.2 billions (Transportation, 2010). Therefore, designing against corrosion of reinforcement in concrete should be of a great concern for materials and bridge engineers, reinforced concrete corrosion specialists and those concerned with the performance of reinforced and pre-stressed concrete bridges, when designing new Reinforced Concrete (RC) structures and when evaluating the residual strength of old RC structures.

It should be emphasized that the reinforcing steel is provided in reinforced concrete to resist the tensile forces, and to produce controlled cracking within that zone. However, corrosion not only deteriorates the steel bar and its function of transferring the tensile

stresses, but it deteriorates the concrete by spalling of the cover. Therefore, corrosion of the reinforcement has a strong influence on the bond behaviour at the interface between the steel reinforcement and concrete. As corrosion of the reinforcing steel progresses, the bond strength between the reinforcing steel and concrete diminishes progressively, and major repairs or replacement is needed. Reinforcement corrosion reduces the bond strength between steel and concrete, deteriorating the load carrying capacity of RC members. Therefore, it is very important to understand the mechanism of bond deterioration and to estimate the bond strength and the residual load carrying capacity of corroded RC beams.

Traditional strength-based design for new concrete structure has failed to provide reliable long-term performance of structures exposed to aggressive environments. Most national building codes aimed at ensuring that the structure being designed, constructed and operated would perform satisfactorily at the ultimate and the serviceability limit states. Therefore, a capacity reduction factor is used in the calculation of the resistance of the concrete structure for consideration of the variation of the material properties, member geometry and details, deficiencies in construction practice and quality control, and the normal variation in the applied loads. However, these considerations do not include the time-dependent behavior of loads and resistances of the concrete structures. For example, the load may change (the highway loading has increased significantly over the past several years), also, the resistance of a concrete structure will decrease due to aging of the material and the deterioration because of various environmental influences (such as corrosion of RC). Therefore, the

long-term performance of the concrete structure over the design service life is not adequately reliable to guarantee the safety of the concrete structure. Considerable experimental and numerical research was undertaken to study the basics of force transfer at the steel rebar-concrete interface, the associated bond stress-slip, and other force–displacement relationships.

While most of the researches regarding bond strength and flexural capacity of corroded RC beams are experimental studies, there are several models for bond strength and very few models for flexural capacity of corroded RC beam. Moreover, all these models are not strictly derived theoretically and have their own limitations and drawbacks. The drawback is that the results are highly dependent on the specific structures considered. Therefore it's very important to propose analytical models for bond strength and flexural strength calculation.

1.2 Previous Research at Ryerson University

The followings are summaries of the previous researches that have been done at Ryerson University, including experimental and theoretical studies.

Hussein (2011) developed an analytical model to describe the deterioration of bond strength at the steel-concrete interface in a reinforced concrete, due to the corrosion of reinforcement. The concrete was assumed to be a thick-walled cylinder subjected to the inner corrosion pressure due to the expansion of steel corrosion products. A friction model was used to combine the action of confining pressure, which consists of radial

pressure produced by reinforcing bar ribs on surrounding concrete and corrosion pressure due to expansion of steel corrosion products. The results from the developed model showed good agreement with several researchers' experimental results.

Al-Bayati (2009) conducted experiments to study the effect of corrosion on shear behavior in both Normal Concrete (NC) and Self-consolidating Concrete (SCC) beams. The use of NC and SCC showed minor influences on failure mode, while the different states of corrosion showed a greater influence on failure mode and the structural capacity of beams made from both NC and SCC.

Joyce (2008) carried out experiments to study the effect of corrosion on the flexural behavior of reinforced concrete (RC) beams. It was observed that the flexural capacity of reinforced concrete beams decreased as the rate of corrosion increased. The study indicated a sharp drop in stiffness at relatively low degrees of corrosion, followed by a slower decline at increasing corrosion levels.

Bhaskar (2008) developed an analytical model of bond which describes the contact pressure between the reinforcing bar and concrete in a RC member. The analytical model was implemented in a finite element analysis, using ABAQUS, of pull-out specimens conducted by Amleh (2000). The results from finite element analysis agreed reasonably with the experimental results.

Smith (2007) conducted experimental investigation into the effects of corrosion on the structural behavior of RC beams. The experimental results of beam tests indicated that the failure mode shifted from predictable ductile flexural failures at mid-span, to more

brittle failures at supports. The load carrying capacity decreased with increasing levels of corrosion. Pull-out tests were also conducted by Smith (2007), and the experimental results showed a gradual bond strength loss with increasing corrosion levels.

Aldulaymi (2007) conducted experimental studies to investigate the influence of increasing levels of corrosion on the progressive deterioration of bond between the steel and concrete. The experimental results indicated that the bond stress-slip response of the embedded bar in the pullout specimen was adversely affected by the width of the crack, and the level of corrosion. The maximum bond strength was affected significantly by the number and size of cracks, and thus, the level of corrosion.

Ghosh and Amleh (2006) modeled the mechanical interaction between the corroding reinforcing steel and the concrete with the nonlinear finite element program ABAQUS. The loss of contact pressure and the decrease in the friction coefficient was modeled first and the relationship between the loss of bond strength and the mass loss of the reinforcing bar was established finally. The model gave accurate predictions of bond strength for three experimental studies.

Hassan (2003) studied the effect of corrosion on bond strength using pullout tests on specimens with four different types of concrete and three different types of steel embedded. The results showed that the bond strength for corroded and un-corroded stainless steel bars was lower than that of the regular carbon steel bars. Low levels of corrosion (about 0.5 to 1% of mass loss) were observed to improve the bond strength

slightly. While, bond strength decreases rapidly with an increase in the corrosion level for all types of specimens.

Lan (2003) investigated the behavior of three different types of specimens analytically, based on fracture mechanics. The finite element program ATENA was used to analyze cracking propagation and bond failure process, with nonlinear material models for concrete. The effect of corrosion on bond-slip relationship in RC structures was also investigated.

1.3 Scope and Objectives of the Present Investigation

The main objective of the current investigation focuses on developing a moment resistance model for the concrete flexural elements under a given aggressive environment (corrosion level). The concrete beams are considered to be corroded to different levels of corrosion. Bond deterioration due to corrosion of the reinforcing steel is the most important parameter in the loss of flexural capacity. Therefore, an analytical model is first developed to calculate the residual bond strength between steel and concrete under corrosion. The model is then implemented within the framework of the moment resistance method. Method for calculating flexural capacity of corroded RC beams is then proposed, which is based on the flexural analysis of normal RC beams that considers the effect of bond degradation as well. A new strain compatibility condition is considered in order to decide the failure modes.

1.4 Thesis Layout

The thesis is composed of six chapters. Chapter 1 addresses the research significance, summarize the researches that have been done in Ryerson University, and presents the scope and objective of this thesis. Chapter 2 presents the fundamentals of corrosion and its influence on structural capacity. Chapter 3 presents the background of the thesis, including the flexural theory, bond basics and the literature reviews of the previous research on bond and flexural behaviors of RC beams. In Chapter 4, an analytical model to calculate bond strength between corroded steel and concrete is proposed and validated by experimental results from other researchers. Chapter 5 presents an analytical procedure to calculate the residual flexural strength of corroded RC beams, which is also validated by experimental studies from other researchers. Conclusions and recommendations are made in Chapter 6. A numerical example is made in Appendix A to demonstrate the calculation method of the residual bond strength and flexural capacity of RC beams after suffering reinforcement corrosion.

Chapter 2

CORROSION OF REINFORCEMENT

2.1 Introduction

As was mentioned earlier, the degree to which performance of reinforced concrete is damaged as a result of reinforcement corrosion is a matter of great concern to those responsible for assessing and maintaining the corroded RC structures. While considerable research effort has been dedicated to the mechanisms and causes of reinforcement corrosion and to researching the durability of repair materials, considerably lower attention has been dedicated to the problem of assessing the residual strength of the corroded structure. A detailed guidance on assessment of residual strength of corrosion-damaged RC structures will be of a great importance to number of practicing and practitioners. Therefore, comprehensive knowledge (that understands and quantifies the effect of reinforcement corrosion on structural behaviour) on the effect of corrosion on structural capacity and integrity is essential for the development of effective tools for the prediction of residual service life and for the development of cost effective repair strategies. This chapter will discuss the available information on the factors that cause and control corrosion of steel in concrete, as several metals will corrode under certain conditions when embedded in concrete. Factors influencing the electrochemical process are also discussed.

2.2 Mechanism of Corrosion

Corrosion is the process of the transformation of a metal to its "native" form, which is the natural ore state, often as oxides, chlorides or sulphates. This transformation occurs because the compounds such as the oxides "involve" less energy than pure metals, and hence they are more stable thermodynamically. The corrosion process does not take place directly but rather as a series of electrochemical reactions with the passage of an electric current. Corrosion also depends on the type and nature of the metal, the immediate environment, temperature and other related factors. The corrosion may be defined as the destructive attack of a metal by chemical or electrochemical reaction with its environment.

Steel in concrete is normally immune from corrosion because of the high alkalinity of the concrete; the pH of the pore water can be greater than 12.5, which protects the embedded steel against corrosion. This alkalinity of concrete causes passivation of the embedded reinforcing bars. A microscopic oxide layer, which is the “passive” film, forms on the steel surface due to the high pH, which prevents the dissolution of iron. Furthermore, the concretes made using low water-cement ratios and good curing practices have a low permeability, which minimizes the penetration of the corrosion inducing ingredients. In addition, low permeability is believed to increase the electrical resistivity of the concrete to some degree which helps in reducing the rate of corrosion by retarding the flow of electrical currents within the concrete that accompany the electrochemical corrosion. Consequently, corrosion of the embedded steel requires the breakdown of its passivity. However, as the global warming becomes worse along with the increase of CO_2 content in air, carbonation may break down the passive layer. Those structures in the tidal zone,

or roads and bridge decks suffering from de-icing salt can also have the passive layer broken down due to the chloride attack. Without the passive layer, the steel is subjected to water and air and so corrosion happens. There are two steps of the corrosion process. The first step of the steel corrosion is shown in Fig. 2-1, and the chemical reactions were given by Mietz, Polder and Elsener (2000) as:

The anodic reaction: $$Fe \rightarrow Fe^{2+} + 2e^{-} \quad (2\text{-}1)$$

The cathodic reaction: $$2e^{-} + H_2O + \frac{1}{2}O_2 \rightarrow 2OH^{-} \quad (2\text{-}2)$$

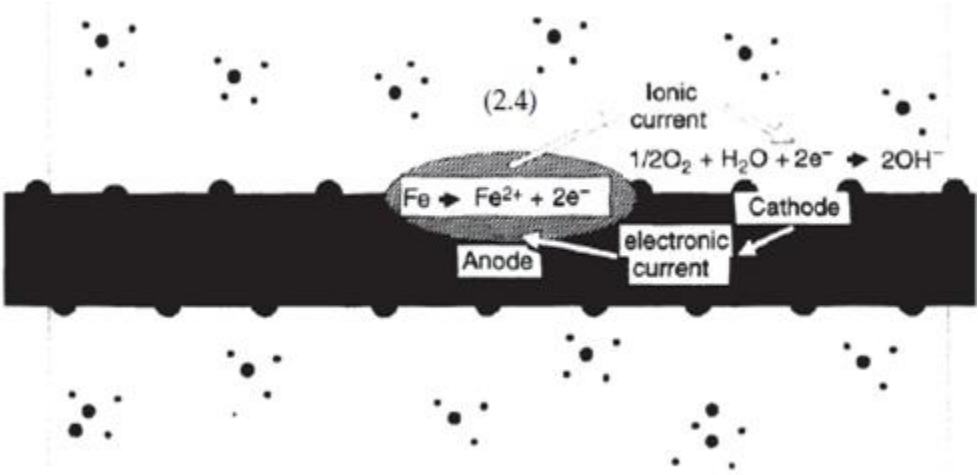

Fig. 2-1: The anodic and cathodic reactions (Mietz, Polder and Elsener, 2000)

The second step of steel corrosion is shown in Fig. 2-2. The chemical reactions were given by Mietz et al. (2000) as:

$$Fe^{2+} + 2OH^{-} \rightarrow Fe(OH)_2 \quad (2\text{-}3)$$

$$4Fe(OH)_2 + O_2 + 2H_2O \rightarrow 4Fe(OH)_3 \quad (2\text{-}4)$$

$$Fe(OH)_3 \rightarrow Fe_2O_3 \cdot H_2O + 2H_2O \quad (2\text{-}5)$$

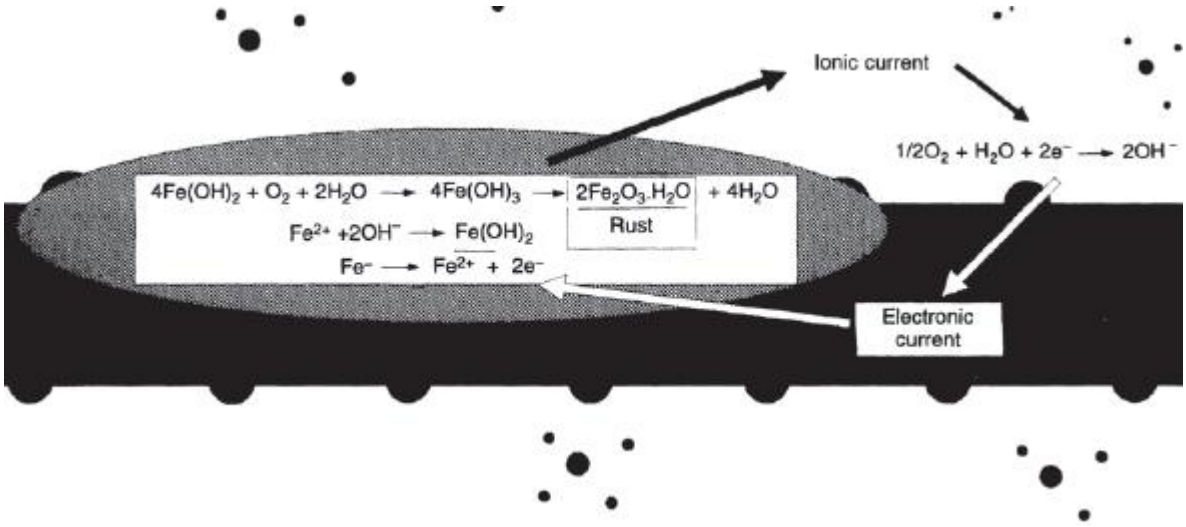

Fig. 2-2: The corrosion reactions on steel (Mietz et al., 2000)

The un-hydrated ferric oxide Fe_2O_3 has a volume of about twice as that of the steel it replaces and will have higher volume up to 10 times when it becomes hydrates (Mietz et al., 2000). In concrete structures, the volume of corrosion products is normally twice of uncorroded steel. The volume expansions of the corrosion products cause the cracking and spalling of concrete, decreasing the load carrying capacity of RC structures.

2.3 Effect of Corrosion on Structural Capacity

There are two classifications of the corrosion of reinforcement namely: general or local corrosion. General corrosion may occur due to either chloride contamination or due to carbonation of the RC structure. The consequences of the steel corrosion are

manifested as a decrease in the bar diameter, deterioration of the mechanical properties of the reinforcing steel (e.g., the change from the normal ductile response of low carbon steel bars to a relatively brittle response in bars damaged by pitting corrosion), cracking and spalling of the concrete by the expansive iron oxides and hydroxides, and a noticeable decrease in the bond at the steel-concrete interface. The oxides and hydroxides occupy a greater volume than the parent metal, and the expansion of the diameter of the bar as it corrodes generally leads to cracking and eventually spalling of concrete cover before an appreciable proportion of the cross sectional area is lost.

Local or pitting corrosion is regularly associated with chloride contamination and not with carbonation. The corrosion products due to local or pitting corrosion do not exhibit the same degree of volumetric expansion as that of the general corrosion. Consequently, the tendency of a corroding bar to split the concrete cover is less with local or pitting corrosion, and extreme loss of bar section may occur without signs of deterioration on the surface of the member.

In general, the residual strength of concrete structures may be affected by local (due to pitting) or general loss of reinforcement cross sectional area, through changes in the concrete cross section as a result of cracking or spalling, or through loss of bond between steel and concrete. It should be noted that the two types of corrosion, pitting and general corrosion, might occur together, and that the presence of general corrosion should not be taken to indicate an absence of local corrosion. It should also be noted that the loss of strength and ductility of reinforcement are of greatest

concern when assessing structures affected by local corrosion, and are not considered in this investigation.

2.3.1 Effect of Corrosion on Steel

In the case of general corrosion, bond is more likely to affect structural capacity than is loss of tensile strength of reinforcement. Experiment results indicated that the level of reinforcement corrosion does not influence the tensile strength of steel bars (calculated on the actual area of cross-section), but reinforcing steel bars with more than 12% corrosion indicates a brittle failure (Almusallam A. A., 2001). It's concluded that the strength ratio and elastic modulus of reinforcement are not significantly affected by corrosion and consequently the strength and modulus of elasticity of non-corroded bars can be adopted in practice (Du et al. 2005).

2.3.2 Effect of Corrosion on Concrete

The corrosion products have higher volume than the original steel. With the increase of corrosion level, the volume expansion of excessive rust products on the surface of steel induces radial compression pressure and hoop tensile pressure on the surrounding concrete after corrosion products fill the pores in concrete. When the hoop tensile stress exceeds the tensile strength of concrete, the concrete will crack. Hence, properties of cracked concrete should be considered to demonstrate the behaviour the RC member after concrete cracks.

2.3.3 Effect of Corrosion on Bond between Steel and Concrete

The transfer of the load between the steel and the concrete is affected by the phenomenon of bond at the steel-concrete interface, which ensures secure gripping of the reinforcement, and the working of the reinforcing steel in conjunction with the concrete, to form a reliable structural element, capable of withstanding both tension and compression forces (Amleh and Mirza, 2004). By simplifying the real behaviour, bond stress may be considered as a shear stress over the surface of a reinforcing bar. Bond strength initially comes from weak chemical bonds between steel and hardened cement, but this resistance is broken at a very low stress. Once slip occurs, friction contributes to bond. In plain reinforcing steel bars, friction is the major component of strength. With deformed (ribbed) reinforcing steel bars, and under increasing slip bond depend principally on the bearing, or mechanical interlock, between ribs rolled on the surface of the bar and the surrounding concrete. In this stage, the reinforcing bar generates bursting forces which tend to split the surrounding concrete. The failure load may be limited by the resistance provided to these bursting forces by concrete cover and confining reinforcement.

Corrosion affects bond strength in several ways. The bond strength between steel and concrete is reduced with the increase of reinforcement corrosion. One reason is that the cracking of concrete implies loss of confinement and thus reduces the bond. Another reason is that the weak layer of corrosion products reduces the friction force. Furthermore, the ribs are also deteriorated and the interlocking force decreases. Corrosion may reduce the height of the ribs of a deformed bar, this is unlikely to be

significant except at advanced stages of corrosion, however, disengagement of ribs and concrete occurs, and the layer of corrosion products formed by oxidation of the steel may force the concrete away from the bar and reduce the effective bearing area of the ribs. Therefore, the bond strength is significantly reduced due to the corrosion of reinforcement. However, it should be noted that within certain level of corrosion (2% to 4% mass loss of steel), the bond strength is observed to increase in many researches (Fu and Chung, 1997), (Al-Sulaimani et al., 1990), (Almusallamet al., 1996), (Chunget al., 2004) and others. The reason is that with the slight formation of corrosion products, increases in the diameter of a corroding bar at first, which increases radial stresses between bar and concrete and hence increases the frictional component of bond. However, further corrosion will lead to more corrosion products, development of longitudinal cracking and a reduction in the resistance to the bursting forces generated by bond action. Corrosion products at the bar-concrete interface will affect friction at the interface.

Chatper 3

BACKGROUND AND LITERATURE REVIEW

3.1 Introduction

The majority of structural members used in practice are subjected to flexural stresses caused by bending moments, such as beams and slabs. Bond between reinforcement and concrete is necessary to ensure composite interaction of the two materials. It is known that the load-carrying capacity of reinforced concrete (RC) beams is reduced with increasing corrosion. In order to analyze the influence of corrosion on flexural capacity of corroded RC beams, the fundamentals of conventional flexural theory, the design and behavior of reinforced concrete members and the bond mechanics for uncorroded beams must be studied first. In addition, this chapter reviews the available information on the changes in bond characteristics of reinforcement induced by corrosion and the consequences of that reduction on residual structural capacity of reinforced concrete elements.

3.2 Strength Requirements for Structures

In order to provide proper safety against failure, structural members must always be proportioned to resist loads greater than service or actual loads. The basic requirement for design and checking the ultimate limit state condition is that the factored resistance be equal to or greater than the effect of factored loads. In equation form, this can be written as:

$$\Phi R \geq \alpha_i S_i \quad (3\text{-}1)$$

where

Φ = resistance factor;

R = nominal resistance of a structural element;

α_i = load factor of ith specified variable load;

S_i = ith specified variable load.

In terms of moment resistance the factored resistance must be greater than or equal to the effect of factored loads (i.e. $M_r \geq M_f$, where M_r represents the factored moment resistance of the cross-section and M_f represents the moment due to the factored loads).

3.3 Flexural Theory of RC Beams

The flexural theory for reinforced concrete is based on three fundamental assumptions (Macgregor and Wight, 2009):

1. Sections perpendicular to the axis of bending that are plane before bending remain plane after bending;
2. The strain in the reinforcement is equal to the strain in the concrete at the same level;
3. The stresses in the concrete and reinforcement can be computed from the strains by using stress-strain curves for concrete and steel.

Figure 3-1(a) shows a beam subjected to a constant bending moment (pure bending). The top half of the beam is subjected to compression and the bottom half is subjected

to tension. There is a plane in the beam, which is not strained, and this is known as the neutral surface. The intersection of the neutral surface with a cross section defines the neutral axis (fundamental assumption of bending theory is that plane sections remain plane). Therefore, the ends of the beam remain plane under the action of the bending moment, resulting in a linear variation of strain with distance from the neutral axis, as shown in Fig. 3-1 (b) (Timoshenko and Gere 1972). In addition, there is a linear stress distribution over the depth of the beam, if the beam is made of a linear-elastic material (a material for which stress is proportional to strain), as shown in Fig. 3-1(c).

The assumption of a linear strain distribution along with the stress-strain curves of the concrete and steel permit determination of the stress distribution in the beam. Figs. 3-2 and 3-3 show schematic stress-strain curves of concrete and steel that are assumed for the design of reinforced concrete members. The compressive stress-strain curve for concrete depends on the testing conditions and the nature and proportions of the concrete mixture. There is no well-defined elastic limit and the curve deviates from a straight line in a gradual fashion.

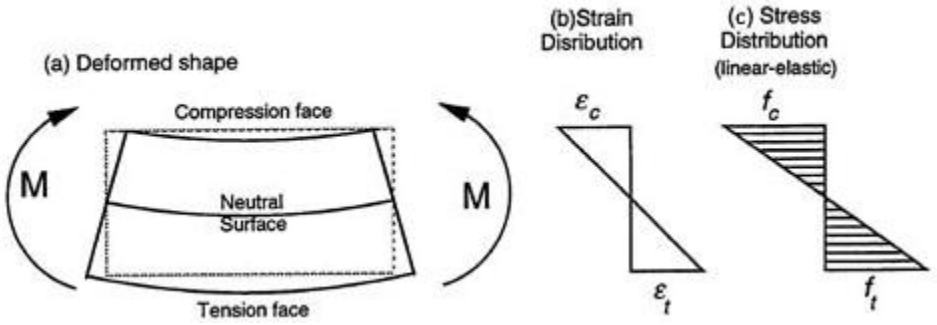

Fig. 3-1: Pure bending of a beam (Timoshenko and Gere 1972)

The mechanical properties of concrete and steel must be defined first. Macgregor and Wight (2009) assumed a elastic-perfectly plastic model for the reinforcing steel in tension and compression in Fig. 3-2. The steel elastic modulus E_s is assumed to be 200 GPa.

$$f_s = \begin{cases} E_s \varepsilon_s, & \varepsilon_s < \varepsilon_y \\ f_y, & \varepsilon_s \geq \varepsilon_y \end{cases} \tag{3-2}$$

where

f_s = steel stress;

E_s = elastic modulus;

ε_s = steel strain;

ε_y = steel strain at yielding;

f_y = yielding strength of steel.

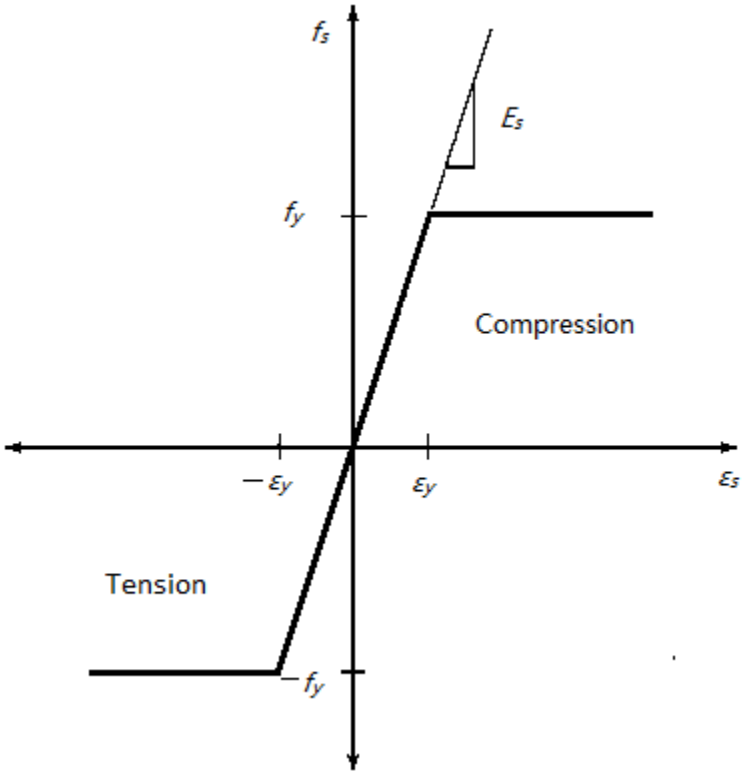

Fig. 3-2: Assumed stress-strain relationship for reinforcing steel (Macgregor and Wight, 2009)

The stress-strain relationship for concrete is assumed by Macgregor and Wight (2009) as shown in Fig. 3-3. The stress-strain relation is originally introduced by Hognestad (1952) as:

$$f_c = \begin{cases} f_c' \left[2\left(\frac{\varepsilon_c}{\varepsilon_o}\right) - \left(\frac{\varepsilon_c}{\varepsilon_o}\right)^2 \right], & \varepsilon_c \leq \varepsilon_o \\ f_c' \left[1 - \frac{Z}{100}\left(\frac{\varepsilon_c - \varepsilon_o}{\varepsilon_o}\right) \right], & \varepsilon_c > \varepsilon \end{cases} \quad (3\text{-}3)$$

where

f_c = stresses in concrete;

f_c' = compressive strength of concrete;

ε_c = strain in concrete;

ε_o = strain in concrete at peak compressive stress, taken as 0.002;

Z = constant controlling the slope of the line, taken as 150.

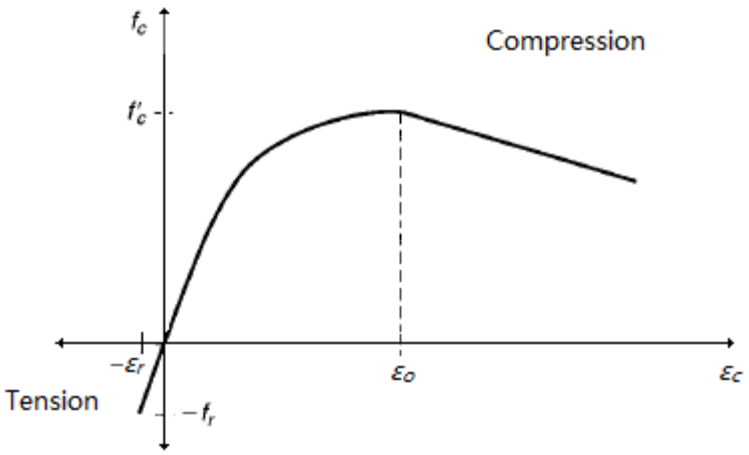

Fig. 3-3: Assumed stress-strain relationship for concrete (Macgregor and Wight, 2009)

To determine the moment capacity of a RC beam, a singly reinforced concrete beam under positive moment is considered in this investigation. The plane section analysis is

drawn in Fig. 3-4, in which d is the distance between the center of principle rebar and the extreme compression fiber, y_c is the distance between neutral axis and extreme compression fiber, Φ is the curvature of the cross section, C_c is the compression force of concrete, T_c is the tensile force of concrete, T is the tension force of reinforcing steel.

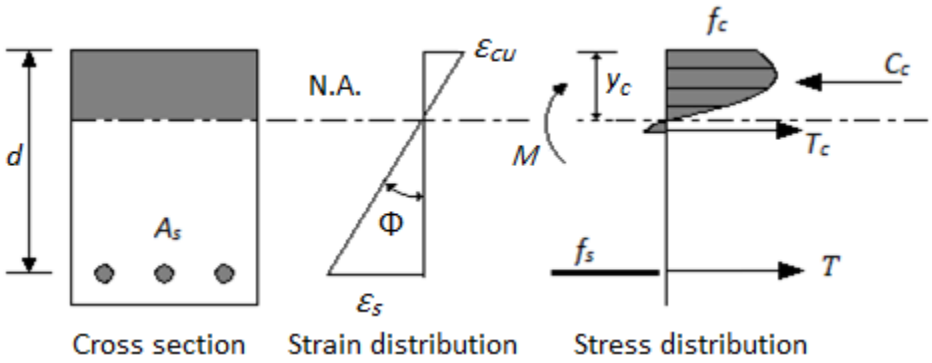

Fig. 3-4: Plane Section Analysis (Macgregor and Wight, 2009)

According to mechanics of materials , e.g. (Gere and Goodno, 2011), three conditions must be satisfied:

1. Geometrical conditions:

$$\Phi = \frac{\varepsilon_y}{y} \tag{3-4}$$

where

Φ = curvature of the section;

ε_y = the strains of concrete and steel at location y;

y = the distance from a point on the section to the neutral axis of the section.

2. Physical conditions:

The stress-strain relationship for steel and concrete, which are Eqs. (3-1) and (3-2), must be met respectively.

3. Equilibrium conditions:

$$C = T \tag{3-5}$$

$$C = \int_0^y f_c \cdot b \cdot dy \tag{3-6}$$

$$T = f_s \cdot A_s \tag{3-7}$$

$$M = \int_0^y f_c \cdot b \cdot y \cdot dy \tag{3-8}$$

where

C = the internal compression force of conrete;

T = the tensile force of reinforcing steel;

A_s = total area of reinforcing steel;

b = width of the beam section;

M = internal moment on the section.

The procedure to calculate the bending moment of a RC beam can be summarized as:

1. Find the cross sectional curvature Φ, and assume the strain of extreme concrete compression fiber is ε_c;
2. According to the "plain section remain plain" assumption, the strain of tensile reinforcing steel is ε_s calculated as:

$$\varepsilon_s = \frac{d - y_c}{y_c}\varepsilon_c \tag{3-9}$$

where

y_c = the distance between the neutral axis and extreme compression fiber.

3. Assuming the location of the neutral axis is y_c, the compression force of concrete C and the tensile force of steel can be calculated based on the the physical condition using Eqs. (3-2) and (3-3);
4. Move up and down the loacation of the neutral axis y_c to meet the equilbrium condition, which is $C = T$. The equibrium moment resistance M of the RC beam can then be calculated using Eq. (3-8).

3.4 Simplification of the Flexural Theory

To make it simple to analyze and design reinforced concrete beams, Macgregor and Wight (2009) suggested the following assumptions:

1. The tensile strength of concrete, T_c is neglected in flexural strength calculations;
2. The section is assumed to reach its norminal flexural strength when the strain in the extreme compression fiber reaches the maximum usable compressive strain, ε_{cu};
3. The compressive stress-strain relationship of concrete may be based on measured stress-strain curves, or may be based on rectangular shape that results in prediction of flexural strength in substantial agreement with the results of compressive tests (ACI Code section 10.2.6).

In this investigation, an equivalent rectangularstress block to represent the parabolic distribution of compression in concrete is used as shown in Fig. 3-4 , which is difined in CSA A23.3-04 (CSA, 2004).

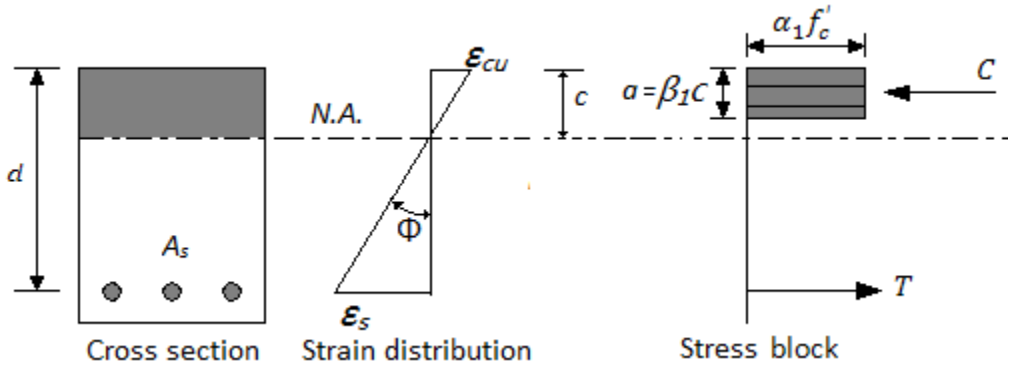

Fig. 3-5: Rectangular Stress Block (CSA, 2004)

In Fig. 3-5, a is the depth of the equivalent rectangular compressive zone; α_1 is the ratio of stress of compression stress block to the compressive strength of concrete which is determined by Cement Association of Canada (2006) as $\alpha_1 = 0.85 - 0.0015 f_c' \geq 0.67$; β_1 is the ratio of depth of stress block and the actual depth of compression zone, which is calculated in the design handbook (Cement Association of Canada, 2006) as $\beta_1 = 0.97 - 0.0025 f_c'$. Once these simplifications are assumed, the procedure of calculation of moment capacity in Section 3.3 will be much easier, which is demonstrated as follows:

1. The compression force of concrete:

$$C = \alpha_1 f_c' a b \tag{3-10}$$

2. Assume the steel yields before crush of conrete, then the tensile force of steel at failure is:

$$T = A_s \cdot f_y \tag{3-11}$$

3. Setting $C = T$ yields the stress block depth:

$$a = \frac{A_s \cdot f_y}{\alpha_1 f_c' b} \tag{3-12}$$

4. The flexural strength is:

$$M = T \cdot \left(d - \frac{a}{2}\right) \tag{3-13}$$

It should be noted that the strain of steel must be checked, because the steel is assumed to yield before the concrete crushes at failure. This assumption must be satisfied to avoid the crushing of concrete. If not, the beam will suffer a brittle failure, which is a bad design. Based on the linear strain distribution, the steel strain is calculated as:

$$\varepsilon_s = \frac{d - a}{a} \varepsilon_{cu} \geq \varepsilon_y = \frac{f_y}{E_s} \tag{3-14}$$

3.5 Influence of Corrosion on Flexural Capacity of RC Members

The majority of structural members used in practice are subjected to flexural stresses caused by bending moments, such as beams and slabs. This section summarizes the current understanding of the influence of corrosion on flexural capacity of a reinforced concrete element. Few researchers have investigated on how the corrosion of

reinforcement influences the flexural capacity of reinforced concrete members, such as strength, deflection and steel and concrete strains in reinforced concrete beams.

1. Malumbela et al. (2009)

Malumbela et al. (2009) studied the flexural behaviour of corroded RC beams under combined effect of corrosion and sustained loads. An accelerated corrosion process using a 5% solution of NaCl and a constant impressed current induced corrosion on tensile steel bars. They tested four RC beams, each with a width of 153 mm, a depth of 254 mm and a length of 3000 mm. Beams were tested under self-weight, under 10% of the ultimate load and under 33% of the ultimate load. Longitudinal tensile strains and longitudinal compressive strains were monitored during the corrosion process. Measured strains were used to determine the depth of the neutral axis, the curvature and the moment of inertia of beams. They concluded that depth of the neutral axis is independent of the level of corrosion for beams free from flexural cracks and beams free from corrosion but significantly reduces with an increase in degree of corrosion for corroded beams with flexural cracks. In addition, the longitudinal strains, depth of the neutral axis and curvature depend on both the level of corrosion and the applied load while the moment of inertia only depends on the level of corrosion.

2. Torres-Acosta et al. (2007)

Torres-Acosta et al. (2007) used specimens of concrete beams with 100 mm × 150 mm cross section and 1500 mm in length casted with chlorides to investigate the flexural capacity loss with steel cross-section loss due to generalized corrosion of the embedded steel. The specimens were tested in flexure under three point loading. The experimental

values of maximum load P_{MAX} were used to estimate the residual load capacity ratio RLC_{COR}. An empirical equation was formulated according to the test data as:

$$RLC_{COR} = -0.8596 \cdot \left(\frac{PIT_{MAX}}{r_0}\right) + 0.9707 \quad (3\text{-}15)$$

where

PIT_{MAX}= maximum pit corrosion depth;

r_0 = rebar radius.

It's observed by Torres-Acosta (2007) that the flexural load capacity decreased 60% with only 10% of the x_{AVER}/r_0 ratio, which is the ratio of average corrosion depth to the rebar radius. PIT_{MAX}/r_0 rather than x_{AVER}/r_0 ratio was the most important parameter affecting flexural load capacity reduction, because pitting corrosion greatly decrease the cross sectional area of the steel at a certain location and change the steel from ductile behavior to brittle behavior.

3. El Maaddawy et al. (2005)

El-Maaddawy et al. (2005) studied the flexural behaviour of corroded RC beams under combined effect of corrosion and sustained loads. Test results showed that the presence of a sustained load and associated flexural cracks during corrosion exposure significantly reduced the time to corrosion cracking and slightly increased the corrosion crack width. For example they found that crack width would propagate 22% faster in loaded conditions. They observed that with 8.9% and 22.2% mass loss, strength losses of 6.4% and 20.0%, respectively. It was also observed that the presence of flexural cracks during corrosion exposure initially increased the steel mass loss rate and, consequently, the

reduction in the beam strength. El-Maaddawy et al. (2005) concluded that at low corrosion levels, the effect of bond loss can be ignored and that the ultimate load carrying capacity of the beam is affected only by the loss on steel reinforcement.

4. Ballim and Reid (2003)

Ballim and Reid (2003) tested beams having dimensions of 160 x 100 x 1500 mm, reinforced with a single 16 mm diameter bottom bar and a pair of 8 mm diameter top bars. Corrosion was initiated through carbonation and was accomplished by placing the beams in a CO_2 filled pressure chamber (that was kept at 80 kPa) and supplying a current of 400 μA/cm^2. The beams were simultaneously corroded and loaded to either 23% or 34% of the ultimate load (P_u).

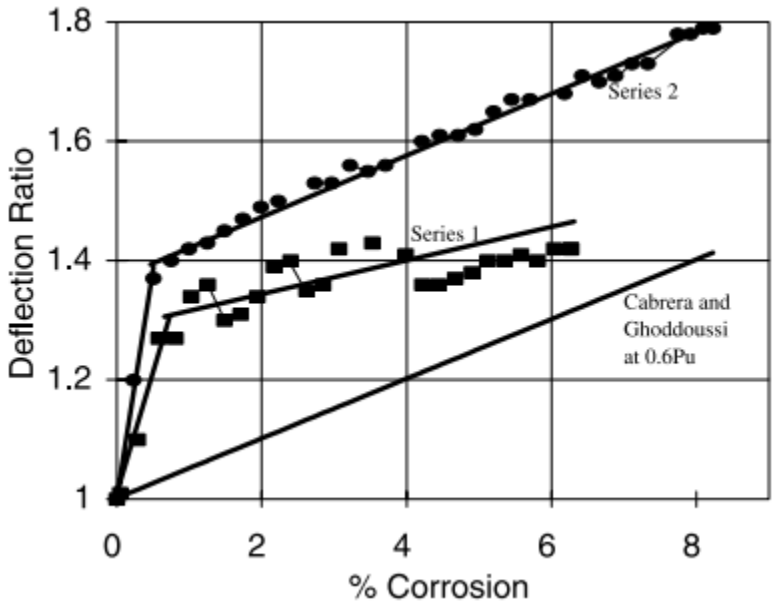

Fig. 3-6: Effect of corrosion on the deflection ratio of RC beams. Series I – loaded to 0.23P_u (Ballim and Reid, 2003)

Fig. 3-6 summarizes the deflection ratios that were observed by Ballim and Reid (2003), which were calculated by dividing the average deflections of the corroded beams with those of the control beams. This graph indicates that the deflection increased as corrosion propagated, particularly at the early stages. The researchers attributed this initial increase in deflection to early crack formation, as the crack creation and widening progressed at a slower rate after a certain point (Ballim and Reid, 2003).

5. Castel et al. (2000)

Castel et al. (2000) studied the mechanical behaviour of RC beams with corroded reinforcement. They conducted two separate experimental studies; the first one consisted of four beams, which were naturally corroded in a salt fog environment for 14 years in an attempt to mimic actual field conditions, with dimensions of 150 x 280 x 3000 mm. Beam ultimate strength were determined by using three-point loading tests. The average reported degree of corrosion was 10% and the reduction in flexural strength was 20% with a 70% reduction in ductility. They concluded that the decrease in stiffness was due to the reduction of both the steel cross-sectional area and bond strength. This was attributed to the fact that the average maximum cross-section loss near the centre of the beam was 20%, which would theoretically result in a stiffness decrease of 15%. However, the total stiffness loss for one of the beams tested was 35%; hence, there was a 20% difference in loss that was unaccounted for, which the researchers suspected to be the result of bond deterioration (Castel et al., 2000). They also said that the concrete cracks resulting from compression reinforcement corrosion have an insignificant effect on the global behaviour of RC beams.

6. Mangat and Elgarf (1999)

Mangat and Elgarf (1999) carried out another investigation into the effect of reinforcement on load carrying capacity on 111 under-reinforced concrete beams. Corrosion was induced at four different rates by applying a current of 1, 2, 3, or 4 mA/cm^2. Nine groups of beams were fabricated, having dimensions of 100 x 150 x 910mm and reinforced with two no. 10 bars in tension. Stirrups (both embedded and external) were applied to avoid shear failure. A significant reduction in the ultimate flexural strength was noticed as under a four-point loading they observed a 77% reduction in ultimate load with a corresponding loss of diameter of 10%. The load-deflection relationships showed that when the degree of corrosion is greater than 2.5%, load-deflection curves become dependent on the rate of corrosion. The rate of corrosion was found to have an effect on the flexural load capacity。 They observed that when corrosion is less than 3.75%, the rate of corrosion had little influence on the residual strength. While, when corrosion is greater than 5%, an increase in the rate of corrosion greatly reduced the flexural strength of RC beams. They suggested that when accelerated corrosion testing is necessary, the lowest practical corrosion rates should be used to induce corrosion, particularly when the desired degree of corrosion is high.

Mangat and Elgarf (1999) proposed a numerical relationship between residual flexural strength and the level of corrosion:

$$B = \left[1 - sin^2\left(7\frac{2Rt}{d_b}\right)\right]100\% \qquad (3\text{-}16)$$

where B is the percent flexural load capacity, R is the rate of corrosion in mm/year, and t is the elapsed time in years after corrosion initiation. The expression $2Rt/d_b$ in the above Eq. (3-16) is the formula for the degree of corrosion as a percentage reduction in bar diameter.

7. Rodriguez et al. (1997)

Rodriguez et al. (1997) studied the effect of varying degrees of corrosion on concrete beams. The beam specimens were 200mm by 150mm with a clear span of 2000mm. Beams had both tensile, compressive as well as shear reinforcement that was corroded using accelerated corrosion techniques by immersing the specimens in a solution made of 3% calcium chlorides by weight to the mixing water, over a period of 101-190 days under a constant current density of 100 μA/cm^2.

The results showed that corrosion increases deflections and crack widths at the service load, decreases strength at the ultimate load, and causes an increase in both the spacing and width of transverse cracking due to bond deterioration. The different types of failure within the beam specimens that was observed by Rodriguez et al. (1997) are shown in Fig. 3-7. They reported that type 1 failure occurred in both corroded and un-corroded beams with a low tensile reinforcement ratio; type 2 failure was observed in beams with un-corroded tensile reinforcement of a high ratio and most corroded beams with a high ratio of shear reinforcement; type 3 failure occurred in nearly all beams having a high ratio of corroded tensile bars and large stirrup spacing; while type 4 failure was found in corroded and un-corroded beams with curtailed tensile reinforcement.

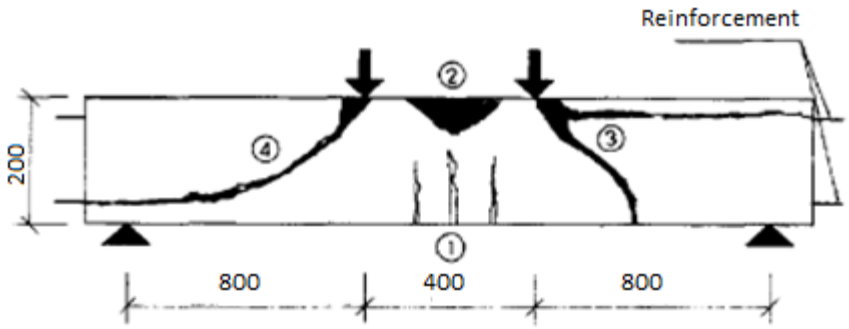

1) Failure by bending (yielding of tensile reinforcement).
2) Failure by bending (crushing of concrete).
3) Failure by shear.
4) Failure by both shear and bond splitting.

Fig. 3-7: Illustration of types of failures of beams with corroded reinforcement (Rodriguez et al., 1997)

It was determined that not only will there be a loss of strength in both shear and bending due to reinforcement corrosion, but also that corrosion can change the mode of failure as well. Failure in some beams shifted from bending to shear upon corrosion of reinforcement. This was prominent in beams with stirrup spacing close to the effective depth of the concrete sections, when combined with a high relative corrosion of the tensile bars. This change in failure mechanism was attributed to the reduction of the stirrups cross-section (shear reinforcement) due to pitting and the reduction of the concrete section due to spalling. In addition, Rodriguez et al. (1997) concluded that by using the reduced sections of steel and concrete with conventional RC models, conservative values of the ultimate moment and shear force could be calculated for RC members damaged by corrosion. However, this method of calculating the strength of damaged members is deficient in that it fails to consider the reduction of bond.

8. Huang and Yang (1997)

Huang and Yang (1997) studied the relationship between the corrosion of RC beams and load-carrying capacity. Two types of beam specimens (150 x 150 x 500 mm, reinforced with two 6 mm bottom bars) were used: beams without cracks (type S) and beams with a middle surface crack (type K). Two concrete mixtures were used: mix A and mix B, having a water to cement ratio (w/c) of 0.4 and 0.3 respectively. Immersing them in seawater and applying a current of 5 A/cm^2 corroded the RC beams. Their results showed significant reduction in load-carrying capacity with the increase in corrosion was more in beams with a low w/c or predetermined cracks (mix B or type K) as shown in Figures 3-8 and 3-9. Huang and Yang (1997) concluded that this behaviour was a result of the chloride ions having easier access to the reinforcing steel in cracked beams than in un-cracked ones.

To explain the fact that the beams made with a lower w/c (which makes for a higher strength concrete), displayed a less favourable response, Huang and Yang (1997) said that, "…lower water/cement ratio concretes have smaller pores, which show lower energy-absorbing capacity", and that after cracking, beams made of high strength concrete may fail before ones of low strength concrete.

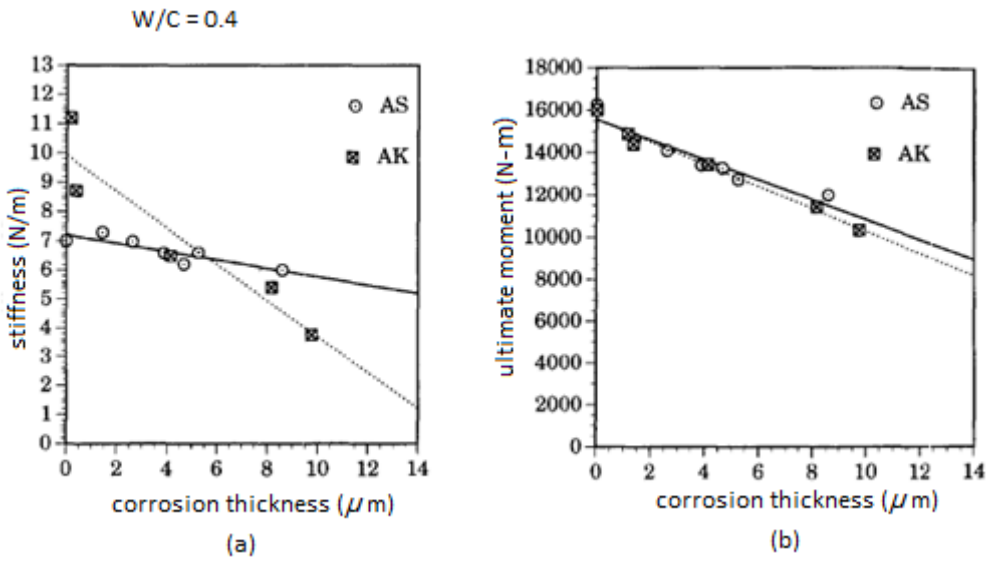

Fig. 3-8: (a) Effect of corrosion on stiffness; (b) effect of corrosion on ultimate moment (AS – beams without cracks and AK – beams with a middle surface crack) (Huang and Yang, 1996).

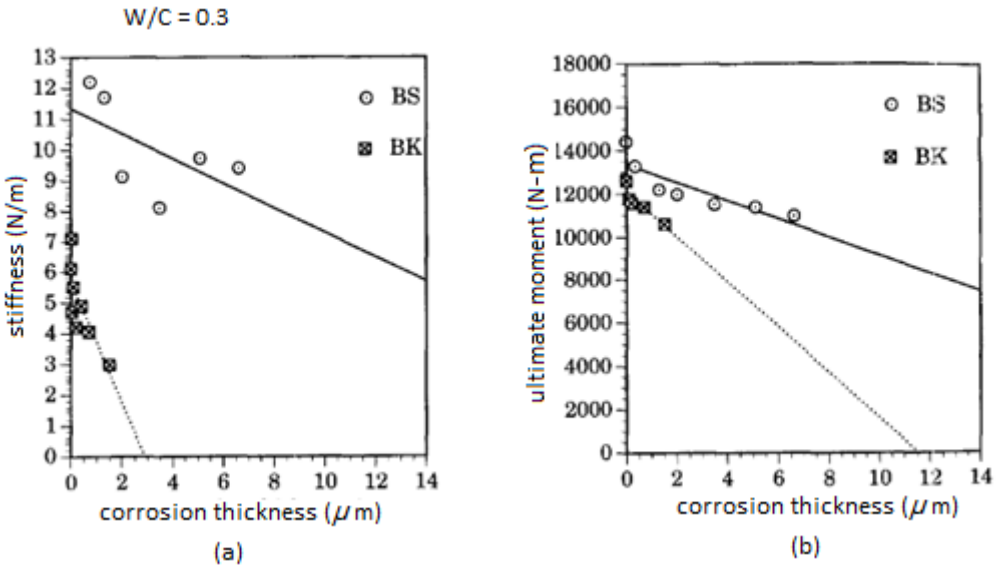

Fig. 3-9: (a) Effect of corrosion on stiffness; (b) effect of corrosion on ultimate moment (BS – beams without cracks and BK – beams with a middle surface crack) (Huang and Yang, 1996).

Amleh (2005) observed similar behaviour with concretes made with low w/c ratios and concluded that concrete that has smaller pores cannot accommodate voluminous rust products as well as concrete with larger pores. This is because the existence of larger pores allows the oxides to migrate more easily into the matrix of the concrete, thus reducing the expansive tensile stresses. Conversely, concrete with smaller pores is more greatly influenced by rust products and experiences larger internal stresses, resulting in a more rapid deterioration of the concrete (Amleh, 2005).

9. Eyre and Nokhasteh (1992)

Eyre and Nokhasteh (1992) studied the behaviour of RC beams simply supported with exposed reinforcement. In the tests performed, the concrete-steel interface was assumed to have zero bond over various lengths of the beam and the capacity of the beam was observed to reduce with smaller bond lengths. They found that even with the use of a critical un-bonded length, the beams failed by the concrete crushing, regardless of steel ratio. Their results have demonstrated that beams may possess considerable strength despite bond being entirely eliminated over part of the span, provided ends of bars remain adequately anchored. Eyre and Nokhasteh (1992) proposed an algebraic method for predicting the ultimate strength of corroded RC beams. However, this method assumes that concrete acts as a linear-elastic material and thus does not properly reflect the stress-strain behaviour of concrete, and presumes a total loss of bond, which does not reflect actual conditions (Maaddawy et al., 2005).

10. Cabrera and Ghoddoussi (1992)

Cabrera and Ghoddoussi (1992) studied the effects of corrosion on beams of 160 x 125 x 1000 mm, reinforced with 2-10 mm diameter bars at the top, 2-12 mm diameter bars at the bottom and 8 mm diameter stirrups. They also used accelerated corrosion techniques to corrode the tensile reinforcement by applying an unknown current density. They reported bond reduction of 35% and a maximum reduction in the steel cross-sectional area was 9%, which resulted in a 20% reduction in the ultimate bending moment and a 40% increase in deflection at the service load. They also developed expressions for the relationship between crack width and corrosion, based on different parameters. Predictions of the two sets of expressions are broadly consistent despite significant differences in conditioning. Others report crack widths in excess of 0.6mm without spalling. Given the importance of confinement from cover and links to bond, it is clear that bond will be severely depleted prior to spalling.

11. AI-Sulaimani et al. (1990)

AI-Sulaimani et al. (1990) conducted two series of tests, one to study the influence of corrosion on the behavior of beams failing in bond, the other to evaluate the behavior of beams designed to fail in flexure. These beam tests were designed to simulate relatively uniform corrosion, while pullout tests were used to simulate severe local corrosion.

These beams and pullout specimens were subjected to different levels of corrosion. In the test program on the study of corrosion-bond behavior for beams designed to fail in bond, beam specimens150x150 mm in cross section and 1000mm in length, with one 12 mm bottom bar having an embedment length of 144mm, were used. In the series aimed at the study of corrosion-bond behavior for beams designed to fail in flexure, the same specimen were used except that the embedment length was increased to 300mm. All beam specimens were cast from a concrete with a water/cement ratio of 0.45 and an average compressive strength of 40 MPa.

Sufficient development length and shear stirrups were provided to prevent bond or shear failures for the beams designed to fail in flexure. They found that the average bond stress over the embedded length was found to be well below the ultimate bond stress observed in pullout tests for bars with similar corrosion, indicating that the failure of the beams was due to the yielding of steel and was not a bond failure (Al-Sulaimani et al., 1990). Furthermore, they concluded that the reduction in beam capacity was not due to a decrease in bond stress but rather, it could be attributed primarily to the reduced area of the reinforcing steel.

12. Minkarah and Ringo (1982)

Minkarah and Ringo (1982) carried out a series of tests on beam specimens in which loss of cover to and full debonding of tension reinforcement due to corrosion damage was simulated. Beam section, which contained 0.95% reinforcement, and span were tested with a varying length of bar exposed. All beams were tested under a single point load

offset from mid-span, and the load was applied at a section where reinforcement remained bonded to concrete. They noted a marked difference in the pattern of crack formation was noted in specimens with bars disbanded. They also noted that the beam strength was not adversely affected by the absence of cover. This structural action was described as changing from flexural to tied arch behaviour with secondary effects. Exposure of reinforcement of about 20% of the span of the beam resulted in a slight loss of load carrying capacity, however, exposure of over 60% of the span of the beam resulted in a strength loss of around 20%.

Cairns (1993, 1995), Eyre and Nokhasteh (1992), and Raoofand Lin (1996) have all conducted tests which demonstrate that beams may possess considerable strength despite bond being entirely eliminated over part of the span, provided ends of bars remain adequately anchored.

3.6 Bond Basics

As mentioned earlier, in the simplified analysis of reinforced concrete structures complete compatibility of strains between concrete and steel is usually assumed, which implies perfect bond. It is the bond that allows the tensile force to transfer from concrete to reinforcing steel to compensate the low tensile strength of concrete. If the bond between steel and concrete is not perfect, the flexural theory for RC beams cannot be used to calculate the flexural capacity of the beam.

3.6.1 Mechanism of Bond Transfer

The transfer of forces from concrete to steel is demonstrated by ACI Committee 408 (2003) in Fig. 3-10.

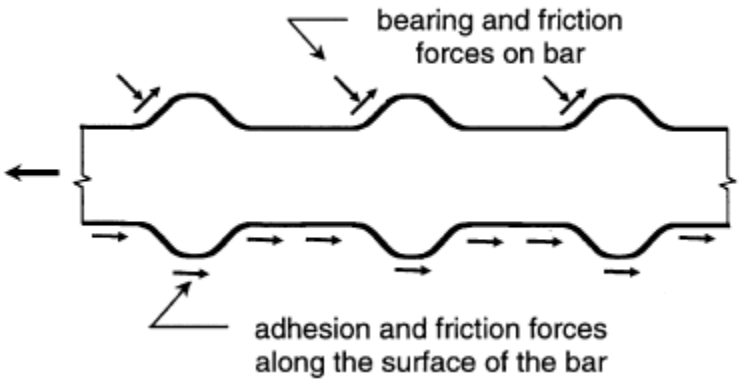

Fig. 3-10: Bond force transfer mechanism (ACI Committee, 2003)

As shown in Fig. 3-10, there are three mechanisms of the bond transfer, illustrated by ACI Committee (2003):

Adhesion: Chemical adhesion between the bar and the concrete. Adhesion is a chemical clinging force at the surface between steel and concrete. Although the chemical adhesion is present when the bar is loaded at the beginning, it is lost quickly as the load is increased, therefore this resisting effects is not reliable.

Friction: The surface characteristics of the rebar influence the frictional bond at the rebar surface. Frictional forces arising from the roughness of the interface, forces transverse to the bar surface, and relative slip between the bar and the surrounding concrete. The friction force plays a significant role between the concrete and the bar deformations (ribs).

Mechanical anchorage: Mechanical anchorage or bearing of the ribs against the concrete surface depends on the surface profile of the rebar. The mechanical anchorage of the ribs plays the most important role for deformed bars at higher load levels. When the ultimate bond strength is reached, shear cracks are formed in the concrete between ribs, while the anchorage forces induce large bearing forces on the ribs. The compressive bearing forces on bars also increase the frictional forces.

3.6.2 Bond Resistance

According to the bond transfer mechanism, the bond resistance for deformed bars consists of three parts:

1. The shear force f_{AD}, which is due to the adhesion between steel and concrete;
2. The friction force f_{fr}, which is the tangential force resulting from the radial compressive stresses due to the bearing force of ribs against the concrete between ribs;
3. The bear force f_b, which is the bearing force on ribs in the direction the rebar.

3.6.3 Bond Failure Modes

As stated by Cairns and Abdullah (1996), three modes of bond failure of ribbed reinforcing bars may be identified as shown in Fig. 3-11.

The first mode, as illustrated in Fig. 3-11 (a), is the pull-out failure, in which concrete is sheared across the tops of the bar ribs. Pull-out failure occurs when the bar is well-confined by a thick cover or by heavy stirrups confining the bar. It is generally agreed

that pull-out failures occur where minimum concrete cover is in excess of three times bar diameter (Cairns and Abdullah, 1996).

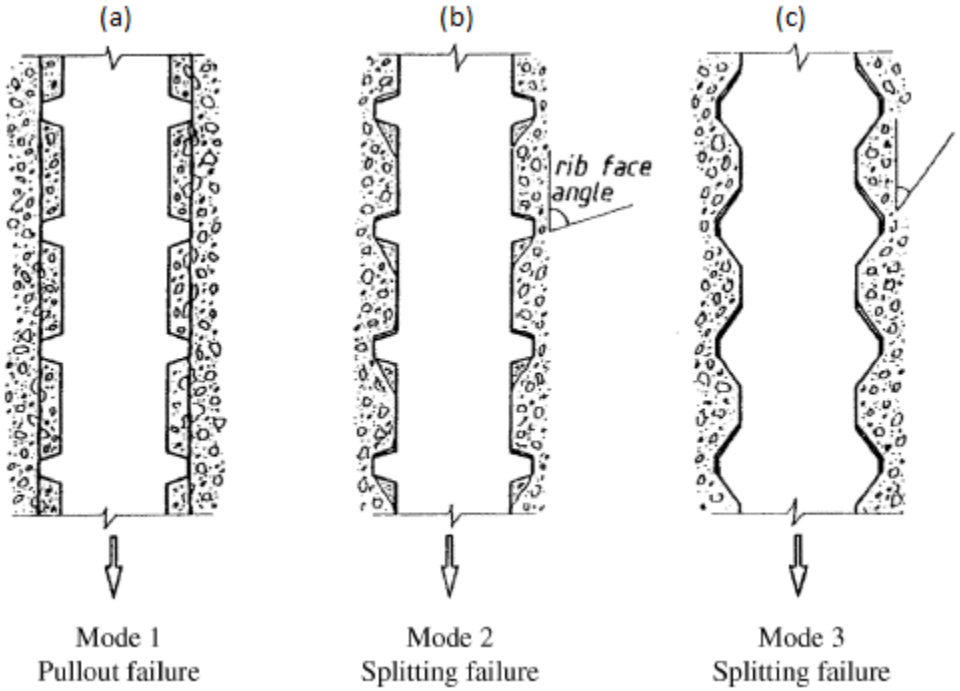

Fig. 3-11: Bond failure modes of ribbed reinforcing bars (Cairns and Abdullah, 1996)

When concrete cover is less than twice the bar diameter, bond-splitting failure will occur as illustrated in Fig. 3-11 (b), where a wedge of concrete is sheared by the bearing of ribs. Fig. 3-11 (c) shows another splitting failure mode, in which concrete is sheared on the inclined surface of ribs.

3.6.4 Factors affecting the bond strength

The bond strength between steel and concrete is affected by many factors, including the structure characteristics, the bar properties and the concrete properties. A summary of the effect of those factors are made by ACI Committee 408 (2003) as follows:

1. Bond force increases with increased concrete cover and bar spacing, development and splice length, and the use of confining transverse reinforcement;
2. Top-cast bars have lower bond strength than bottom-cast reinforcing bars;
3. Noncontact lap splices provide a higher bond strength than contact lap splices;
4. For a given length of bar, the bond force contributed by both concrete and transverse reinforcement increases as the bar diameter increases;
5. The bond strength of bars confined by transverse reinforcement increases with increased relative rib area;
6. Bond strength increases with increased concrete compressive strength;
7. The bond strength provided by transverse reinforcement increases approximately with the 3/4 power of the compressive strength;
8. An increase in aggregate strength and quantity results in an higher bond strength;
9. Fiber reinforcement act as transverse reinforcement, providing increased bond strength;
10. Improved consolidation of concrete results in higher bond strength.

3.7 Influence of Corrosion on Bond Behavior

A lot of researchers have investigated the influence of corrosion on the bond strength between steel and concrete.

1. Chung et al. (2004)

Chung et al. (2004) carried out experimental research in order to determine the way in which corrosion affects bond strength and development length. Seventy concrete slab specimens having one steel reinforcing bar were corroded to different levels of corrosion to evaluate the effect of corrosion level on bond stress and development length of flexural tension members. The average bond stress increases before corrosion level reached 2% and then starts to decrease after 2% corrosion level. Chung et al. (2004) explains that below actual corrosion of 2%, the corrosion rusts on the surface of corroded steel bar causes increase in friction stress between reinforcing bar and concrete, which overrides the decreasing bond stress due to corrosion.

They also suggested a correction factor δ in development length when designing concrete structures by ACI318 Code:

$$\delta = \begin{cases} 1.0, & C_0 \leq 2.0 \\ 2.09 C_0^{-1.06}, & C_0 > 2.0 \end{cases} \quad (3\text{-}17)$$

where C_0 is the corrosion level in percentage.

2. Jin and Zhao (2001)

Jin and Zhao (2001) carried out a series of experimental studies using pull-out cubic concrete specimens (100 mm × 100 mm × 100mm) with 12 mm diameter plain bars and

deformed bars respectively. Optimizing the aggressive line of test data, they gave the following empirical equations to calculate the bond strength:

$$\tau_u = \eta \tau_{u0} \tag{3-18}$$

where τ_{u0} is the bond strength between uncorroded steel bar and concrete, η is the bond strength coefficient, η_p as the bond strength coefficient for plain bar in Eq. (3-19) and η_D as the coefficient for deformed bars in Eq. (3-21).

$$\eta_p = \begin{cases} 1 + 22\delta, & \delta \le \delta^* \\ 1 - 15 + 37\delta^*, & \delta > \delta^* \end{cases} \tag{3-19}$$

where δ is the corrosion layer depth, δ^* is the depth corresponding to the cracking time, which was calculated by Jin and Zhao (2001):

$$\delta^* = D_0 \cdot \left(\sqrt{n\rho^* + 1 - \rho^*} - 1\right)/2 \tag{3-20}$$

where D_0 is the diameter of the steel bar, ρ^* is the percentage of rebar corrosion corresponding to cracking time, and n is the volume expansion ratio taken as 2 to 3.

The bond strength coefficient for deformed bars was expressed as:

$$\eta_D = \begin{cases} 1.00 + 7.0\delta, & \delta \le 0.05 \\ 1.46 - 2.3\delta, & \delta > 0.05 \end{cases} \tag{3-21}$$

Jin and Zhao (2001) also conducted beam tests on 1140-mm-long beams with a cross section of 150 mm × 150 mm, reinforced with two 12 mm bottom bars, two 6 mm top bars and 6 mm stirrups at 100 mm. Based on the test data, they proposed the following empirical equation to calculate the bending capacity of corroded RC beams:

$$M_u = \beta' M_{u0} \tag{3-22}$$

where M_{u0} is the bending strength of uncorroded RC beam, β' is the comprehensive reduction coefficient considering rebar corrosion and was expressed as:

$$\beta' = \begin{cases} 1, & \rho < 1.2 \\ 1.04514 - 0.03762\rho, & 1.2 \leq \rho \leq 6 \end{cases} \quad (3\text{-}23)$$

where $\rho\%$ is the corrosion percentage.

3. Amleh and Mirza (1999)

Amleh and Mirza (1999) investigated the influence of corrosion on bond between the reinforcing steel and concrete, using a series of tests on 14 cylinder tension specimens. The cylinder was 100 mm in diameter and 1-m long and reinforced with one No. 20 bar. 12 of the 14 specimens were placed in a tank filled with a 5% NaCl solution. The study was carried out for seven different levels of corrosion, ranging from no corrosion to extensive corrosion, with a 9-mm longitudinal crack caused by the bursting pressure due to the volume expansion of the corrosion products. They have reported a 9% loss of bond strength due to 4% loss of weight from corrosion accompanied by transverse cracks, and a 17.5% weight loss with no transverse cracks before yielding of the bar resulted in 92% loss of bond between the steel and the surrounding concrete.

The width of these transverse cracks increased as the corrosion level increased, and it signified a reduction of bond between the reinforcing steel bar and concrete.

4. Stanish et al. (1999)

Stanish et al. (1999) investigated 10 one-way slab specimens having a cross section of 350 mm (width) by 150 mm (thickness) and 1300 mm span. The slabs were immersed in a 3% NaCl solution up to the mid-depth of the rebars and were tested under four-point loading. Based on the experimental program and subsequent mathematical analysis, the peak bond strength at various corrosion levels was estimated. A linear regression analysis was performed with the available data and the empirical average bond stress was expressed as:

$$\frac{U}{\sqrt{f_c'}} = 0.63 - 0.04ML \tag{3-24}$$

where ML is the percentage of mass loss.

5. Fu and Chung (1997)

Fu and Chung (1997) reported that the corrosion of steel rebar in concrete which is immersed in saturated $Ca(OH)_2$ solution caused the bond strength to increase while the contact resistivity increased within the first 5 weeks of corrosion. Further corrosion caused the bond strength to decrease while the contact resistivity continued to increase. This means that slight corrosion increased the bond strength, while severe corrosion decreased the bond strength.

6. Almusallam et al. (1996)

Almusallam et al. (1996) investigated the effect of reinforcement corrosion on the bond strength between reinforcing steel and concrete. They noticed that in the pre-cracking stage (0-4% corrosion), the ultimate bond strength increases. However, when

reinforcement corrosion is in the range of 4 to 6%, the bond failure occurs suddenly at a very low free-end slip. Beyond 6% rebar corrosion, the bond failure occurs because of a continuous slippage of rebars. The ultimate bond strength initially increased with an increase in the degree of corrosion within 4% rebar corrosion, after which there was a sharp decrease in the ultimate bond strength up to 6% rebar corrosion. Beyond the 6% rebar corrosion, the ultimate bond strength did not vary very much even up to 80% corrosion.

7. Cabrera and Ghoddoussi (1992)

Cabrera and Ghoddoussi (1992) investigated the effect of reinforcement corrosion on bond strength. They studied two types of specimens: pull-out test specimens and beam test specimens. The pull-out tests were carried out on 150 mm concrete cubes, in which diameter reinforcing bars were centrally embedded. The beam specimens were 125 × 160 × 1000 mm, reinforced with two 10 mm top bars, two 12 mm bottom bars and plain stirrups of 8 mm at 40 mm spacing along the shear span of 384 mm. The experimental results were used to determine the relationships between bond stress and the corrosion rate. They discussed the influence of the cement type on the rate of corrosion and their effect on the bond strength. Maximum reduction of the cross section (9%) at bottom bar caused a reduction of 20% of the ultimate bending moment and increased the deflection by 40% at mid-span corresponding to the service load.

8. Al-Sulaimani et al. (1990)

Al-Sulaimani et al. (1990) studied the influence of reinforcing bar corrosion and the associated longitudinal cracking on the steel-concrete interface bond behaviour using the

standard pull-out and beam tests. The bond behaviour at the steel-concrete interface was examined at four different stages of corrosion, no corrosion stage, pre-cracking stage, cracking stage, post-cracking stage. They found that when the mass loss of the reinforcement due to corrosion reaches approximately 2%, concrete cracks. A small amount of corrosion increases the bond, but the slip at failure decreases considerably. However, when the mass loss exceeds 2%, bond strength decreases considerably. Even when there is extensive corrosion, bond is not completely destroyed. Bond strength exists even when the mass loss approaches 6%. This can explain the fact that structures with extensively corroded reinforcement sustain loads.

3.8 Theoretical and Analytical Models

A few researchers have proposed models to calculate the bond strength between reinforcement and concrete. Models to calculate the residual flexural strength were also suggested by few researchers.

1. Coronelli Bond model (2002)

Coronelli (2002) studied the interface pressure caused by the expansion of corrosion product at different confinement stages and developed a model predicting the bond strength for corroded bars in reinforced concrete structures. He studied the role of the interface pressure caused by bar expansion in different confinement situations.

In order to determine the interface pressure, the total crack width with regard to corrosion depth X, which was proposed by Molina, Alonso and Andrade (1993), was used:

$$W_{cr} = \sum_i u_{i_{corr}} = 2\pi t \tag{3-25}$$

with

$$t = \frac{r_b(v_{rs} - 1)}{r_b + c} X \tag{3-26}$$

where

$u_{i_{corr}}$ = opening of each single radial crack;

t = bar expansion;

v_{rs} = ratio between the volumes of corroded and virgin steel;

c = extension of the crack across the cover;

r_b = bar radius;

X = the corrosion depth.

Fig. 3-12 shows the relation between corrosion depth X and bar expansion t.

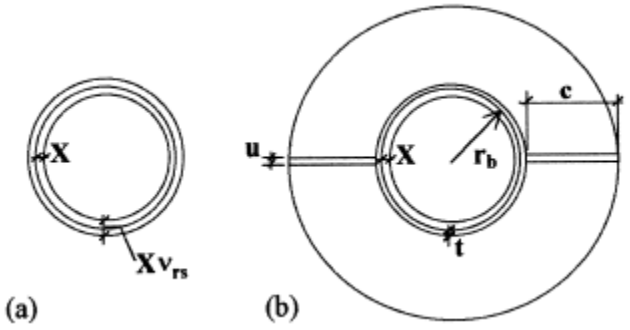

Fig. 3-12: Corrosion depth X and bar expansion t (Coronelli, 2002)

Once the crack width is determined, the confinement pressure at failure p^{max} can be achieved by adding confinement of stirrups and confinement of concrete.

Coronelli (2002) modified a model proposed by Cairns and Abdullah (1996) for splitting bond failure by considering corroded bars and formulated the bond strength as:

$$\tau_{bu} = k(X)p^{max}(X) + \tau_b^0(X) + \mu(X)p_{corr}(X) \tag{3-27}$$

where

τ_{bu} = bond strength;

p^{max} = maximum confining pressure at bond failure;

τ_b^0 = cohesive bond strength contribution determined by Eq. (3-28);

p_{corr} = corrosion pressure;

k = a factor determined by Eq. (3-29);

μ = friction coefficient determined by Eq. (3-30).

$$\tau_b^0 = nA_r f_{coh}[cot\delta + \tan(\varphi + \delta)]/(\pi d_b s_r) \tag{3-28}$$

$$k = nc_r\, tan(\varphi + \delta)\,/\pi \tag{3-29}$$

where

n = number of transverse ribs at section;

s_r = rib spacing;

A_r = rib area in the plane at right angles to bar axis;

c_r = coefficient, depending on the rib shape and area;

δ = orientation of the ribs;

φ = friction angle between steel and concrete;

f_{coh} = adhesion strength determined by Eq. (3-31).

Coronelli (2002) considered the influence of corrosion on the friction coefficient and adhesion strength and proposed the following equations:

$$\mu = \tan\varphi = 0.3 - 0.2(X - X_{cr}) \quad (3\text{-}30)$$

$$f_{coh} = 2 - 10(X - X_{cr}) \quad (3\text{-}31)$$

The drawback of this model is that the corrosion pressure is not theoretically derived but based on experimental results.

2. Wang and Liu Bond Model (2006)

Wang and Liu (2006) modeled the bond strength of corroded reinforcements theoretically. They firstly calculated the corrosion pressure with reference to Fig. 3-13, where R_0 is the initial radius of rebar, R_c is the cover dimension, R_i defines the cracking front, p_{cor} is the corrosion pressure caused by expansive action of corrosion products, p_i is the radial pressure at the cracking front. It should be noted that in this section, they used different notations for cover dimension, cracking front and initial radius from those in the present research in Chapter 4.

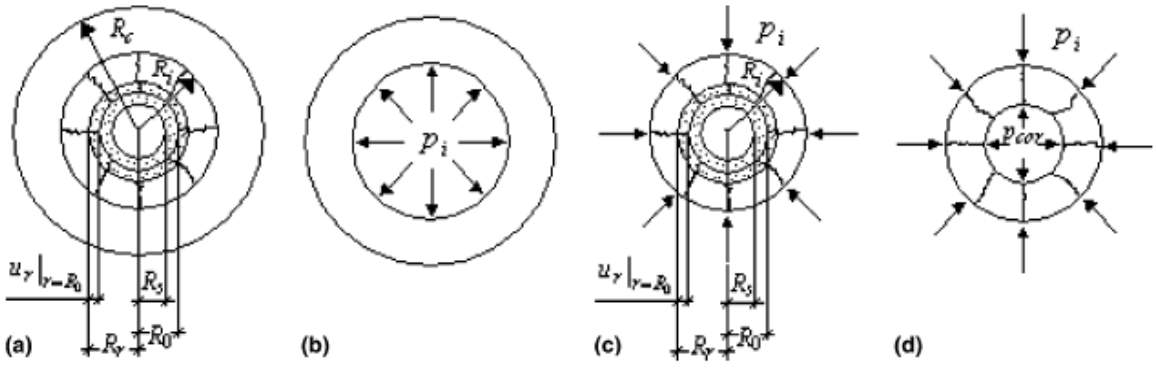

Fig. 3-13: Idealization of cover concrete as thick-walled cylinder: (a) geometry; (b) elastic outer part; (c) cracked inner part with radial displacement $u_r \mid_{r=R_0}$; (d) equivalence of (c). (Wang and Liu, 2006)

Wang and Liu (2006) calculated the corrosion pressure before corrosion cracking ($x \leq x_{cr}$) and after corrosion cracking ($x > x_{cr}$) respectively.

Before corrosion cracking, the thickness of the rust layer t_r was calculated by Wang and Liu (2006) as:

$$t_r = \frac{n(2R_0x - x^2) + x(R_i - R_0 + x)}{R_i + R_0} \tag{3-32}$$

The radial displacement $u_r \mid_{r=R_0}$ caused by corrosion expansion is then:

$$u_r \mid_{r=R_0} = R_r - R_0 = t_r - x = \frac{(n-1)(2R_0x - x^2)}{R_i + R_0} \tag{3-33}$$

The radial displacement was simply considered as elastic and is given as:

$$u(r) = \frac{f_t}{E_0} \cdot r \cdot \frac{(R_c/r)^2 + 1}{(R_c/R_i)^2 + 1} \tag{3-34}$$

where E_0 is the modulus of elasticity of concrete.

Set $r = R_0$ in Eq. (3-34) and equal it to Eq. (3-33) yields the corrosion depth x at certain cracking front R_i.

In order to calculate the corrosion pressure p_{cor}, an equilibrium condition along any radially cracked section was given by Wang and Liu (2006) as:

$$p_{cor} \cdot R_0 = p_i \cdot R_i + \int_{R_0}^{R_i} \sigma_\theta(r) dr \tag{3-35}$$

where

$$p_i = f_t \cdot \frac{R_c^2 - R_i^2}{R_c^2 + R_i^2} \tag{3-36}$$

When the hoop stress $\sigma_\theta(\mathrm{r})$ reaches the tensile strength of concrete f_t at the cracking front, the inner cracked cylinder is considered to perform a strain softening behaviour and the stress-strain relationship is illustrated in Fig. 3-14.

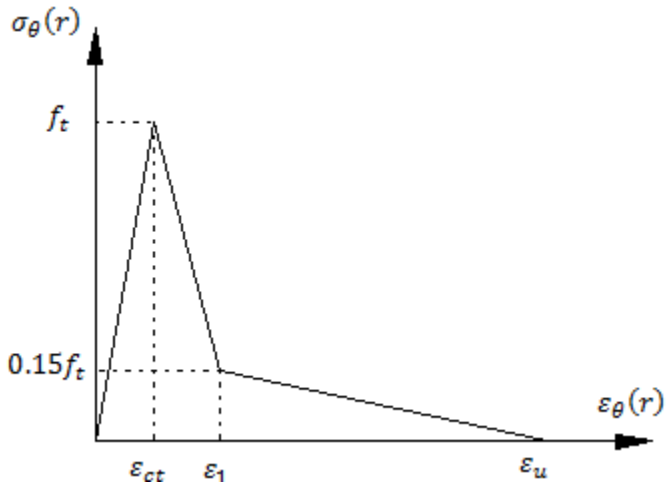

Fig. 3-14: Average stess-strain relationship of concrete in tension (Pantazopoulou and Papoulia, 2001)

The hoop strain at position r was given:

$$\varepsilon_\theta(r) = \frac{u_r}{r} = \frac{f_t}{E_0} \cdot \frac{(R_c/r)^2 + 1}{(R_c/R_i)^2 + 1} \tag{3-37}$$

The hoop stress was expressed for different hoop strains in Fig. 3-14 as:

$$\sigma_\theta(r) = \begin{cases} E_0 \cdot \varepsilon_\theta(r), & \varepsilon_\theta(r) \le \varepsilon_{ct} \\ f_t \cdot \left[1 - 0.85 \dfrac{\varepsilon_\theta(r) - \varepsilon_{ct}}{\varepsilon_1 - \varepsilon_{ct}}\right], & \varepsilon_{ct} < \varepsilon_\theta(r) \le \varepsilon_1 \\ 0.5 f_t \dfrac{\varepsilon_u - \varepsilon_\theta(r)}{\varepsilon_u - \varepsilon_1}, & \varepsilon_1 < \varepsilon_\theta(r) \le \varepsilon_u \end{cases} \tag{3-38}$$

After corrosion cracking, the calculation process is similar. The Equilibrium equation was formulated as:

$$p_{cor} \cdot R_0 = \int_{R_0}^{R_i} \sigma_\theta(r) dr \tag{3-39}$$

The hoop strain was expressed as:

$$\varepsilon_\theta(r) = \varepsilon_{\theta c} \cdot \frac{(R_c/r)^2 + 1}{2} \tag{3-40}$$

where $\varepsilon_{\theta c}$ is the average hoop strain at R_c .

The hoop stress can be determined by Eq. (3-38) and then corrosion pressure can be obtained by Eq. (3-39).

Wang and Liu (2006) used Fig. 3-15 to calculate the normal compressive pressure p_x and the friction pressure provided by the bond action of corroded ribbed bars in splitting failure. . In Fig. 3-15, the rib face angle $\varphi = 45°$; the core diameter $d_0 = 0.96d$, where

d is the nominal diameter of the non-corroded reinforcing bar; the rib spacing $l_r = 0.6d$. When the corrosion depth reaches$x$, the nominal diameter will be $d_x = d - 2x$. According to Xu (1990), the average rib height of noncorroded bar is 0.07d; the average rib height of the corroded bar in Fig. 3-15 (a) at corrosion level x can be taken as h_x = $0.07d_x$; α is the angle of face of crushed concrete, the average value of α is taken as α = 25^o; the concrete cover c_e is given in Eq. (22) by Wang and Liu (2006); p_x and $fp_x$are the normal compressive force and friction force on the bearing face; f is the friction coefficient of crushed concrete, and f = 0.6 according to Xu (1990); p_{crx} isthe average radial force and s_{crx} is the splitting bondanchorage strength.

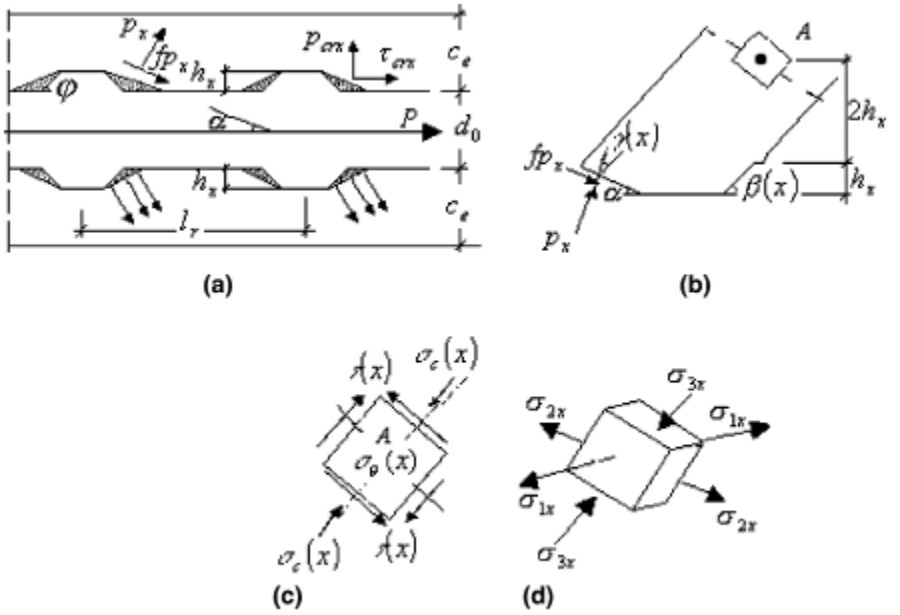

Fig. 3-15: (a) Geometry of a ribbed bar and the mechanical interaction between bar and concrete; (b) point A at the end of concrete key; (c) stresses of A; (d) principal stresses of A (Wang and Liu, 2006)

The splitting bond strength produced by p_x and fp_x was as:

$$\tau_{crx} = (sin\alpha + f \cdot cos\alpha) \cdot p_x \cdot \frac{\pi(d_0 + h_x)h_x}{\pi l_r d_x sin\alpha} \quad (3\text{-}41)$$

Considering the corrosion pressure p_{cor} prior to loading, the ultimate bond strength of corroded reinforcements was formulated by Wang and Liu (2006) as follows:

$$\tau_{ux} = \tau_{crx} + tan\alpha \cdot p_{cor} \quad (3\text{-}42)$$

The drawback of the model is that a same modulus of elasticity of cracked concrete as that of uncracked concrete is used, which overestimates the behaviour of cracked concrete.

3. Wang and Liu Flexure Model (2008)

Wang and Liu (2008) proposed an analytical model to calculate the flexural capacity of corroded RC beam. The development of this model is as following:

Wang and Liu (2008) took into consideration of properties of the corroded bar. The yield strength of corroded bar that was proposed by Lee et al. (1998):

$$f_{yx} = \begin{cases} \left(1 - \frac{1.24\Delta w}{100}\right) f_y, & uniform\ corrosion \\ \left(1 - \frac{1.98\Delta w}{100}\right) f_y, & pitting\ corrosion \end{cases} \quad (3\text{-}43)$$

where

f_y = yielding strength of noncorroded reinforcement;

Δw = the corrosion mass loss percentage (%).

And the elastic modulus of corroded reinforcement that was proposed by Lee et al.(1998):

$$E_{sx} = \begin{cases} \left(1 - \dfrac{0.75\Delta w}{100}\right) E_s, & uniform\ corrosion \\ \left(1 - \dfrac{1.13\Delta w}{100}\right) E_s, & pitting\ corrosion \end{cases} \quad (3\text{-}44)$$

where E_s is the modulus of elasticity of noncorroded reinforcement.

The bond strength for corroded reinforcement can be determined from the Wang and Liu (2006). The ultimate bond strength $\tau_u(0)$ of the uncorroded reinforcement is determined according to Xu (1990). The average bond strength $\bar{\tau}_u(0)$ of uncorroded reinforcement was assumed to be half of $\tau_u(0)$ (Kim & White, 1991).

A schematic drawing of RC beam for analysis is shown in Fig. 3-16.

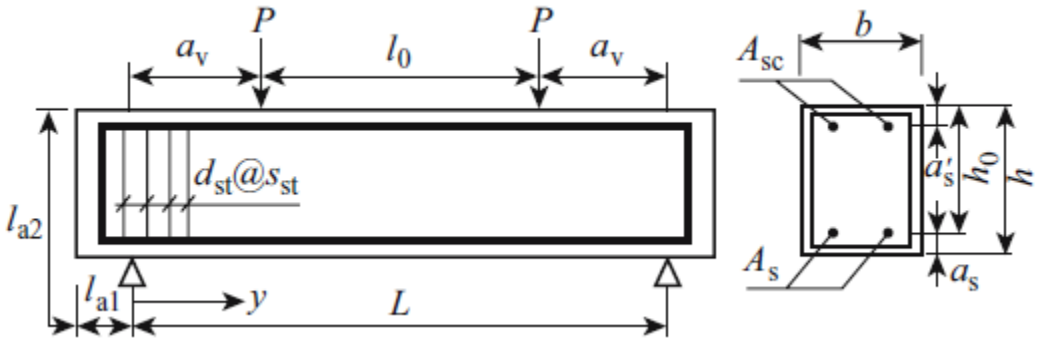

Fig. 3-16: A schematic drawing for RC beam (Wang & Liu, 2008)

If $\bar{\tau}_u(x) \geq \bar{\tau}_u(0)$, flexural capacity of corroded RC beam can be calculated by conventional RC models. If $\bar{\tau}_u(x) < \bar{\tau}_u(0)$, the assumed strain compatibility in code equations is no longer satisfied. Wang and Liu (2008) made use of condition of

equilibrium of forces and compatibility of the total deformations to develop a new compatibility equation, which is:

$$\varepsilon_{sx} = \left[\frac{\bar{\tau}_u(x)}{\bar{\tau}_u(0)} + \frac{l_0}{L} \cdot \frac{\bar{\tau}_u(0) - \bar{\tau}_u(x)}{\bar{\tau}_u(0)}\right] \varepsilon_{cx} \frac{h_{0x} - x_{cx}}{x_{cx}} \tag{3-45}$$

where

ε_{sx} = tensile strain of steel;

ε_{cx} = compressive strain of concrete in extreme fiber;

x_{cx} = depth of compression zone;

h_{0x} = effective depth of corroded RC beam;

l_0 = length of constant moment zone;

L = span of the beam.

The tensile strain of reinforcement ε_{sx} is determined by the relationship of $T_{sx} = \varepsilon_{sx} E_{sx} A_s$, T_{umax} and $f_{yx} A_s$, where T_{umax} is the tensile force can be provided by the corroded RC beam. The flexural carrying capacity M_{fx} can be obtained by simultaneously solving Eqs. (3-46) to (3-49), and considering the equilibrium of forces of the corroded RC beam (Wang and Liu, 2008).

$$F_{scx} = \frac{E_{scx}(x_{cx} - a'_{sx})}{x_{cx}} \cdot \varepsilon_{cx} A_{sc} \leq A_{sc} f_{ycx} \leq \bar{\tau}_u(x') n' \pi d'_{x'} l'_a \tag{3-46}$$

$$A_s \varepsilon_{sx} E_{sx} = f'_c b x_{cx} \left(\frac{\varepsilon_{cx}}{\varepsilon_0} - \frac{{\varepsilon_{cx}}^2}{3{\varepsilon_0}^2}\right) + F_{scx} \tag{3-47}$$

$$M_{fx} = f'_c b x_{cx} \left(\frac{\varepsilon_{cx}}{\varepsilon_0} - \frac{{\varepsilon_{cx}}^2}{3{\varepsilon_0}^2}\right) z_{0x} + F_{scx}(h_{0x} - a'_{sx}) \tag{3-48}$$

$$z_{0x} = h_{0x} - x_{cx}\frac{4\varepsilon_0 - \varepsilon_{cx}}{12\varepsilon_0 - 4\varepsilon_{cx}} \quad (3\text{-}49)$$

where

A_{sc} = the area of the compressive steel;

f_{ycx} = yield strength of corroded compressive reinforcing steel;

E_{scx} = modulus of elasticity of corroded compressive reinforcing steel;

$\bar{\tau}_u(x')$ = average ultimate bond strength of the compressive reinforcing steel at corrosion depth x';

n' = the number of compressive rebar;

$d'_{x'}$ = diameter of corroded compressive reinforcing bar;

l'_a = the anchorage length of compressive rebar;

z_{0x} = the lever arm between tensile force in reinforcement and compression force in concrete;

b = the width of the RC beam.

Fig. 3-17 shows a flow chart of the analytical procedure proposed by Wang and Liu (2008) for flexural carrying capacity.

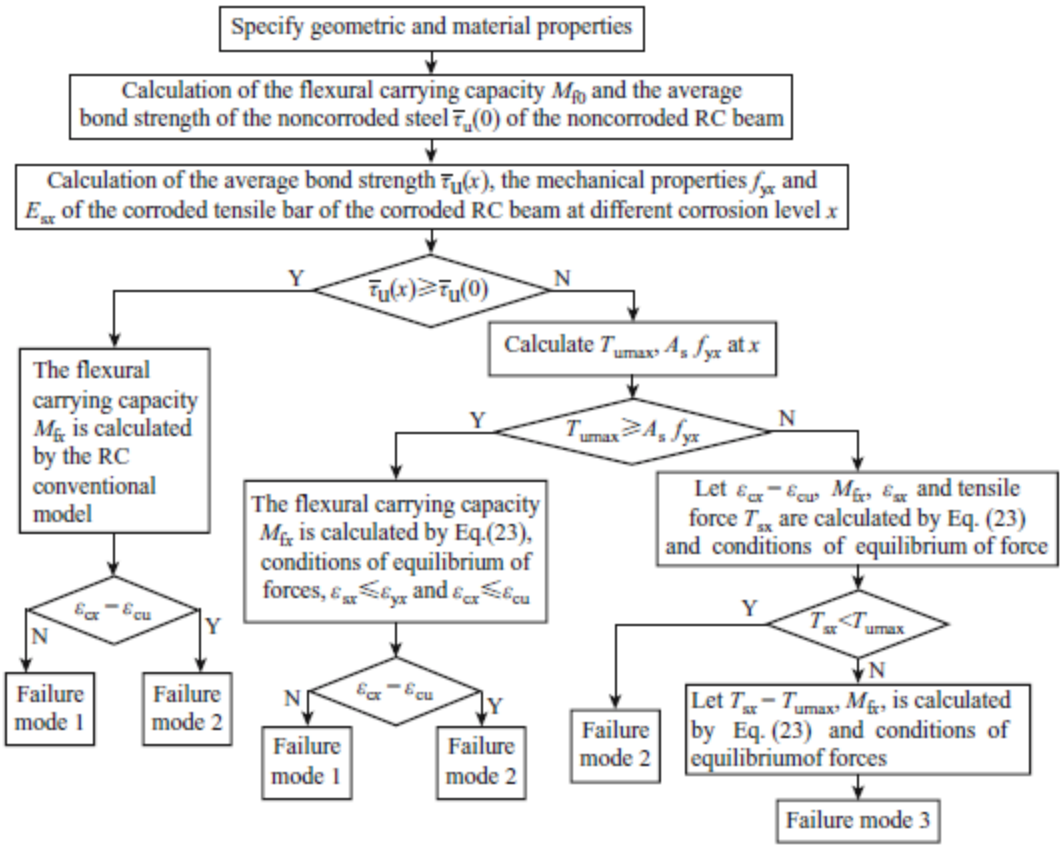

Fig. 3-17: Analytical procedure for flexural carrying capacity and failure mode of corroded RC beams (Wang and Liu, 2008)

4. Maaddawy et. al Flexure Model (2005)

Maaddawy et al (2005) studied the combined effect of corrosion and sustained loads on the structural performance of reinforced concrete beams. Test results showed that the presence of a sustained load and associated flexural cracks during corrosion exposure significantly reduced the time to corrosion cracking and slightly increased the corrosion crack width. The presence of flexural cracks during corrosion exposure initially increased the steel mass loss rate and, consequently, the reduction in the beam strength.

They also proposed an analytical model to predict the nonlinear flexural behavior of corroded RC beams. In the model, the deflection of a RC beam was calculated from the elongation of the rebar between concrete cracks rather than from curvatures of beam sections. A schematic drawing of the model is shown in Fig. 3-18.

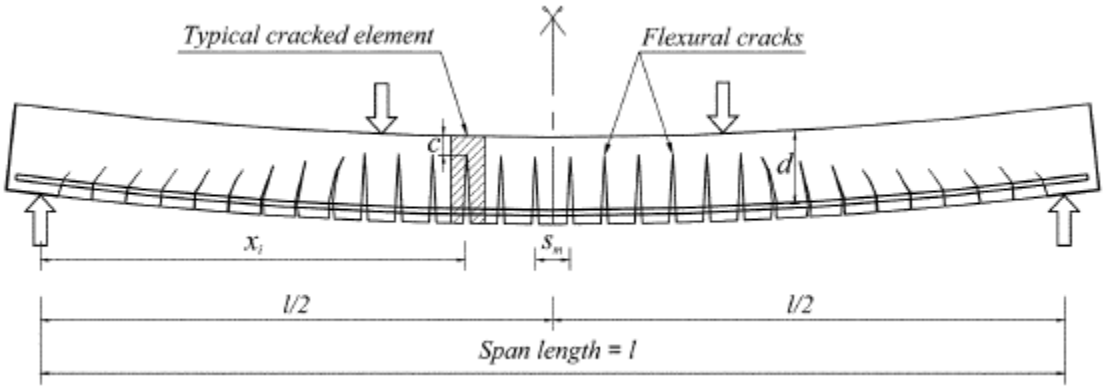

Fig. 3-18: Modeling of test specimens (Maaddawy et al., 2005)

The beam was modeled as a series of elements and was assumed to be subjected to a pure bending moment that is constant along the element length. Each element has a length equal to mean crack spacing. The element has a single crack at its middle point which initiates when the moment is larger than cracking moment. The maximum stress of steel locates at the middle of the element. The deflection of beam and the elongation of steel were calculated using this model by Maaddawy et al. (2005).

To calculate the flexural capacity of corroded and uncorroded beam, Maaddawy et. al (2005) considered both compatibility and equilibrium requirements. The strain and stress distribution and relationship is shown in Fig. 3-19 and Fig. 3-20.

The strain compatibility conditions are:

$$\varepsilon_s' = \frac{\varepsilon_c(c - d')}{c} \tag{3-50}$$

$$\varepsilon_s = \frac{\varepsilon_c(d - c)}{c} \tag{3-51}$$

$$\varepsilon_{ct} = \frac{\varepsilon_c(h - c)}{c} \tag{3-52}$$

where

ε_s = strain of tensile reinforcing bar;

ε_s' = strain of compressive reinforcing bar;

ε_c = strain of concrete at extreme compression fiber;

ε_{ct} = strain of concrete at extreme tension fiber;

c = depth of neutral axis measured from top face of beam;

d' = depth of compressive reinforcing bar measured from top face of beam;

d = depth of tensile reinforcing bar measured from top face of beam;

h = height of concrete cross section.

The stress block factors α_1 and β_1 for a parabolic stress-strain curve that were proposed by Collins and Mitchell (1987):

$$\alpha_1\beta_1 = \frac{\varepsilon_c}{\varepsilon_{c_0}} - \frac{1}{3}\left(\frac{\varepsilon_c}{\varepsilon_{c_0}}\right)^2 \tag{3-53}$$

$$\beta_1 = \frac{4 - \frac{\varepsilon_c}{\varepsilon_{c_0}}}{6 - 2\frac{\varepsilon_c}{\varepsilon_{c_0}}} \tag{3-54}$$

where ε_{c_0} is the concrete strain corresponding to concrete compressive strength.

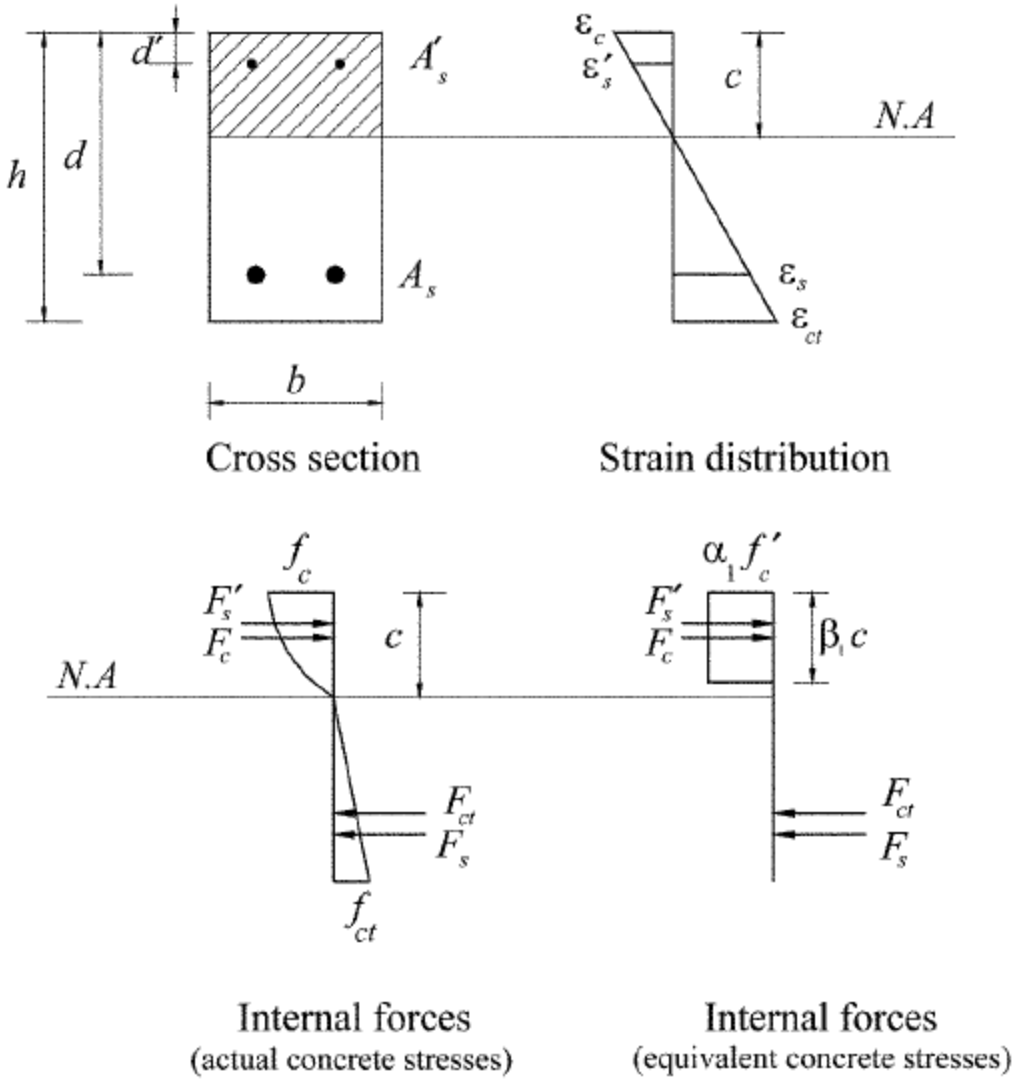

Fig. 3-19: Vertical strain and stress distribution at middle of uncracked element (Maaddawy et al., 2005)

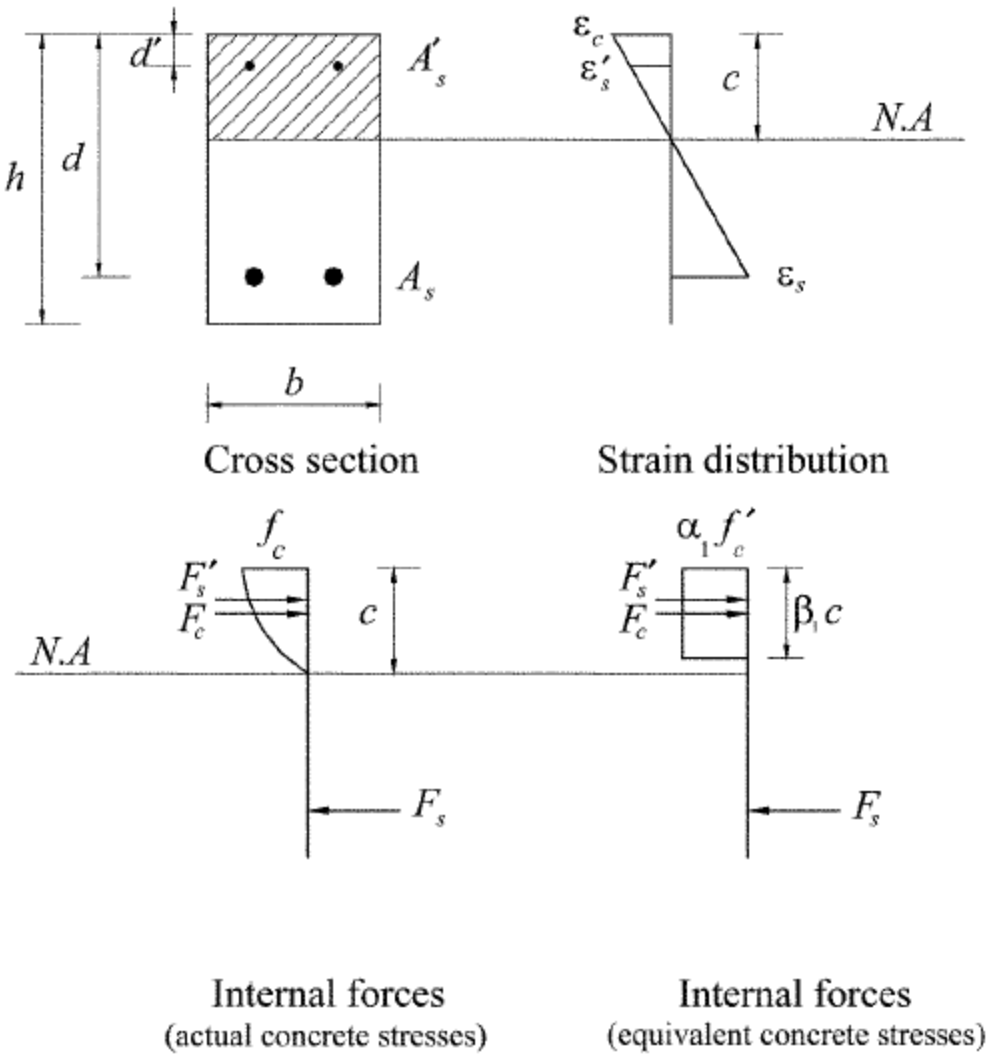

Fig. 3-20: Vertical strain and stress distribution at middle of cracked element (Maaddawy et al., 2005)

Equilibrium equations in the pre-yield stage were formulated by Maaddawy et al. (2005) as:

$$\alpha_1 f_c' \beta_1 cb + A_s' E_s \frac{\varepsilon_c (c - d')}{c}$$

$$-E_c b \frac{\varepsilon_c (h - c)^2}{2c} - A_s E_s \frac{\varepsilon_c (d - c)}{c} = 0 \qquad (3\text{-}55)$$

$$\alpha_1 f_c' \beta_1 cb\left(c - \frac{\beta_1 c}{2}\right) + A_s' E_s \frac{\varepsilon_c (c - d')^2}{c}$$

$$+E_c b \frac{\varepsilon_c (h - c)^3}{3c} + A_s E_s \frac{\varepsilon_c (d - c)^2}{c} = M_{ext} \quad (3\text{-}56)$$

and in the post-yield stage are:

$$\alpha_1 f_c' \beta_1 cb + A_s' E_s \frac{\varepsilon_c (c - d')}{c}$$

$$-A_s \left[f_y + E_{sp}\left(\frac{\varepsilon_c (d - c)}{c} - \frac{f_y}{E_s}\right)\right] = 0 \quad (3\text{-}57)$$

$$\alpha_1 f_c' \beta_1 cb\left(c - \frac{\beta_1 c}{2}\right) + A_s' E_s \frac{\varepsilon_c (c - d')^2}{c}$$

$$+A_s (d - c)\left[f_y + E_{sp}\left(\frac{\varepsilon_c (d - c)}{c} - \frac{f_y}{E_s}\right)\right] = M_{ext} \quad (3\text{-}58)$$

where M_{ext} is the external moment.

The drawback of this model is that no analytical analysis is done to account the effect of corrosion for bond degradation.

Chapter 4

ANALYTICAL MODEL OF BOND DEGRADATION

Considerable experimental, numerical and analytical research was undertaken to study the basics of force transfer at the steel rebar-concrete interface, the associated bond stress-slip, and other force–displacement relationships within corroded reinforced concrete members.

A model proposed by Cairns et al. (1996) for splitting bond failure and later modified by several researchers first by Coronelli (2002) to consider the corroded bars, then by Bhargava et al. (2006) with their contributions toward the estimation of various parameters associated with the bond strength evaluation of corroded bars at different corrosion levels, then lately was modified by Hussein (2011). Coronelli (2002) formulated the bond strength as follows:

$$\tau_{bu} = k(x)p^{max}(x) + \tau_b^0(x) + \mu(x)p_{corr}(x) \quad (4\text{-}1)$$

where

τ_{bu} = total bond strength;

x = corrosion depth (mm);

p^{max} = maximum confining pressure at bond failure, including confinement of concrete and stirrups;

τ_b^0 = adhesive bond strength contribution;

k = coefficient as a function of the rib properties and friction angle between steel and concrete;

μ = friction coefficient between steel and concrete;

p_{corr} = corrosion pressure.

However, it's very likely that the bond will not fail in splitting especially in heavy corrosion when the ribs are severely corroded and pull-out failure occurs. Hussein (2011) has modified the equation for corrosion pressure p_{corr} and assumed concrete as a thick-walled cylinder subjected to internal pressure, radial pressure produced by principal bar ribs on surrounding concrete, exerted from the growth of corrosion products on the concrete at the interface between the steel bar and the surrounding concrete. Therefore, it can be concluded that the bond stress at the steel-concrete interface is a function of contact pressure at the steel-concrete interface. Hussein (2011) bond strength model consists of the contribution of the confining pressure of cracked concrete, the corrosion pressure and the adhesion between corrode steel and cracked concrete:

$$\tau_{bu} = \mu(x) \cdot p_{conf}(x) + \mu(x) \cdot p_{corr}(x) + \tau_{AD}(x) \quad (4\text{-}2)$$

where

x = corrosion depth in mm;

τ_{bu} = total bond strength;

$\mu(x)$ = friction coefficient between steel and concrete;

$p_{conf}(x)$ = confining pressure by cracked concrete;

$p_{corr}(x)$ = corrosion pressure;

$\tau_{AD}(x)$ = bond strength contribution due to adhesion between corroded steel and cracked concrete.

However, this model doesn't include the contribution of the confinement of the stirrups, which is a very important factor affecting the bond strength between steel and concrete. Therefore, to include the contribution of stirrups, the present investigation proposes the following equation for calculating bond strength between corroded rebar and concrete:

$$\tau_{bu} = \mu(x) \times \left[p_{c,c}(x) + p_{c,st}(x) + p_{corr}(x)\right] \quad (4\text{-}3)$$

where

$p_{c,c}(x)$ = the confinement by concrete;

$p_{c,st}(x)$ = the confinement by stirrups.

4.1 Friction Coefficient

Influence of corrosion on interfacial friction was taken into account in a number of analytical models, e.g. Coronelli (2002), Amleh and Ghosh (2006), and Bhargava et al. (2006). Friction is incorporated into existing numerical models only implicitly as a part of interfacial resistance (Val, 2011).

In this model, the friction coefficient $\mu(x)$ that was suggested by Coronelli (2002) is used:

$$\mu(x) = 0.37 - 0.26(x - x_{cr}) \quad (4\text{-}4)$$

where

x_{cr} = corrosion depth associated with through concrete cracking.

4.2 Confining Pressure by Cracked Concrete

With the use of transverse reinforcement, the splitting cracks resistance and the confining pressure on bars increases. Hence, to consider the effect of stirrups, the confining stress produced by stirrups is added. The confining pressure by cracked concrete and stirrups can be calculated based on the model proposed by Giuriani et al. (1991).

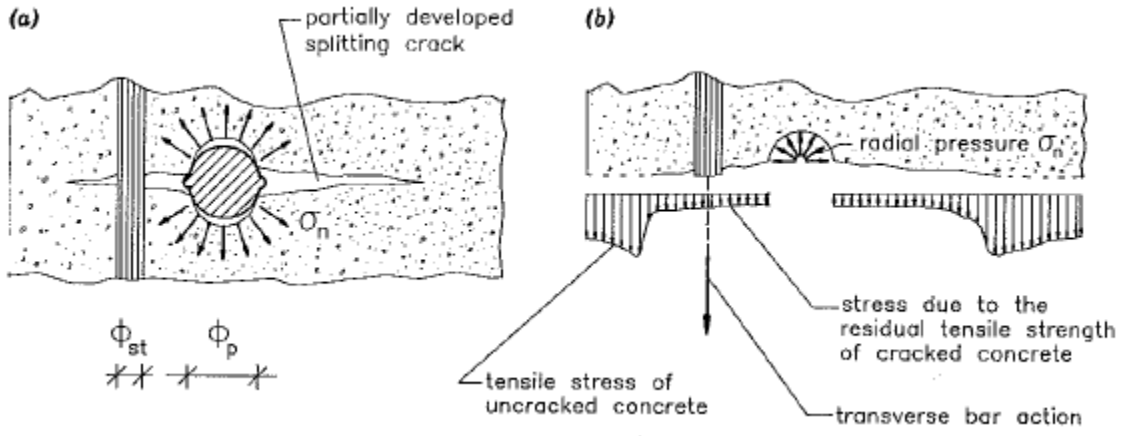

Fig. 4-1: Splitting crack and confining actions around ribbed bar

(Giuriani et al., 1991)

With splitting cracks, the bond stress becomes sensitive to confinement of reinforcing bar. This confining action could be provided by the residual stresses transmitted between the faces of the cracked concrete and by transverse reinforcement distributed along the main bar as illustrated in Fig. 4-1. As shown in Fig. 4-1, the radial pressure σ_n is equilibrated by the stress due to the residual tensile strength of cracked concrete, tensile stress of uncracked concrete, and the tensile force by the stirrups.

The confining pressure by cracked concrete was formulated by Giuriani et al. (1991) as:

$$p_{c,c} = \frac{(b - n_p \Phi_p)\Delta z}{A_p^*} \sigma_{rc} \tag{4-5}$$

where

b = the width of the member;

n_p = number of longitudinal reinforcing steel (principle bar);

Φ_p = diameter of principle bar;

Δz = stirrups spacing;

A_p^* = area of principle bar in the splitting plane (Fig. 4-2);

σ_{rc} = residual tensile strength of cracked concrete.

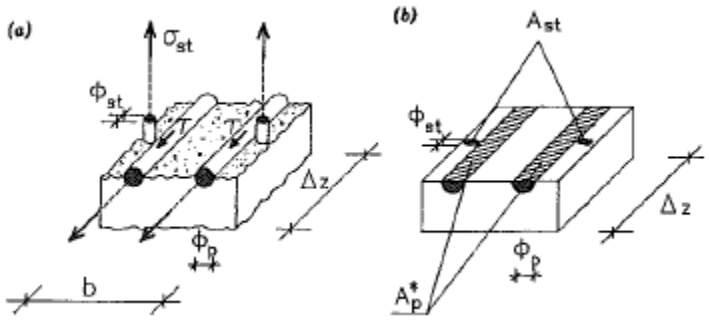

Fig. 4-2: Geometrical parameters of principal and transverse bars

The residual tensile strength of cracked concrete σ_{rc} was suggested by Giuriani et al. (1991) as:

$$\sigma_{rc} = \frac{f_{ct0}}{\kappa \frac{\Phi_p}{\Phi_a} \frac{w}{\Phi_p} + 1} \tag{4-6}$$

where

f_{ct0} = tensile strength when concrete begin to crack (w=0);

κ = coefficient experimentally determined;

Φ_a = maximum size of aggregate;

w = crack opening;

The value of f_{ct0} and κ can be taken from Fig. 4-3.

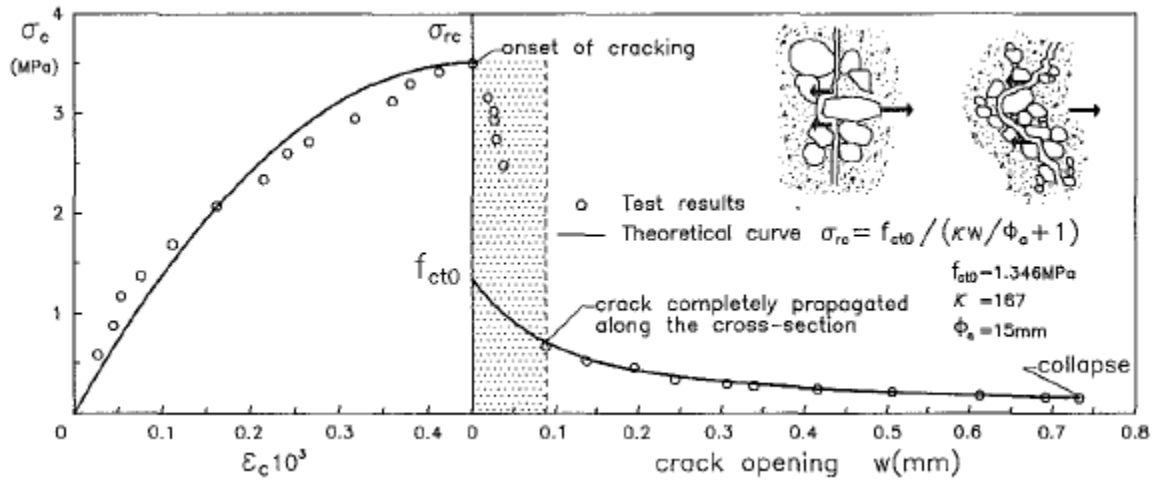

Fig. 4-3: Residual tensile stress of cracked concrete at increasing crack opening

The crack width can be calculated based on the model proposed by Molina et al. (1993):

$$\Sigma \frac{w_i}{x} = 2\pi\left(\nu_{r/s} - 1\right) \tag{4-7}$$

where

$\nu_{r/s}$ = ν_r / ν_s , which is the ratio between specific volumes of rust and steel.

As suggested by Molina et. al (1993), there are normally three principle cracks developed, thus

$$\sum_1^3 \frac{w_i}{x} = 2\pi\left(v_{r/s} - 1\right) \tag{4-8}$$

Therefore, the average crack width can be taken as:

$$w = \frac{2\pi\left(v_{r/s} - 1\right)x}{3} \tag{4-9}$$

4.3 Confining Pressure by Stirrups

The confining pressure contributed by stirrups that was suggested by Giuriani et al. (1991) is used:

$$p_{c,st} = \frac{A_{st}^*}{A_p^*}\sigma_{st} \tag{4-10}$$

where

A_{st}^* = global cross-section area shown in Fig. 4-2;

σ_{st} = stress in stirrups.

The stress in stirrups was proposed by Giuriani et al. (1991) as:

$$\sigma_{st} = E_s\sqrt{\frac{a_2}{\left(\alpha\frac{\Phi_{st}}{\Phi_p}\right)^2}\left(\frac{w}{\Phi_p}\right)^2 + \frac{a_1}{\alpha\frac{\Phi_{st}}{\Phi_p}}\frac{w}{\Phi_p} + a_0} \tag{4-11}$$

where

E_s = modulus of elasticity of steel;

Φ_{st} = diameter of stirrups;

α = coefficient experimentally determined regarding stirrups geometry;

a_0, a_1 , and a_2 are coefficient related to the ideal trilateral local bond-slip law of the stirrups (Fig. 4-4) and were formulated by Giuriani et al. (1991) as:

$$a_0 = \frac{a_1^2 \frac{T_{12}}{T_{11}}}{4a_2\left(\frac{T_{12}}{T_{11}} - 1\right)} \tag{4-12}$$

$$a_1 = \frac{8T_{02}}{E_s} \tag{4-13}$$

$$a_2 = \frac{4T_{12}\Phi_{st}}{E_s} \tag{4-14}$$

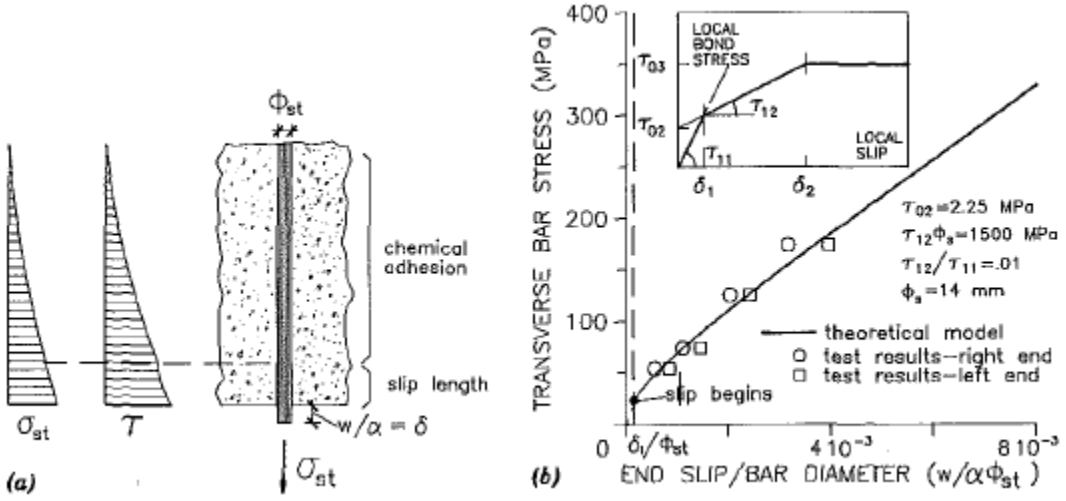

Fig. 4-4: Transverse-bar response at increasing crack opening

It should be noted that the bond contribution by stirrups has an upper limit. The maximum value of the bond force contributed by stirrups that was suggested by ACI Committee 408 (2003) is used:

$$T_s = K_1 t_r t_d \frac{NA_{tr}}{n} f_c'^p \quad (4\text{-}15)$$

where

K_1 = a constant, taken as 31.14;

t_r = a factor that depends on the relative rib area R_r of the reinforcement;

t_d = a factor that depends on the diameter d_b of the developed or spliced bar;

N = the number of transverse stirrups, or ties, within the development or splice length;

A_{tr} = area of each stirrup or tie crossing the potential plane of splitting adjacent to the reinforcement being developed or spliced;

n = number of bars being developed along the plane of splitting;

f_c' = concrete compressive strength;

p = a constant taken as 0.5.

The values of t_r and t_d were represented as linear functions of relative rib area R_r and bar diameter d_b, respectively by Zuo and Darwin (1998, 2000) as:

$$t_r = 9.6R_r + 0.28 \quad (4\text{-}16)$$

$$t_d = 0.78d_b + 0.22 \quad (4\text{-}17)$$

with d_b in inches and $R_r \leq 0.14$.

4.4 Corrosion Pressure

To calculate the corrosion pressure, a corrosion-cracking model must be proposed first. Thick-walled cylinder models have been used by many researchers such as Xu et al. (2007), Bhargava et al. (2006), Wang and Liu (2004) and can be demonstrated in Fig. 4-5. The concrete thick-walled cylinder subjected to internal pressure, radial pressure produced by principal bar ribs on surrounding concrete, exerted from the growth of corrosion products on the concrete at the interface between the steel bar and the surrounding concrete. The concrete in the inner cylinder is considered as an anisotropic material, while at the outer cylinder, the concrete is treated as isotropic material. A frictional model is used to combine the action of confining pressure resulted from radial pressure produced by principal bar ribs on surrounding concrete, and corrosion pressure resulted from the expansion of corrosion products.

In Fig. 4-5, R_i is the initial radius of reinforcing steel. As corrosion increases, the corrosion depth x increases. The corrosion products first occupy the space where steel is corroded then expand outside and form a rust layer of thickness t. The expansion pressure makes the surrounding concrete crack and reaches a radius R_c, which is the crack front. R_0 is the radius of concrete cover front.

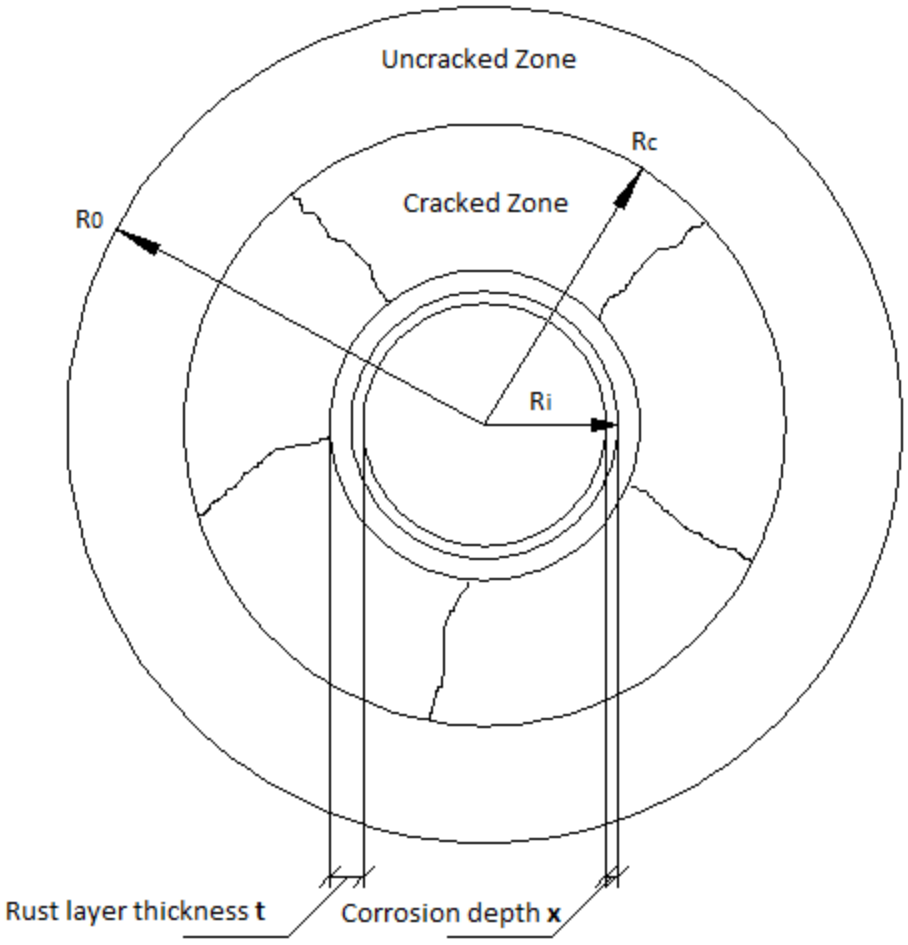

Fig. 4-5: Corrosion cracking model

4.4.1 Corrosion Pressure before Through Cracking

When cracks propagate and reach the outmost cover, it's called through cracking. Before through cracking, the hollow concrete cylinder is divided into an inner partially cracked zone and an outer uncracked zone, which was initially proposed by Tepfers (1979). The outer uncracked cylinder performs an isotropic linear elastic behaviour. However, the inner cracked concrete should be treated as tensile softening by a bi-linear stress-strain relationship as proposed in the CEB-FIP Model Code (CEB-FIP, 1993).

When the penetration depth reaches x, the radius of bar is reduced to $R_s = R_i - x$, and the reduced volume per unit length of bar is $\Delta V_s = \pi R_i^2 - \pi R_s^2 = \pi R_i^2 - \pi(R_i - x)^2 = \pi(2R_i x - x^2)$. Hence, the newly formed rust volume is:

$$\Delta V_r = \nu_{r/s} \Delta V_s = \nu_{r/s} \pi(2R_i x - x^2) \tag{4-18}$$

The ratio of rust volume to steel volume $\nu_{r/s}$ can be taken from 1.7-6.15 according to different corrosion products (Lundgren, 2002). In this research, the value of $\nu_{r/s}$ is taken as 3.

It should be noted that not all the corrosion products form the rust layer. In fact, some of the rust penetrates into the open cracks in cracked zone of the cylinder. The total crack width along the surface at $r = R_i$ that was formulated by Pantazopoulou and Papoulia (2001) is used:

$$\Sigma w = 2\pi R_i \times \varepsilon_{\theta,R_i} \tag{4-19}$$

with the hoop strain at $r = R_i$:

$$\varepsilon_{\theta,R_i} = \frac{u_{R_i}}{R_i} \tag{4-20}$$

where u_{R_i} is the radial displacement at $r = R_i$.

Substituting Eq. (4-20) to Eq. (4-19) yields the crack width:

$$\Sigma w = 2\pi u_{R_i} \tag{4-21}$$

As stated by Pantazopoulou and Papoulia (2001), the total space available within cracks can be approximated as $\Sigma w(R_c - R_r)/2$ with reference to the model in Fig. 4-6.

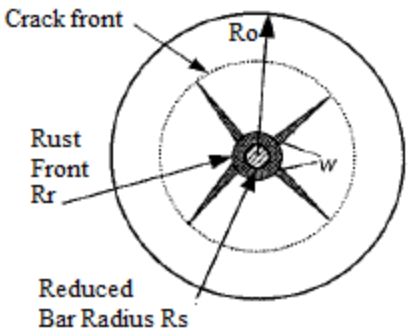

Fig. 4-6: Rust deposited within open cracks (Pantazopoulou and Papoulia, 2001)

Then the accumulated rust volume is consisted of two parts: the rust layer and the one penetrating into the cracks. Now by letting R_s to be the reduced radius of bar, and R_r to be the rust front, then

$$\Delta V_r = [\pi {R_r}^2 - \pi {R_s}^2] + \Sigma w(R_c - R_r)/2 \tag{4-22}$$

Substitute Eq. (4-21) into Eq. (4-22), and noticing that that $t = u_{R_i} + x, R_s = R_i - x$, and $R_r = R_i + u_{R_i}$, then Eq. (4-22) becomes:

$$\Delta V_r = \pi u_{R_i}(R_c + R_i) + \pi x(2R_i - x) \tag{4-23}$$

Equating Eq. (4-23) into Eq.(4-18), and solving u yields:

$$u_{R_i} = \frac{x\left(v_{r/s} - 1\right)(2R_i - x)}{R_c + R_i} \tag{4-24}$$

Similar derivation of the radial displacement that considers the volume expansion was also done by other researchers, such as Wang and Liu (2006), Pantazopoulou and Papoulia (2001), and Xu et al. (2007).

The uncracked concrete ($R_c < r \leq R_0$) behaves as isotropic linearly elastic material. Fig. 4-7 shows the pressure within uncracked cylinder.

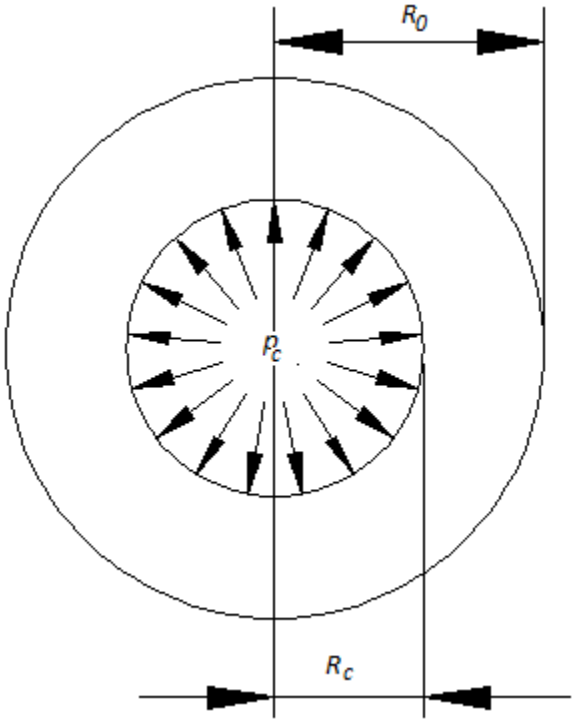

Fig. 4-7: Free-body diagram of uncracked cylinder

The problem of a hollow cylinder suffered from inner and outer constant pressure was solved by Xu et al. (2002) as a plain stress problem. The radial and hoop stress and the radial displacement that were expressed by Xu et al. (2002) are used in this investigation:

$$\sigma_r = \frac{A}{r^2} + 2C \tag{4-25}$$

$$\sigma_\theta(r) = -\frac{A}{r^2} + 2C \tag{4-26}$$

$$u_r = \frac{1}{E_0}\left[-(1+\nu)\frac{A}{r} + 2(1-\nu)rC\right] \tag{4-27}$$

where ν is the poison's ratio; A and C are constants to be determined by boundary conditions; E_0 is the initial modulus of elasticity of concrete.

By applying the boundary conditions, i.e. when $r = R_o$, σ_r = 0; when $r = R_c$, $\sigma_\theta(r) = f_t$, the constants A and C are solved as:

$$A = -f_t \frac{R_0^2}{\left(\frac{R_0}{R_c}\right)^2 + 1} ; C = \frac{f_t}{2} \frac{1}{\left(\frac{R_0}{R_c}\right)^2 + 1} \tag{4-28}$$

The radial and hoop stress and radial displacement then becomes:

$$\sigma_r(r) = f_t \frac{1 - \left(\frac{R_0}{\mathrm{r}}\right)^2}{1 + \left(\frac{R_0}{R_c}\right)^2} \tag{4-29}$$

$$\sigma_\theta(r) = f_t \frac{1 + \left(\frac{R_0}{\mathrm{r}}\right)^2}{1 + \left(\frac{R_0}{R_c}\right)^2} \tag{4-30}$$

$$u_r = \frac{f_t}{E_0} \frac{1}{\left(\frac{R_0}{R_c}\right)^2 + 1} \left[(1+\nu) \frac{R_0^2}{r} + (1-\nu)\mathrm{r} \right] \tag{4-31}$$

It should be noted that the value of radial stress is negative because it is in compression.

The inner partially crack concrete should be treated as inhomogeneous orthotropic linearly elastic material, as suggested by Chernin et al. (2010), but solving the differential equation for the radial displacement u_r is not an easy work. To make it simple, it can be assumed that the radial displacement u_r follows the elastic distribution, which was proposed by Nielsen (2002), in Eq. (4-27) within the range $R_i < r \leq R_c$. Thus

setting $r = R_i$ in Eq. (4-31) yields the radial displacement of concrete contacting with the bar:

$$u_{R_i} = \frac{f_t}{E_0} \frac{1}{\left(\frac{R_0}{R_c}\right)^2 + 1} \left[(1+\nu) \frac{R_0^2}{R_i} + (1-\nu) R_i \right] \tag{4-32}$$

Using the theory of elasticity, the strain-displacement relationship that was proposed by Chernin et al. (2010) is used in this investigation:

$$\varepsilon_r(\mathrm{r}) = \frac{du_r}{dr}; \quad \varepsilon_\theta(\mathrm{r}) = \frac{u_r}{r} \tag{4-33}$$

Substituting Eq. (4-33) into (4-31) yields the radial and hoop strain in partially cracked concrete:

$$\varepsilon_r(\mathrm{r}) = \frac{f_t}{E_0} \frac{1}{\left(\frac{R_0}{R_c}\right)^2 + 1} \left[(1-\nu) - (1+\nu) {R_0}^2 r^{-2} \right] \tag{4-34}$$

$$\varepsilon_\theta(\mathrm{r}) = \frac{f_t}{E_0} \frac{1}{\left(\frac{R_0}{R_c}\right)^2 + 1} \left[(1-\nu) + (1+\nu) {R_0}^2 r^{-2} \right] \tag{4-35}$$

To take into consideration that the hoop stiffness is different from the radial stiffness, based on theory of elasticity of orthotropic materials, the following constitutive relationship between stress and strain, which was proposed by Li et al. (2006), is used in this investigation:

$$\sigma_\theta(r) = \frac{E_\theta}{1 - \nu_1 \nu_2} [\varepsilon_\theta(r) + \nu_1 \varepsilon_r(r)] \tag{4-36}$$

where ν_1 and ν_2 is the Poison's ratio in the radial and tangential directions. For simplicity, it can be assumed that the Poision's ratio $\nu_1 = \nu_2 = \nu$. Then Eq. (4-36) can be rewritten as:

$$\sigma_\theta(r) = \frac{E_\theta}{1-\nu^2}[\varepsilon_\theta(r) + \nu\varepsilon_r(r)] \tag{4-37}$$

To calculate the hoop stiffness E_θ, Chernin et al. (2010) used their previous work (Val et al., 2009) in which a FE analysis was performed and the tension softening in the direction normal to a crack is based on the model proposed by Hillerborg et al. (1976), who adopted a stress-displacement curve from CEB-FIP model code (CEB-FIP, 1993). The hoop stiffness that was proposed by Chernin et al. (2010) is used:

$$E_\theta(r) = E_0\left(\frac{r}{R_c}\right)^n \tag{4-38}$$

with recommended value of n as:

$$n = \begin{cases} 1.5, & f_t \leq 3.07\ MPa \\ 0.081e^{0.95f_t}, & f_t > 3.07\ MPa \end{cases} \tag{4-39}$$

The normalised modulus of elasticity is shown in Fig. 4-8.

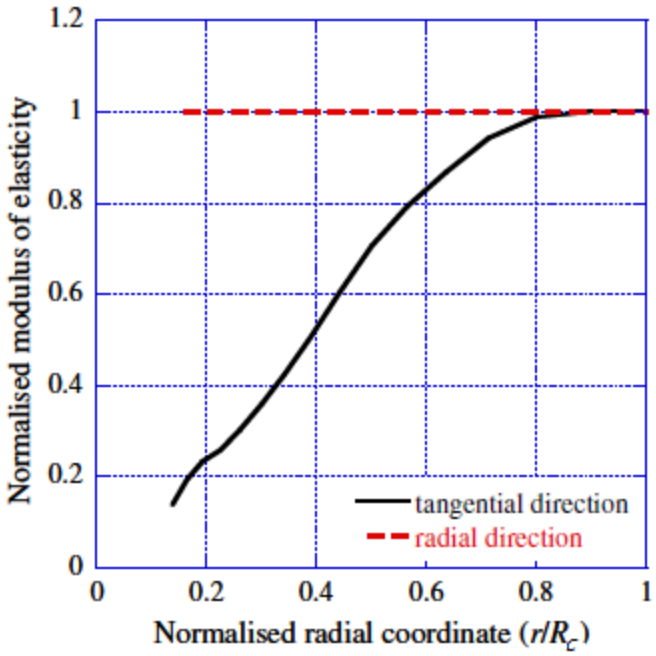

Fig. 4-8: Residual stiffness of partially cracked thick-walled concrete cylinder (FE analysis) (Cabrera & Ghoddoussi, 1992)

Assuming the crack front R_c to be between the initial bar radius R_i and the radius of the concrete front R_0 ($R_i < R_c \leq R_0$), and substituting Eqs. (4-34), (4-35), and (4-38) into Eq. (4-37) yields the hoop stress in partially cracked concrete:

$$\sigma_\theta(r) = \frac{f_t}{R_c^n} \cdot \frac{1}{\left(\frac{R_0}{R_c}\right)^2 + 1} (r^n + R_0^2 \cdot r^{n-2}) \tag{4-40}$$

The above Eq. (4-40) is the solution to the hoop stress in partially cracked concrete, based on the elastic mechanics, which also considers the stiffness reduction of cracked concrete in the hoop direction. To calculate the corrosion pressure p_{corr}, a free body diagram was drawn by Xu et al. (2007), but the they considered the hoop stress as a linear triangle distribution from f_t at the crack front to zero at the bar surface, which is

not the real case. An improved and more realistic free-body diagram is drawn in Fig. 4-9 in this research.

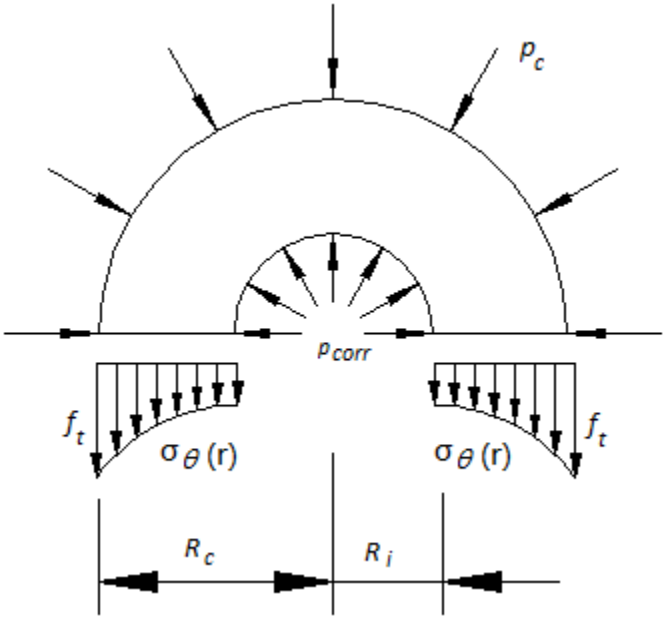

Fig. 4-9: Schematic fee-body diagram of inner cracked concrete

In Fig. 4-9, p_{corr} is the corrosion pressure on bar surface and p_c is the radial pressure on the crack front, which can be calculated from Eq. (4-29) by setting $r = R_c$:

$$p_c = f_t \frac{\left(\frac{R_0}{R_c}\right)^2 - 1}{\left(\frac{R_0}{R_c}\right)^2 + 1} \tag{4-41}$$

It should be noted that the hoop stress along the crack front and on the surface of the bar are not plotted, but they themselves are in equilibrium. The integration of the projection of corrosion pressure on half of the cutting side of the section is:

$$\int_0^{\pi/2} \cos\theta \, p_{corr} R_i d\theta = p_{corr} R_i \tag{4-42}$$

Similarly,

$$\int_0^{\pi/2} \cos\theta \, p_c R_c d\theta = p_c R_c \tag{4-43}$$

So the equilibrium gives the following equation

$$p_{corr} R_i = p_c R_c + \int_{R_i}^{R_c} \sigma_\theta(r) dr \tag{4-44}$$

Eq. (4-44) was also expressed in Wang and Liu (2006), but the they didn't explain how it was derived in details.

Substituting Eqs. (4-40) and (4-41) into Eq. (4-44) yields the corrosion pressure before through cracking:

$$p_{corr} = \frac{R_c}{R_i} \cdot f_t \frac{\left(\frac{R_0}{R_c}\right)^2 - 1}{\left(\frac{R_0}{R_c}\right)^2 + 1} + \frac{1}{R_i} \cdot \frac{f_t}{{R_c}^n} \frac{1}{\left(\frac{R_0}{R_c}\right)^2 + 1} \left(\frac{R_c^{n+1} - R_i^{n+1}}{n+1} + \frac{R_c^{n-1} - R_i^{n-1}}{n-1} \right) \tag{4-45}$$

The steps to calculate the corrosion pressure corresponding to corrosion depth x or ML(Mass Loss) before through cracking are summarized as follows:

1. Assume the crack front R_c in the range of $R_i < R_c \leq R_0$;

2. Calculate the value of n for the hoop stiffness $E_\theta(r)$ of cracked concrete using Eq. (4-39);

3. Calculate the corrosion pressure using Eq. (4-45), which was derived in this research;
4. Calculate the corresponding radial displacement u_{R_i} using Eq. (4-32);
5. Solve the corrosion depth x by Eq. (4-24) and the solution is given by the present author:

$$x = R_i - \sqrt{R_i^2 - \frac{(R_c + R_i)u_{R_i}}{(\nu_{r/s} - 1)}} \tag{4-46}$$

6. Calculate the corresponding ML (Mass Loss):

$$ML = \frac{R_i^2 - (R_i - x)^2}{R_i^2} \tag{4-47}$$

4.4.2 Corrosion Pressure after Through Cracking

The critical corrosion depth x_{cr} can be obtained by setting $R_c = R_0$ in Eq. (4-46). After through cracking, i.e., $> x_{cr}$, it should be noted that there has not been any research done to properly calculate the hoop stiffness E_θ after through cracking. However, the stress-strain relationship can be assumed as shown in Fig. 4-10. The hoop stress can be calculated by the method proposed by Wang and Liu (2006).

Since there is no outer uncracked concrete confining the cracked concrete, the equilibrium equation Eq. (4-44) becomes:

$$p_{corr} R_i = \int_{R_i}^{R_0} \sigma_\theta(r) dr \tag{4-48}$$

The stress-strain of cracked concrete in tension relationship that was proposed by Pantazopoulou and Papoulia (2001) is used:

$$\sigma_\theta(r) = \begin{cases} f_t \cdot \left[1 - 0.85 \cdot \dfrac{\varepsilon_\theta(r) - \varepsilon_{ct}}{\varepsilon_1 - \varepsilon_{ct}}\right], & \varepsilon_{ct} < \varepsilon_\theta(r) \le \varepsilon_1 \\ 0.15 f_t \dfrac{\varepsilon_u - \varepsilon_\theta(r)}{\varepsilon_u - \varepsilon_1}, & \varepsilon_1 < \varepsilon_\theta(r) \le \varepsilon_u \end{cases} \quad (4\text{-}49)$$

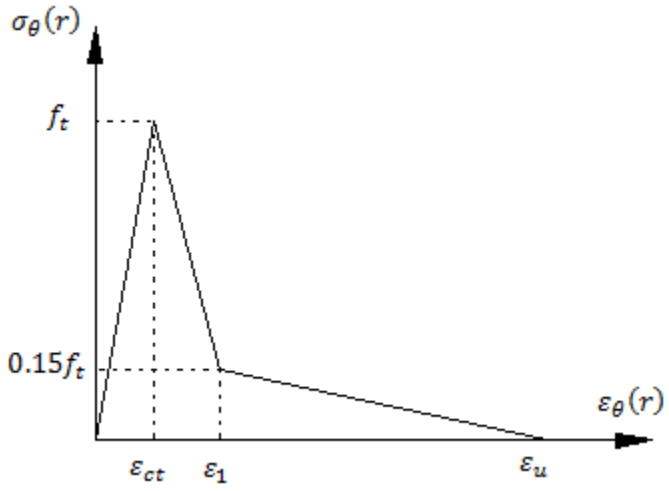

Fig. 4-10: Stress-strain relationship of concrete in tension

(Pantazopoulou & Papoulia, 2001)

The radial displacement at $r = R_i$ can be calculated using Eq. (4-24) by setting $R_c = R_0$:

$$u_{R_i} = \frac{x(\nu_{r/s} - 1)(2R_i - x)}{R_0 + R_i} \quad (4\text{-}50)$$

Set $R_c = R_0$, replace $\frac{f_t}{E_0}$ with $\varepsilon_{\theta 0}$, i.e., the hoop strain at $r = R_0$, and neglect Poison's effect, then Eq. (4-32) was formulated by Wang and Liu (2006) as:

$$u(r) = \varepsilon_{\theta 0} \cdot r \cdot \frac{1 + (R_0/r)^2}{2} \quad (4\text{-}51)$$

Then, the hoop strain at any location r was:

$$\varepsilon_\theta(r) = \frac{u(r)}{r} = \varepsilon_{\theta 0} \cdot \frac{1 + (R_0/r)^2}{2} \tag{4-52}$$

Equating $u(R_i)$ in Eq. (4-51) to Eq. (4-50) yields the unknown$\varepsilon_{\theta 0}$:

$$\varepsilon_{\theta 0} = 2x \cdot \frac{(\nu_{r/s} - 1)(2R_i - x)}{(\frac{R_0}{R_i} + 1)(\frac{R_0^2}{R_i^2} + 1)} \tag{4-53}$$

The steps to calculate the corrosion pressure after through cracking $x > x_{cr}$ are:

1. Assume the penetration depth x, and the corresponding *ML* is calculated using Eq.(4-47);

2. Calculate the hoop strain at $r = R_0$ "$\varepsilon_{\theta 0}$" using Eq. (4-53);

3. Calculate the hoop strain at any location, $\varepsilon_\theta(r)$ using Eq. (4-52);

4. Find out in which range the strain, ε_θ is in Fig. 4-10 and use the corresponding stress-strain relationship in Eq. (4-49) to calculate the stress $\sigma_\theta(r)$;

5. Substitute the stress $\sigma_\theta(r)$ into Eq. (4-48) and integrate r from R_i to R_0 to calculate the corrosion pressure.

The specific integration procedure and equations can be found in Wang and Liu's paper (Wang and Liu, 2006) except one error in Eq. (15c) in their paper and is corrected by the present author as:

$$I_c = \frac{0.15 f_t}{\varepsilon_u - \varepsilon_1}\left[\varepsilon_u(RR1 - RRu) - \frac{f_t}{E_0} \cdot \frac{1}{(R_c/R_i)^2} \cdot \left(\frac{R_c^2}{RRu} - \frac{R_c^2}{RR1} + RR1 - RRu\right)\right] \tag{4-54}$$

The model to calculate the corrosion pressure is mainly based on the model proposed by Wang and Liu (2006), modified by the present author by treating the inner cracked concrete cylinder as inhomogeneous orthotropic linearly elastic material, and the solution of the corrosion pressure before through cracking is given by the present author as in Eq. (4-45).

After calculating the confinement by concrete and stirrups, and the corrosion pressure, the bond strength between steel and concrete can be obtained using Eq. (4-3).

4.5 Comparison with Experimental Results and Discussion

The model developed to determine the bond stress at uncorroded and corroded steel-concrete interface is validated by analyzing and comparing the results obtained from the model versus experimental results done by other researchers.

4.5.1 Comparison with Al-Sulaimani's experiment

The bond model is used to calculate the results of pull-out tests conducted by Al-Sulaimani et al. (1990). As was mentioned earlier, the pull-out tests were conducted on 150 mm cubic concrete specimens with different reinforcing bar diameters (10 and 14 mm) embedded centrally. The average compressive strength of concrete is 30 MPa. The calculated results and the experiment results are shown in Fig. 4-11 and 4-12, in which τ_c is the bond contribution from concrete confinement, τ_{corr} is the bond contribution from corrosion pressure and τ_{bu} is the total ultimate strength of concrete.

The calculated results correspond well with the experimental results before about 50% bond loss but the bond strength is over-estimated after 50% bond loss. The reason is that the cracked concrete is assumed to be an elastic material, but the concrete has more plastic behaviour as cracking propagates so the concrete should deform more than expected and release more corrosion pressure, leading to lower bond strength.

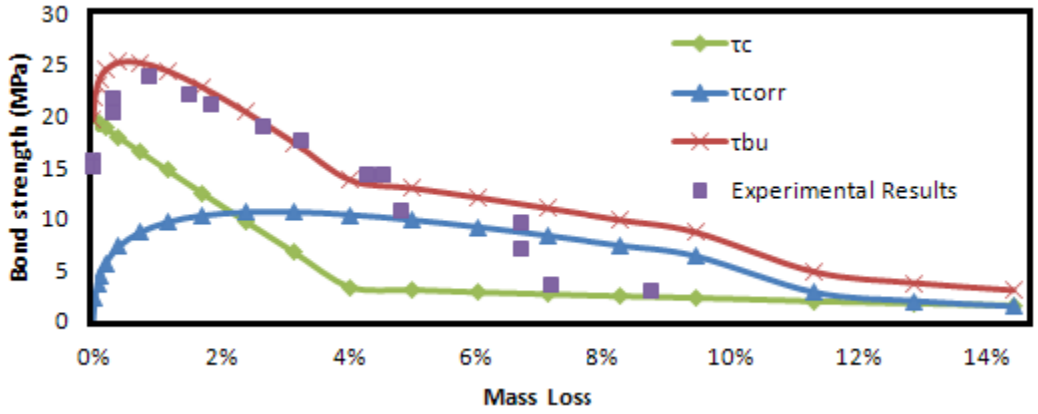

Fig. 4-11: Comparison with experimental results (10-mm bar) from Al-Sulaimani (1990)

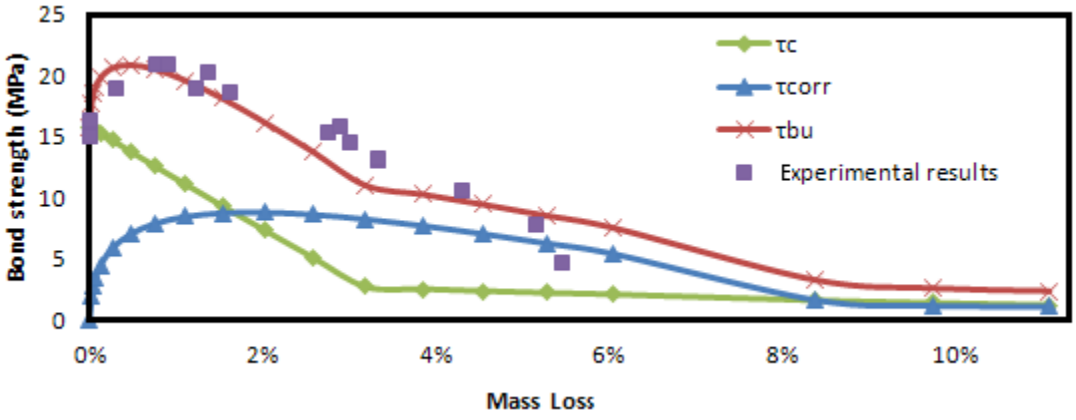

Fig. 4-12: Comparison of bond strength between analytical calculation and experimental results (14-mm bar) from Al-Sulaimani (1990)

4.5.2 Comparison with Zhao's experiment

The bond model is used to calculate the results of pull-out tests conducted by Zhao and Jin (2002). The pull-out test was conducted on 100-mm cubic concrete specimens with 12-mm-diameter rebar. The concrete has an average 28-day compressive strength of 22.13 MPa. The comparison of the calculated results using the developed model and experimental test results are shown in Fig. 4-13. The calculated results correspond well with the experimental results.

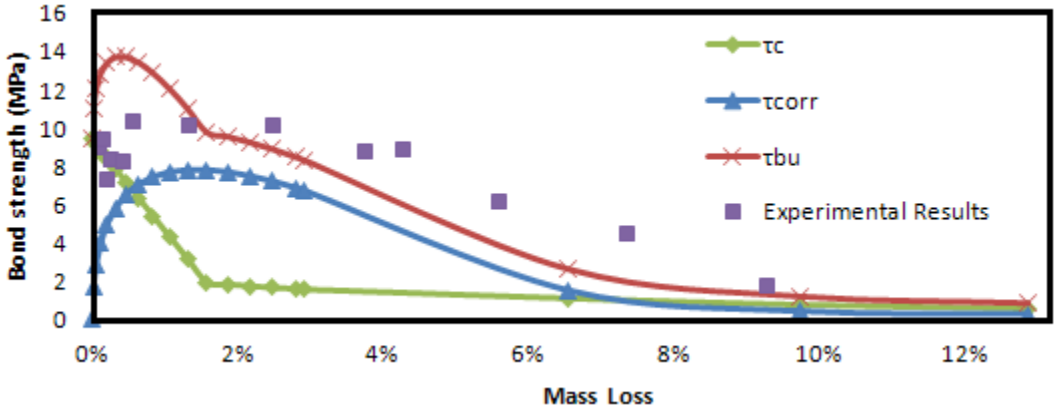

Fig. 4-13: Comparison of bond strength between analytical calculation and experimental results from Zhao and Jin (2002)

4.5.3 Comparison with Smith's experiment

The bond model is used to calculate the results of beam tests conducted by Smith (2007). The beam tests were conducted on 12 beams with two No. 15 tension reinforcing bars, two No. 10 top rebars and 6-mm stirrups at 40 mm in the shear zone. The beams are 1000 mm in span, and have a cross section of 156 mm in width and 176 mm in depth. The ultimate loads were converted to bond strength. The converted bond strength and the calculated results are shown in Fig. 4-14, in which τ_{st} is the bond

contribution from stirrups. It can be seen that the calculated results are close to the experimental results. The main contribution to bond strength is from the confinement of stirrups.

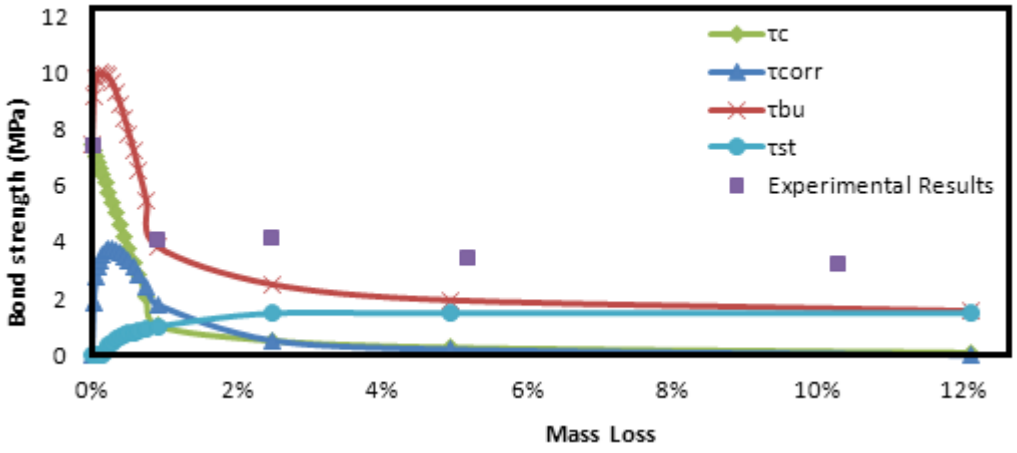

Fig. 4-14: Comparison of bond strength between analytical calculation and experimental results from Smith (2007)

4.5.4 Comparison with Joyce's experiment

The bond model is used to calculate the results of beam tests conducted by Joyce (2008). The beam tests were conducted on beams with two 15 M tension rebars, two 10 M top rebars and 10M stirrups at 40 mm. The beams have an 1100-mm-long span and have a cross section of 156 mm in width and 176 mm in depth. The 28-day compressive strength of concrete is 35 MPa. Ultimate load is converted to bond strength. Fig. 4-12 shows the comparison of bond strength between analytical calculation and the experimental results. The calculated results correspond well with the experimental results. Similar like Smith's results, the bond strength increases at the beginning and

then decreases as corrosion level increases. The main contribution of the bond strength after 5% is the confining pressure by stirrups.

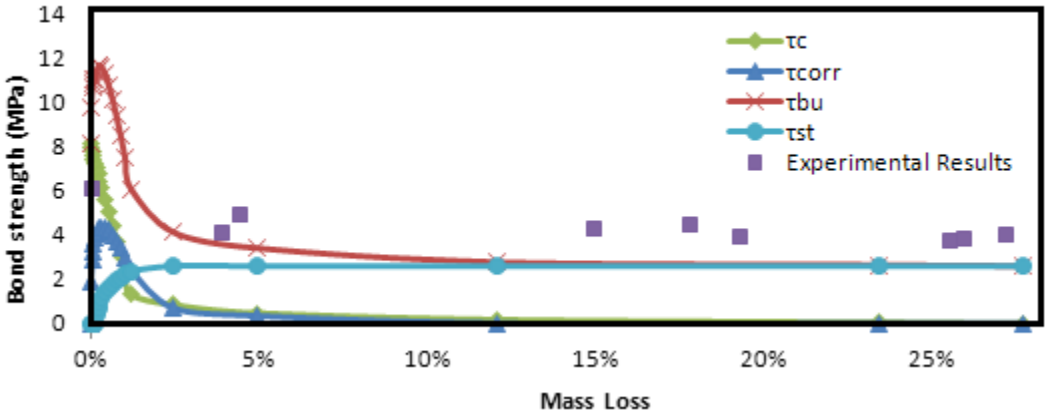

Fig. 4-15: Comparison of bond strength between analytical calculation and experimental results from Joyce (2008)

Chapter 5

RESIDUAL FLEXURAL CAPACITY OF CORRODED RC BEAMS

The flexural capacity of uncorroded RC beam can be calculated by traditional methods provided by concrete design books, in which both the strain compatibility and equilibrium must be satisfied. However, if reinforcement is corroded, bond degradation occurs and the tensile force in concrete will not be well transferred to reinforcement. The strain of steel may be less than the strain of concrete at the same level. In other words, strain compatibility condition cannot be met anymore. A new strain compatibility analysis must be developed to enable a realistic analysis of a corroded RC beams.

5.1 Strain Compatibility Analysis of a Corroded RC beam

As stated by Wang and Liu (2010), due to the loss of bond strength over regions of corroded bars, the compatibility condition of the perfectly bonded RC beam will shift to a new compatibility condition. Wang and Liu (2010) introduced an "interpolation" method to obtain the strain compatibility equation, which lies in between that of perfectly bonded and that of unbonded beam. They analyzed a partially corroded doubly reinforced RC beam. To illustrate the compatibility condition in a simpler way by this method, this investigation considers a whole length corrosion of a singly reinforced RC beam shown in Fig. 5-3.

For an uncorroded perfectly bonded beam, the strain distribution is shown in Fig. 5-1. To meet the geometric condition in Fig. 5-1 and assuming steel and concrete deform compatibly at one cross section, the strain of the tension reinforcing bars ε_s and the strain of compressive extreme fiber ε_c must satisfy the following equation:

$$\frac{\varepsilon_s}{\varepsilon_c} = \frac{d - c}{c} \tag{5-1}$$

where

d = effective depth of beam section;

c = depth of compression zone.

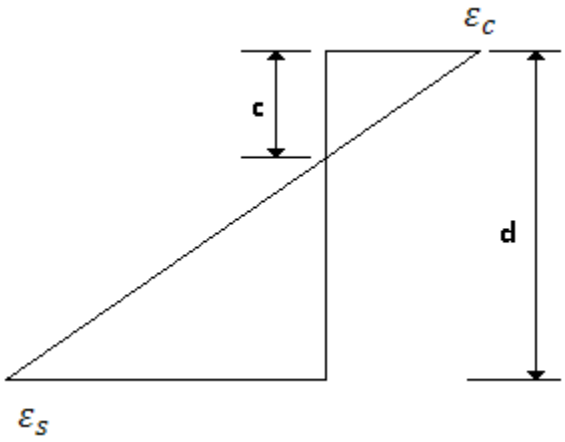

Fig. 5-1: Strains

For an unbonded beam with good anchorage at the end, the strain compatibility cannot be obtained by a cross section, because the reinforcement and the surrounding concrete at steel level on a cross section do not have the same amount of deformation. However, the conditions of equilibrium of forces and compatibility of deformations

must be satisfied, whether or not steel is bonded to the concrete (Cairns and Zhao, 1993). Wang and Liu (2010) gave the following deformation compatibility:

$$\int_0^l \varepsilon_s \, dl = \int_0^l \varepsilon_{cd} \, dl \tag{5-2}$$

The above equation means the elongation of the steel is equal to the total deformation of concrete at steel level. Thus, for an unbonded beam, the elongation of steel is:

$$\int_0^l \varepsilon_s \, dl = l \cdot \varepsilon_s^{ub} \tag{5-3}$$

where ε_s^{ub} is the strain of the tensile steel over the unbonded RC beam.

To determine the right side of Eq. (5-2), i.e. the total deformation of concrete at steel level, the concept of "equivalent plastic region length l_{eq}" proposed by Pannell (1969) was used by Wang and Liu (2010) to assume that the lengthening of the concrete at steel level was mainly due to the plastic deformations occurring within l_{eq}" in the vicinity of applied load.

The concept of equivalent plastic region length is illustrated in Fig. 5-2, in which the length L_0 means the equivalent plastic length l_{eq} in the present investigation. Au and Du (2004) carried out a detailed study and suggested the equivalent plastic length l_{eq} as:

$$l_{eq} = 9.3c \tag{5-4}$$

where c is the depth of compression zone.

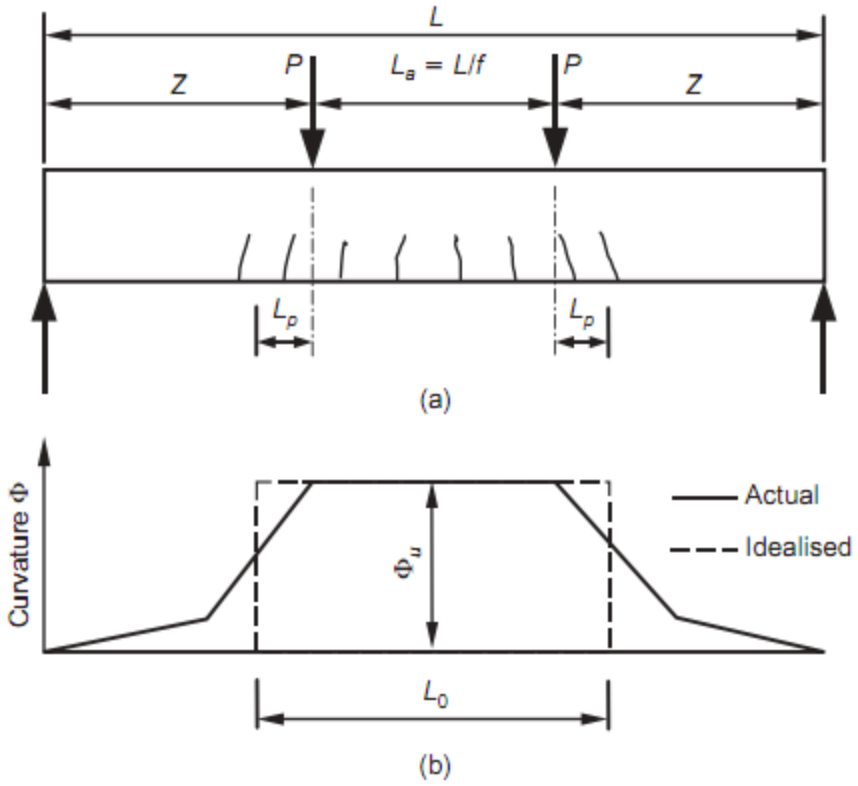

Fig. 5-2: A simply supported prestressed concrete beam with unbonded tendons under two symmetrically disposed point loads: (a) arrangement of loading; (b) actual and idealised curvature distribution along the beam (Au and Du, 2004)

For unbonded RC beam, steel and concrete at a section don't deform compatibly, but concrete itself still satisfy the assumption that a plain section remains plain after loading. Then according to the geometric condition in Fig. 5-1, the total deformation of concrete at steel level is:

$$\int_0^l \varepsilon_{cd}\, dl = l_{eq}\varepsilon_c \frac{d - c^{ub}}{c^{ub}} \tag{5-5}$$

where c^{ub} is the depth of compressive zone for an unbonded beam.

Eq. (5-5) is different from the original paper (Wang and Liu, 2010) in that the compressive extreme fiber strain ε_c is used in this investigation instead of ultimate compressive strain of concrete ε_{cu} because the compressive extreme fiber doesn't necessarily reach its limit for unbonded beam and for corroded beam at failure. Besides, the interpolation, which will be discussed later in this section, must be based on the actual strain of compressive extreme fiber, not the ultimate compressive strain of concrete.

The total deformation of concrete at steel level equating the elongation of steel, i.e. equating Eq. (5-3) to Eq. (5-5), yields:

$$\frac{\varepsilon_s^{ub}}{\varepsilon_c} = \frac{l_{eq}}{l} \cdot \frac{d - c^{ub}}{c^{ub}} \tag{5-6}$$

The ratio of steel strain to the strain of concrete at compressive extreme fiber for perfectly bonded and unbonded RC beam are expressed respectively in Eq. (5-1) and Eq. (5-6). Noticing the form of the two equations, and assuming that the strain compatibility of the corroded beam lies in between that of perfectly bonded and unbonded beam, Wang and Liu (2010) proposed a factor $\mathrm{g}(x)$ to account for the corrosion and the following relation was suggested:

$$\frac{\varepsilon_{sx}}{\varepsilon_{cx}} = \mathrm{g}(x) \cdot \frac{d - c_x}{\mathrm{c}_x} \tag{5-7}$$

where

ε_{sx} = strain of reinforcing bar at corrosion depth x;

ε_{cx} = strain of compressive extreme fiber at corrosion depth x;

c_x = depth of compression zone at corrosion depth x and the value of c_x can be calculated using Eq. (5-23) in section 5.2;

$g(x)$ = interpolating function of x.

To solve $g(x)$, Table 5-1 is developed by interpolating the function of x.

Table 5-1: Interpolation factor $g(x)$

Bond condition	Average bond strength	Interpolation factor
Perfectly bonded	$\tau_{bu}(0)$	1
Corroded	$\tau_{bu}(x)$	$g(x)$
Unbonded	0	$\frac{l_{eq}}{l}$

According to Table 5-1, linear interpolation yields the following equation:

$$\frac{g(x)-1}{\tau_{bu}(x)-\tau_{bu}(0)} = \frac{1-\frac{l_{eq}}{l}}{\tau_{bu}(0)-0} \tag{5-8}$$

The interpolation factor is solved as:

$$g(x) = 1-\left(1-\frac{\tau_{bu}(x)}{\tau_{bu}(0)}\right)\cdot\left(1-\frac{l_{eq}}{l}\right) \tag{5-9}$$

where

$\tau_{bu}(x)$ = bond strength at corrosion depth x;

$\tau_{bu}(0)$ = bond strength of perfectly bonded beam, or say at corrosion depth 0.

Substituting Eq. (5-9) and (5-4) into Eq. (5-7) yields the compatibility equation for RC beam at corrosion depth x:

$$\frac{\varepsilon_{sx}}{\varepsilon_{cx}} = 1 - \left(1 - \frac{\tau_{bu}(x)}{\tau_{bu}(0)}\right) \cdot \left(1 - \frac{9.3c_x}{l}\right) \cdot \frac{\mathrm{c}_x}{d - \mathrm{c}_x} \tag{5-10}$$

5.2 Flexural Capacity of Corroded RC Beams at Anchorage Failure

Various RC mechanics books provided the explanation of the developmental length, such as Macgregor and Wight (2009), which discusses the relationship between bond and moment capacity of RC beam. To illustrate the influence of bond on flexural capacity of a RC beam, a simply supported reinforced concrete beam is shown in Fig. 5-3. The flexural compressive force *C* is resisted by concrete and the flexural tensile force *T* is provided by reinforcement as shown in Fig. 5-4, while the forces acting on the reinforcement are shown in Fig. 5-5.

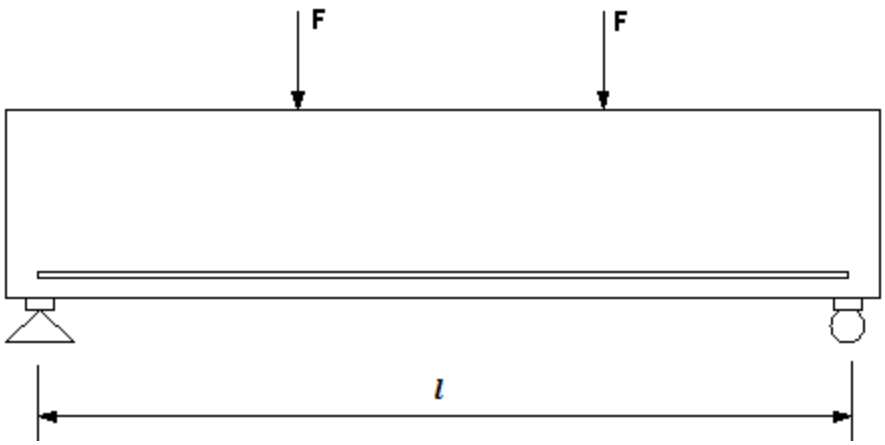

Fig. 5-3: Simply supported beam under 4-point load

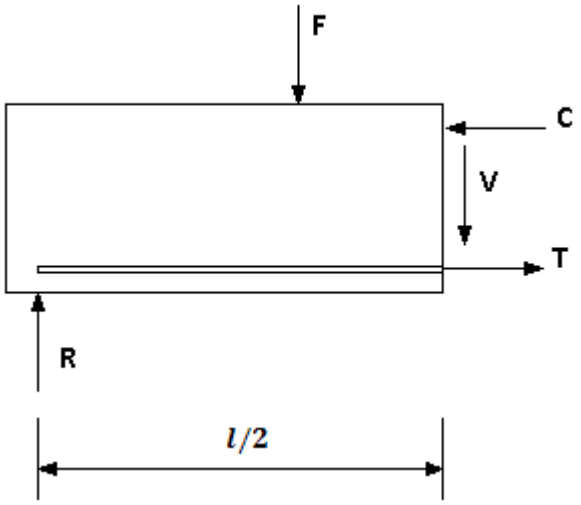

Fig. 5-4: Internal forces in the beam (Macgregor and Wight, 2009)

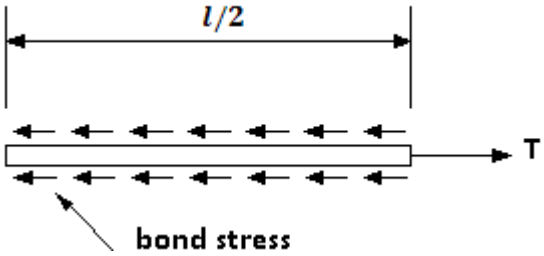

Fig. 5-5: Forces on reinforcement (Macgregor and Wight, 2009)

At flexural failure, the bond force on the surface of rebar should be in equilibrium with the ultimate tensile force of rebar:

$$\tau_{avg} \cdot \pi d_b \cdot \frac{l}{2} = T = f_y \cdot \frac{\pi {d_b}^2}{4} \tag{5-11}$$

The average bond stress on the reinforcing bar at flexural failure is:

$$\tau_{avg} = \frac{f_y \cdot d_b}{2l} \tag{5-12}$$

where

τ_{avg} = average bond stress;

f_y = yielding strength of reinforcing bar;

d_b = diameter of rebar;

l = total length of tensile rebar.

According to Fig. 5-6, the variation in steel stresses transferred from surrounding concrete follow the shape the moment diagram, so the average bond strength $\tau_{bu,avg}$ can be assumed to be:

$$\tau_{bu,avg} = \tau_{bu} \cdot \frac{l_b + \frac{l - l_b}{2}}{l} = \tau_{bu} \cdot \frac{l + l_b}{2l} \tag{5-13}$$

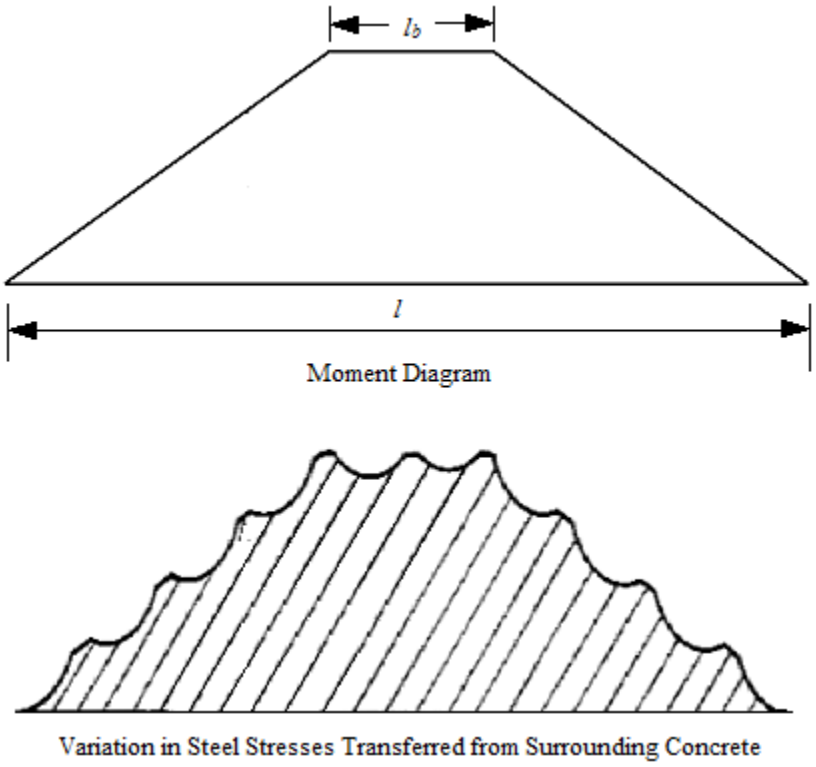

Fig. 5-6: Moment and variation in steel stresses transferred from surrounding concrete (Macgregor and Wight, 2009)

If the average bond strength at a certain corrosion level $\tau_{bu,avg} \geq \tau_{avg}$, then conventional method provided by design codes or design handbook, such as the Cement Association of Canada (2006) should be used to calculate the flexural capacity.

While $\tau_{bu,avg} < \tau_{avg}$, which means the tensile force cannot be fully transferred to reinforcement due to insufficient bond, then the tensile reinforcement can only provide the following flexural tensile force:

$$T = \tau_{bu,avg} \cdot \pi d_{bx} \cdot \frac{l}{2} \tag{5-14}$$

where

$\tau_{bu,avg}$ = average bond strength at corrosion depth x;

d_{bx} = diameter of rebar at corrosion depth x.

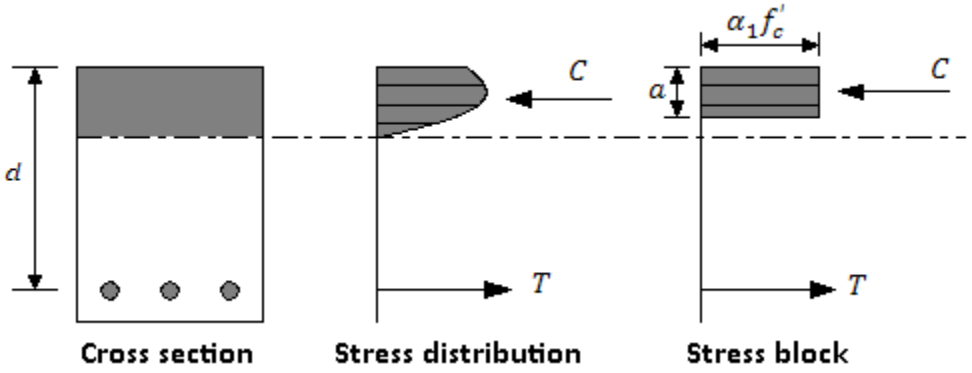

Fig. 5-7: Flexural analysis of a RC beam section

Consider a RC beam section in Fig. 5-7 to analyze the flexural capacity of the beam. Because corrosion doesn't affect the force equilibrium conditions and the concrete itself still abide by the assumption that "plain section remains plain after loading", so a similar flexural analysis can be done compared with that in the handbook (Cement Association of Canada, 2006). Yet, the compression strain of extreme fiber is calculated using the new compatibility condition illustrated in section 5.1.

The moment resistance is:

$$M_{rx} = T \cdot \left(d - \frac{a}{2}\right) \tag{5-15}$$

where

d = effective depth of beam section;

a = depth of the equivalent rectangular compressive zone.

The depth a can be determined from the equilibrium of internal forces:

$$C = T \tag{5-16}$$

where

C = compressive force provided by concrete:

$$C = \alpha_1 f_c^{'} ab \tag{5-17}$$

α_1 = the ratio of stress of compression stress block to the compressive strength of concrete which is determined by Cement Association of Canada (2006):

$$\alpha_1 = 0.85 - 0.0015 f_c^{'} \geq 0.67 \tag{5-18}$$

$f_c^{'}$ = compressive strength of concrete;

b = width of the beam cross section.

Solving Eqs. (5-14), (5-16) and (5-17) simultaneously yields the depth of the compressive stress block:

$$a = \frac{\tau_{bu,avg} \cdot \pi d_{bx} \cdot l}{2\alpha_1 f_c^{'} b} \tag{5-19}$$

Substituting Eq. (5-14) and (5-19) into Eq. (5-15) yields the ultimate flexural capacity:

$$M_{rx} = \tau_{bu,avg} \pi d_{bx} \frac{l}{2}\left(d - \frac{\tau_{bu,avg} \cdot \pi d_{bx} \cdot l}{2\alpha_1 f_c^{'} b}\right) \tag{5-20}$$

The value of steel strain and strain of compressive extreme fiber must be checked. Steel strain can be calculated as:

$$\varepsilon_{sx} = \frac{f_s}{E_s} = \frac{T}{A_{sx} E_s} \tag{5-21}$$

Using the ratio in Eq. (5-10), strain of compressive extreme fiber is expressed as:

$$\varepsilon_{cx} = \frac{\varepsilon_{sx}}{1 - \left(1 - \frac{\tau_{bu,avg}(x)}{\tau_{bu,avg}(0)}\right) \cdot \left(1 - \frac{9.3c_x}{l}\right) \cdot \frac{\mathrm{c}_x}{d - \mathrm{c}_x}} \tag{5-22}$$

and c_x is calculated using the following equation:

$$\mathrm{c}_x = \frac{a}{\beta_1} \tag{5-23}$$

where β_1 is the ratio of depth of stress block and the actual depth of compression zone, which is suggested in the design handbook (Cement Association of Canada, 2006) as:

$$\beta_1 = 0.97 - 0.0025 f_c' \tag{5-24}$$

It should be noted that if the strain of the principle reinforcing bar, $\varepsilon_{sx} > 0.002$, the tension rebar yields before anchorage failure occurs, then refer to section 5.3; and if $\varepsilon_{cx} > 0.0035$, which is the ultimate compressive strain of concrete, the compression concrete crushes before the yielding of the steel or anchorage failure, then refer to section 5.4.

5.3 Yielding Controlled Flexural Capacity of Corroded RC Beams

If $\varepsilon_{sx} > 0.002$, which means that the steel yields before anchorage failure occurs, because the cross-sectional area is seriously degraded by corrosion, or the bond strength is adequate enough for the stress transfer between the steel and concrete then the ultimate tensile force of the reinforcing bar is:

$$T = n \cdot f_y \cdot \frac{\pi d_{bx}^2}{4} \tag{5-25}$$

where n is the number of tensile rebars and f_y is the yielding strength of steel.

The compressive force provided by concrete is given in Eq. (5-17) and the equilibrium condition of the compressive and tensile forces is given in Eq. (5-16). Solving Eqs (5-16), (5-25) and (5-17) simultaneously yields the depth of stress block:

$$a = f_y \cdot \frac{\pi d_{bx}^2}{4\alpha_1 f_c' b} \tag{5-26}$$

The ultimate moment resistance is:

$$M_{rx} = T \cdot \left(d - \frac{a}{2}\right) \tag{5-27}$$

Substituting Eq. (5-25) and (5-26) into Eq. (5-27) yields the residual flexural capacity:

$$M_{rx} = n \cdot f_y \cdot \frac{\pi d_{bx}^2}{4}\left(d - f_y \cdot \frac{\pi d_{bx}^2}{8\alpha_1 f_c' b}\right) \tag{5-28}$$

5.4 Compression Controlled Flexural Capacity of Corroded RC Beams

If ε_{cx} as is calculated in section 5.2 is larger than the ultimate compressive strain of concrete, ε_{cu}, the concrete crushing failure controls the ultimate moment capacity. In this study, the value of ε_{cu} is taken as 0.0035 (Cement Association of Canada, 2006). The strain of steel is calculated using Eq. (5-10) by substituting ε_{cu} for ε_{cx} and is expressed as:

$$\varepsilon_{sx} = \varepsilon_{cu} \cdot \left[1 - \left(1 - \frac{\tau_{bu,avg}(x)}{\tau_{bu}(0)}\right) \cdot \left(1 - \frac{9.3c_x}{l}\right) \cdot \frac{d - c_x}{\mathrm{c}_x}\right] \tag{5-29}$$

The tensile force provided by steel is:

$$T = n \cdot \varepsilon_{sx} E_s \cdot \frac{\pi d_{bx}^2}{4} \tag{5-30}$$

The compressive force by concrete is given by Eq. (5-17). The force equilibrium condition is C=T as shown in Eq. (5-15). Solving Equations (5-16), (5-17), (5-23), (5-27) and (5-28) simultaneously yields the depth a of stress block.

$$a = \frac{n \cdot \varepsilon_{cu} \left[1 - \left(1 - \frac{\tau_{bu}(x)}{\tau_{bu}(0)} \right) \cdot \left(1 - \frac{9.3 \frac{a}{\beta_1}}{l} \right) \cdot \left(\frac{d - \frac{a}{\beta_1}}{\frac{a}{\beta_1}} \right) \right] \cdot E_s \cdot \frac{\pi d_{bx}^2}{4}}{(0.85 - 0.0015 f_c') \cdot f_c' \cdot b} \tag{5-31}$$

The general solution of the above quadratic equation is not made here because of the complexity of the expression. It's suggested to solve the equations with specific corrosion depths. Given a corrosion depth x, the ultimate bond strength at corrosion level x can be calculated using the proposed model in Chapter 4. Then the only unknown variation in Eq. (5-31) is the stress block depth a. Once a is solved, ε_{sx} and T are obtained using Eqs. (5-23), (5-29) and (5-30). The ultimate moment $M_{rx} = T\left(d - {}^{a}/_{2}\right)$ can then also be obtained.

5.5 Doubly Reinforced RC Beams

As stated in the concrete design handbook (Cement Association of Canada, 2006), the compression reinforcement usually yields when the section reaches its capacity. Even if it doesn't yield, it's very close to yielding. With this assumption, the beam can be divided into an imaginary beam and a coupling reinforcement shown in Fig. 5-8.

The ultimate moment capacity can be obtained by Cement Association of Canada (2006):

$$M_r = M_{r1} + M_{r2} \tag{5-32}$$

where M_{r1} and M_{r2} is the moment resistance provided by the imaginary beam and the coupling reinforcement shown in Fig. 5-8.

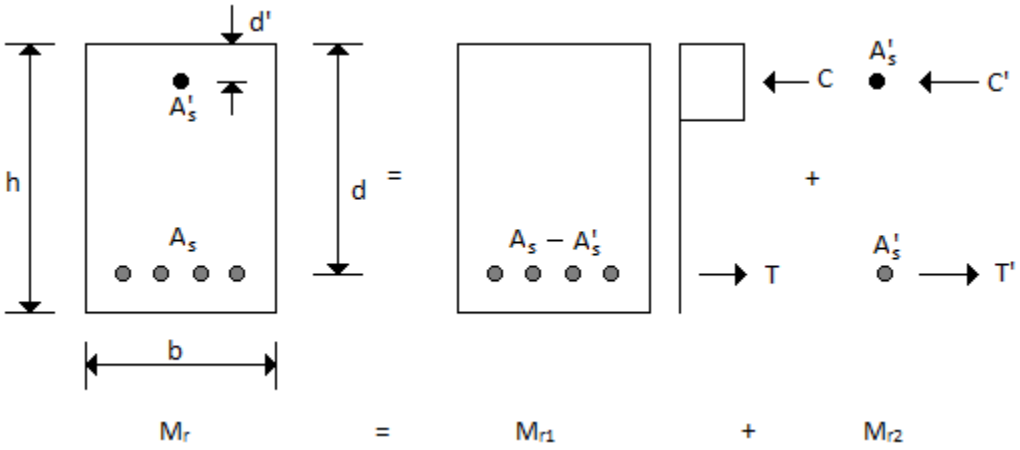

Fig. 5-8: Imaginary Beam Section for Doubly Reinforced Beam (Cement Association of Canada, 2006)

The calculation of M_{r1} is the same as is illustrated in section 5.2. M_{r2} is taken as:

$$M_{r2} = A'_s f_y (d - d') \tag{5-33}$$

However, if the reinforcement is highly corroded that the bond strength is not adequate for the concrete and tension reinforcing bars to fully work together ($\tau_{bu,avg} < \tau_{avg}$), the compression reinforcing bars are not likely to yield. Then the contribution of compression bar, which is actually decreasing a small amount of the value of the compression depth, a, can be ignored. Treating the beam as a singly reinforced beam will give a close and conservative value compared with assuming a doubly reinforced beam.

5.6 Flexural Capacity Calculation Steps

The following general steps are presented to illustrate how to calculate flexural carrying capacity of a corroded RC beam using the above proposed method:

1. Assume a balanced failure in which C = T, and calculate the average bond stress needed to prevent anchorage failure as in section 5.2. If the needed bond stress is smaller than the bond strength, concrete works well with steel and traditional methods in concrete design book can be used. If the needed bond stress is larger than bond strength, then the following steps should be taken.
2. First assume the beam suffers anchorage failure and calculate the stain of steel and concrete using the analysis in section 5.1 and 5.2. If the steel strain at extreme tension fiber $\varepsilon_{sx} \leq 0.002$, which is the strain when concrete reaches its tensile strength, anchorage failure may occur. Calculate the flexural capacity by the procedure in section 5.2.
3. If the steel strain at extreme tension fiber $\varepsilon_{sx} > 0.002$, the surrounding concrete reaches its tensile strength, and steel yields before anchorage failure, then refer to section 5.3 for yielding controlled beam.
4. If the concrete strain at extreme compression fiber ε_{cx} as is calculated in section 5.2 is larger than the ultimate compressive strain ε_{cu}, the beam is highly reinforced and reinforced beams fail in crushing the compression concrete. Section 5.4 should be referred to calculate the flexural capacity.

5.7 Comparison with Experimental Results and Discussion

5.7.1 Comparison with Smith's experiment

Beam tests were conducted on 12 beams with two No. 15 principle reinforcing bars, two No. 10 top reinforcements and 6-mm stirrups at 40 mm spacing in shear zone by Smith (2007). The beams are 1000 mm in span, and have a cross section of 156 mm in width and 176 mm in depth. The calculation is done in excel, following steps proposed in Section 5.6. The results are shown in Fig. 5-9.

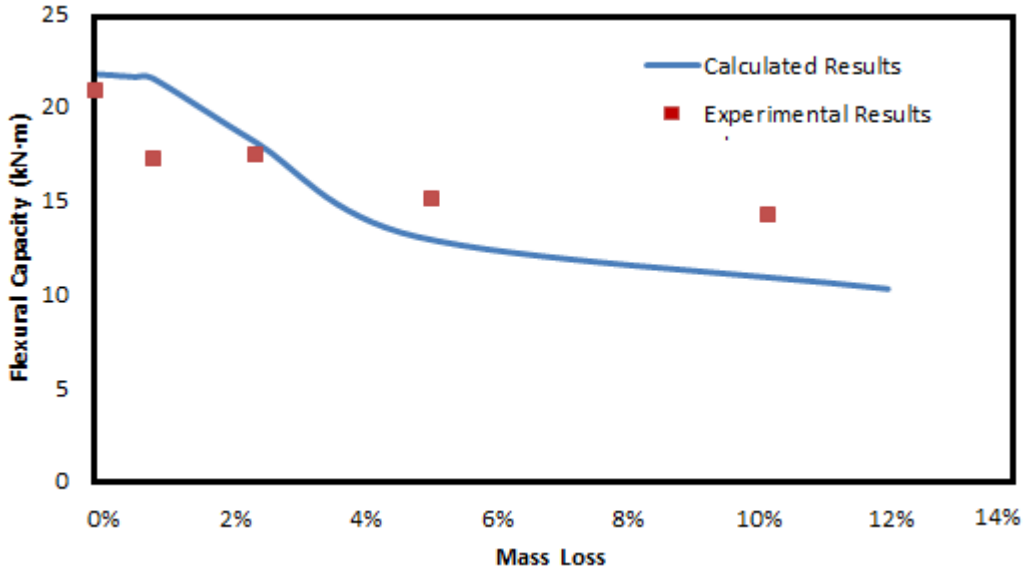

Fig. 5-9: Comparison of flexural strength between analytical calculation and experimental results from Smith (2007)

As shown in Fig. 5-9, the experimental results correlate well with the calculated results except the result of mass loss 1%. This may be due to the experimental error, because no other researches showed such a large drop of flexural strength at corrosion level 1%. The residual flexural strength is decreased as the corrosion propagates.

5.7.2 Comparison with Joyce's experiment

Beam test was conducted on beams with two 15 M principle rebars, two 10 M top rebars and 10 M stirrups at 40 mm spacing (Joyce, 2008). The beams have an 1100-mm-long span and have a cross section of 156 mm in width and 176 mm in depth. Following the procedure in Section 5.6, calculation is made in excel and results are shown in Fig. 5-9.

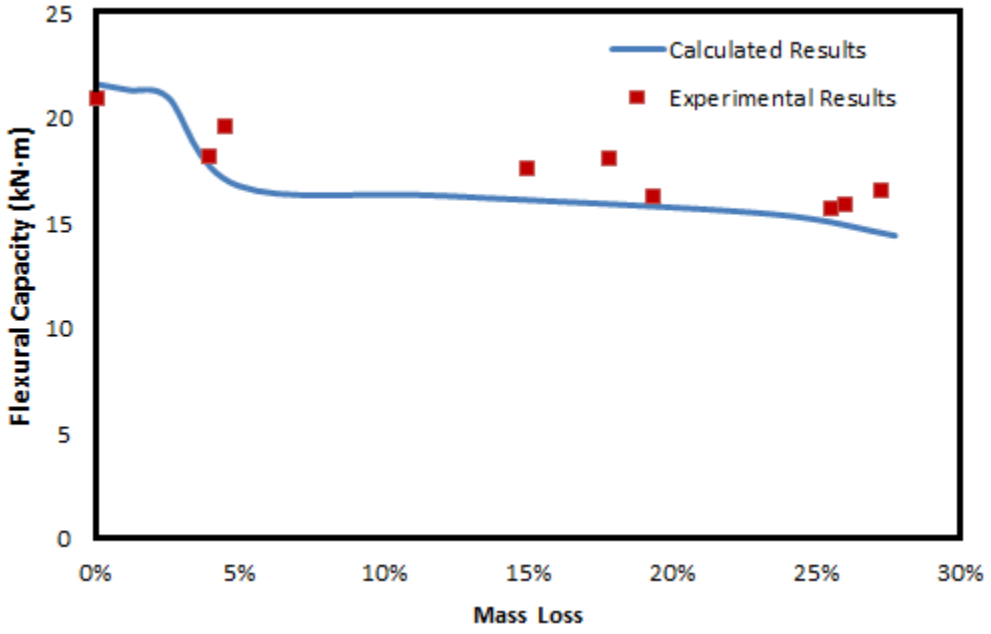

Fig. 5-10: Comparison of flexural strength between analytical calculation and experimental results from Joyce (2008)

As shown in Fig. 5-10, the experimental results compare well with the calculated ones. The flexural strength doesn't drop a lot after mass loss of 5%, because the bond strength doesn't drop significantly due to the good confinement of stirrups.

5.7.3 Comparison with Jin and Zhao's experiment

Beam tests were carried out on beams with two 12 M principle bars, 6 M top bars and 6 M stirrups at 100 mm by Jin and Zhao (2001). The beams were 1140 mm in length and 150 mm × 150 mm in cross section. The comparison between the experimental results and that from calculation is shown in Fig. 5-11.

As shown in Fig. 5-11, the experimental results compare well with the calculated results using the procedure developed in this research. The flexural strength before corrosion level of 3% remained almost the same as the un-corroded beam, because although the bond strength was reduced, it was not highly reduced to the critical bond strength, which is required to ensure the perfect bond between the steel and concrete and prevent the beam from anchorage failure.

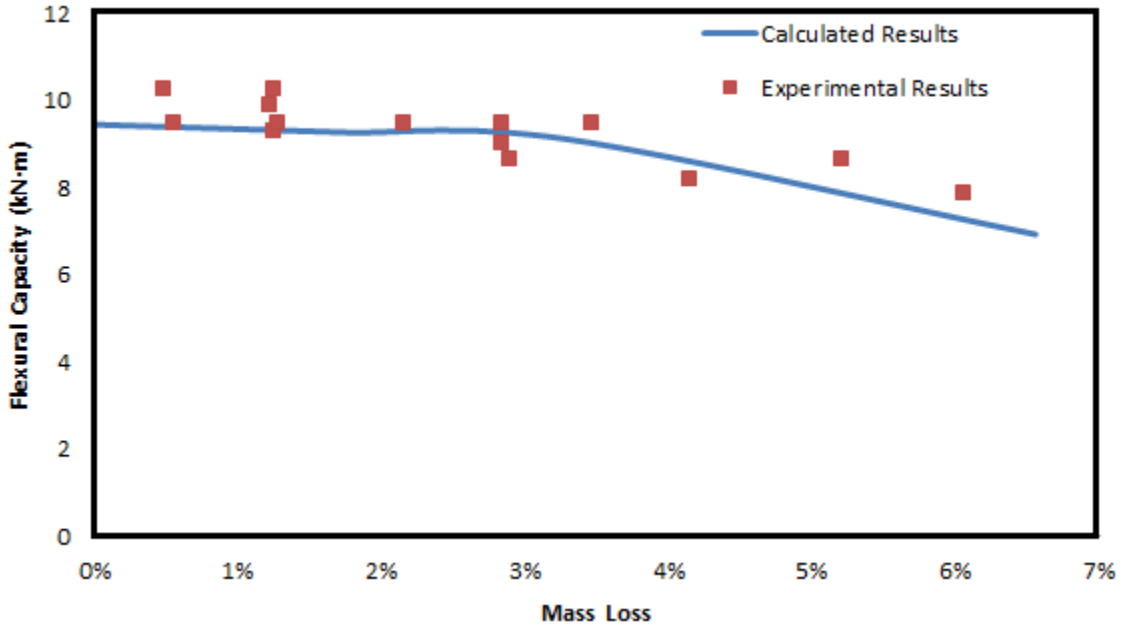

Fig. 5-11: Comparison of flexural strength between analytical calculation and experimental results from Jin and Zhao (2001)

5.7.4 Comparison with Rodriguez's experiment

Rodiguez (1997) carried out beams tests on several groups of beams. In this research, the test results from beams with 10M principle bars and 6M stirrups are used for comparison. The beams were 2300 in length, 150 mm in width and 200 mm in depth. The experiment results and calculation results are shown in Fig. 5-12.

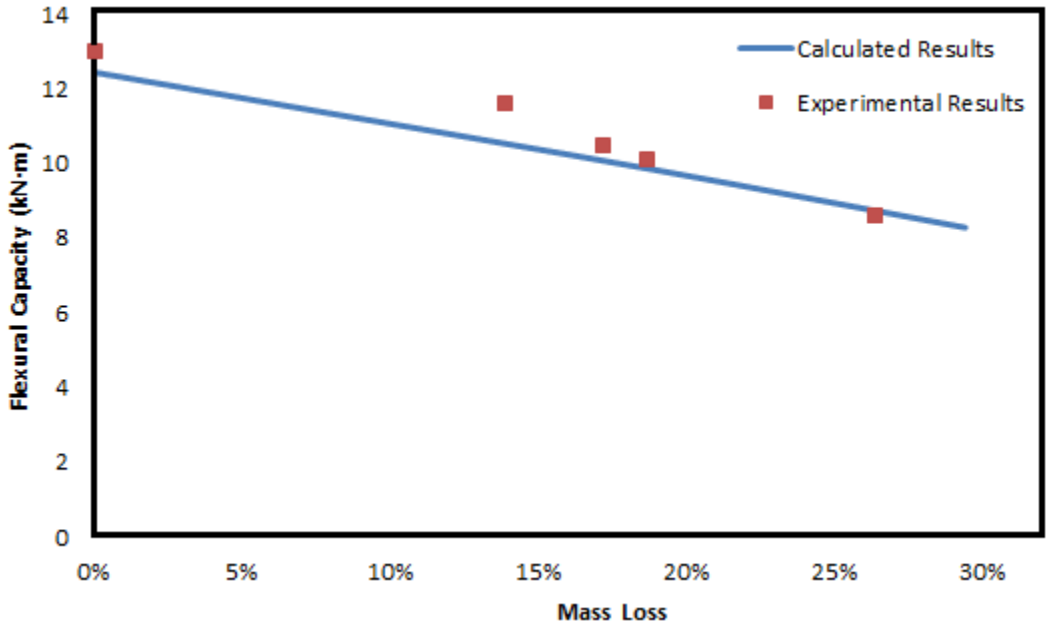

Fig. 5-12: Comparison of flexural strength between analytical calculation and experiment results by Rodriguez (1997)

As shown in Fig. 5-12, the experimental results follow the trend of the calculated results. The calculated result were plotted almost as a straight line because Rodriguez (1997) used longer beams, which is 2 meters in length, while other researchers used around 1 meter-long beams. From the calculated results, the beam failed in yielding of tension rebar rather than anchorage failure even at higher corrosion level. The main cause of the flexural strength drop of such long beams is the decrease of the cross-sectional area.

5.8 Summary of the results from the analytical calculation

To acquire an overall understanding of the effect of corrosion on bond strength and the residual flexural strength of corroded reinforced concrete beams, the relative bond strength and the relative flexural strength are obtained by considering that the uncorroded specimen to be 100%. The relative percentages for the corroded specimens were calculated and plotted versus the mass loss percentage as shown in Fig. 5-13 and Fig. 5-14.

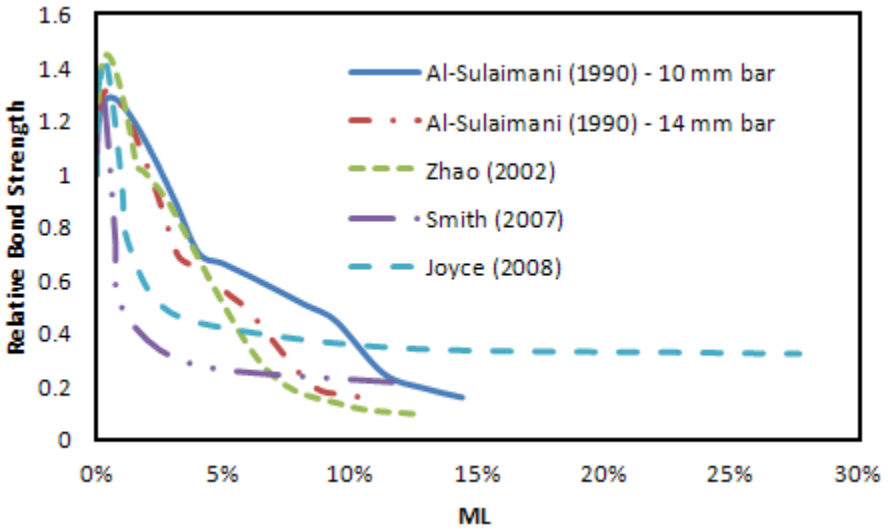

Fig. 5-13: Relative bond strength of corroded RC members

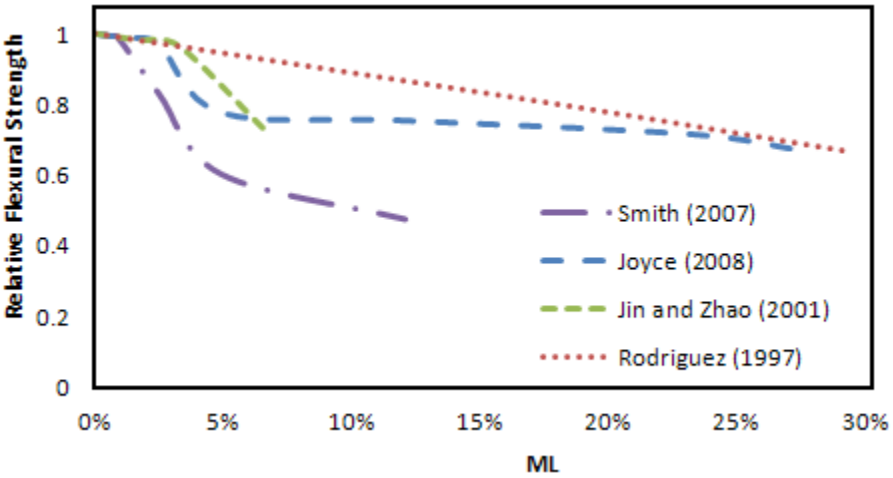

Fig. 5-14: Relative flexural strength of corroded RC beams

The relative bond strength is the ratio of the residual bond strength to the bond strength of uncorroded RC members. The relative flexural strength is the ratio of residual flexural strength of corroded RC beams to the flexural strength of uncorroded RC beams. It can be noted from this qualitative plot, Figure 5-13, that the between the concrete and the reinforcing steel increases initially with slight corrosion (basically, this very slight corrosion enhances the adhesive and cohesive properties of the steel-concrete interface). After which the bond strength deteriorates increasingly as the level of corrosion increases. While, the flexural strength (Fig. 5-14) decreases increasingly as the level of corrosion increases.

It should be noted that the relative bond strength is much less than that of the relative flexural strength at the same corrosion level. For example, by observing Joyce's results, at the corrosion level of 5% mass loss, the relative bond strength is 0.45, but the relative flexural strength is 0.8. Some amount of the bond strength loss is not reflected on the flexural strength loss, because the beam still suffers yielding controlled flexural failure, or the flexural strength is still based on the yielding strength of the steel rather than bond strength between steel and concrete, until the bond strength is reduced to the critical value to allow the anchorage failure occur.

5.9 Limitations of the proposed model

Some limitations of the proposed model are listed as follows:

1. Stirrups reinforcement is considered free of corrosion (uncorroded). Actually, stirrups are always corroded in field situations, so the effect of corrosion on stirrups should be studied in the future.

2. The hoop stress-strain relationship of the cracked concrete is based on the properties of unconfined concrete. Actually, the stirrups have certain confining effect on the cracked concrete and the stirrups improve the tensile strength and stiffness of the concrete, so the effect of stirrups confinement on concrete properties should be studied to obtain more realistic results.

3. The reinforcement anchorage at the end of the beam is not studied in this research. In field situations, the beams are usually continuous or well anchored at the end of the beam. At high corrosion level, the beam will perform as a tied arch action mode behavior, which should also be studied in the future.

Chapter 6

CONCLUSIONS AND RECOMMENDATIONS

An analytical study was performed to investigate the influence of corrosion on the flexural capacity of RC members. The results confirm that, the reinforcement corrosion has a strong effect on the flexural strength of the concrete beams failing in bond as has been notably observed by many other studies. Analytical models were proposed to predict the residual bond and the residual flexural capacity of a RC member, establishing practice-oriented design tools for concrete flexural elements under a given corroded environment. The predicted results of these models correlated very well with the results observed in the various experimental studies. The major conclusions from this study and recommendation for future work are presented in the following sections.

6.1 Conclusions

The increase of corrosion level leads to a decrease of the load carrying capacity of the RC beam. The reduction of the bond between steel and concrete is the main factor of the mechanical degradation for flexural capacity.

1. An analytical model to estimate the bond strength between corroded steel and concrete is developed:

$$\tau_{bu} = \mu(x) \times \left[p_{c,c}(x) + p_{c,st}(x) + p_{corr}(x)\right] \quad (6\text{-}1)$$

   The bond strength depends mainly on the confining forces including the confinement by the cracked concrete, the confinement by stirrups and the corrosion pressure. The friction coefficient is also a factor influencing the bond strength.

In the proposed analytical model, it was observed that at low corrosion levels (approximately ML < 1%), the bond strength increases as corrosion depth increases. Beyond that, the bond strength gradually decreases because the corrosion pressure cracks the concrete when the hoop stress exceeds the tensile strength of concrete, decreasing the confinement of concrete around the reinforcing steel, and bond becomes negligible at higher corrosion levels. The bond strength at higher corrosion level (approximately ML > 8%) is mainly contributed by the confinement of stirrups. Therefore, stirrups are very important in RC members to maintain the bond strength especially when the corrosion level is high. These trends as observed in the various experimental studies are well matched by the model predictions in the present study.

2. The corrosion pressure is a very important parameter influencing the bond strength. A thick-walled cylinder model is used and the cracked concrete is assumed to be an inhomogeneous orthotropic linearly elastic material in this report. The stiffness of cracked concrete is different in radial and hoop direction. However, the radial displacement for cracked concrete is assumed to be linearly distributed, which makes the material not continuous. It is recommended that a finite element method be used to overcome the difficulty of solving the differential equation for radial displacement. Eq. (4-45) is developed to calculate the corrosion pressure before through cracking. Corrosion pressure after through cracking can be calculated using Eq. (4-48).

3. A model for the prediction of flexural capacity of reinforced concrete beams is proposed. A new strain compatibility equation initially proposed by Wang and Liu (2010) is used to calculate flexural capacity and determine the failure mode of corroded RC beam. In the present flexure model, both force equilibrium and new strain compatibility are satisfied. The relationship between average bond stress needed and average bond strength determines the method that should be used to calculate flexural capacity of corroded RC beam.

4. Different failure modes, which are determined by the strain of concrete at extreme compression fiber $\varepsilon_{sx}$and the strain of tensile steel ε_{sx}, are considered in this report with different solutions.

   At anchorage controlled failure ($\tau_{bu,avg} \geq \tau_{avg}\ and\ \varepsilon_{sx} \leq 0.002$), the ultimate moment resistance is:

$$M_{rx} = \tau_{bu,avg}\pi d_{bx} l\left(d - \frac{\tau_{bu,avg} \cdot \pi d_{bx} \cdot l}{\alpha_1 f_c^{'} b}\right) \tag{6-2}$$

   At yielding controlled failure ($\varepsilon_{sx} > 0.002$), the ultimate moment resistance is:

$$M_{rx} = n \cdot f_y \cdot \frac{\pi d_{bx}^2}{4}\left(d - f_y \cdot \frac{\pi d_{bx}^2}{8\alpha_1 f_c' b}\right) \tag{6-3}$$

   At compression controlled failure($\varepsilon_{cx} > 0.0035$), the ultimate moment resistance is:

$$M_{rx} = n \cdot \varepsilon_{sx} E_s \cdot \frac{\pi d_{bx}^2}{4} \cdot (d - a) \tag{6-4}$$

   where a is calculated by simultaneously solving Eqs. (5-16), (5-17), (5-23), (5-29) and (5-30).

6.2 Recommendations for Future Research

The future research can focus on the followings:

1. More experimental work is necessary to monitor and assess the structural behavior of corroded concrete beams. The influence of the different parameters, such as the reinforcing bar diameter, type of loading, concrete cover thickness, concrete strength and the steel yield strength on the behavior of reinforced concrete beams subjected to corrosion need to be studied both in the laboratory and in the field.
2. A long-term data collection and study of the deterioration of concrete structures due to the ingress of various aggressive substances is needed.
3. The effect of corrosion on the shear capacity of corroded RC beams should be studied in the future so that load carrying capacity considering both flexural and shear failure can be achieved.
4. Furthermore, the effect of corrosion on the performance of reinforced concrete structures should be studied theoretically, because the previous and current studies are only within the local and member levels not the structure level.
5. More effort should also be done to analytically study the deflection of corroded structures to meet the serviceability requirement.
6. Regarding the limitations of the proposed model, the effect of corrosion on stirrups should be studied. The effect of stirrups on the properties of cracked concrete should also be studied.
7. The reinforcement anchorage at the end of the beam should be studied in the future.

APPENDIX A: NUMERICAL EXAMPLE

To demonstrate the calculation method of the residual bond strength and flexural capacity of RC beams after suffering reinforcement corrosion, the beam configuration in the experiment by Roger Smith (2007) was used as an example. The beams, having dimensions 156 mm wide by 176 mm high by 1050 mm long, were reinforced with two 15M principle rebars at the bottom and two 10 M rebars at the top, and with 6 mm stirrups at 40 mm spacing. The cover of the reinforcing steel was 30 mm. The compressive strength of the concrete was 39 MPa.

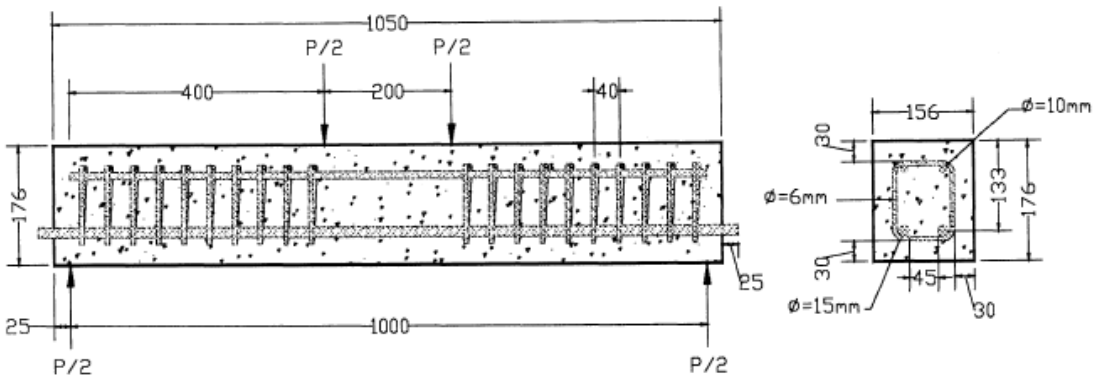

Fig A-1: Geometry of a typical beam specimen used in Smith (2007)

To calculate the flexural strength of the beam at different corrosion level x or mass loss *ML*, the bond strength should be calculated first.

The total bond strength proposed in this research is shown in Eq. (4-3):

$$\tau_{bu} = \mu(x) \times \left[p_{c,c}(x) + p_{c,st}(x) + p_{corr}(x)\right]$$

Corrosion pressure before through cracking:

The most important factor in the above equation is the contribution of corrosion pressure $p_{corr}(x)$. Following the procedure in Chapter 4, the steps of calculating the corrosion pressure before through cracking are as follows:

1. Find the cracking front R_c. The initial radius of reinforcing steel, which is the inner radius of the cylinder, is $R_i = 8\ mm$, the outer radius is $R_0 = 30 + 6 + 8 = 44\ mm$. Values of R_c used are between 8 mm to 44 mm to make sure the concrete is before through cracking. To demonstrate the method in Chapter 4, the value of R_c is taken as 27 mm as an example.

2. The exponent n for the hoop stiffeness is calculated using Eq. (4-39):

$$n = 0.081e^{0.95 f_t} = 0.081 \times 2.71828^{0.95 \times 4.3715} = 5.153$$

while the tensile strength of concrete is calculated as:

$$f_t = 0.7\sqrt{f_c'} = 0.7 \times \sqrt{39} = 4.3715\ MPa$$

3. The corrosion pressure is calculated using Eq. (4-45):

$$p_{corr} = \frac{R_c}{R_i} \cdot f_t \frac{\left(\frac{R_0}{R_c}\right)^2 - 1}{\left(\frac{R_0}{R_c}\right)^2 + 1} + \frac{1}{R_i} \cdot \frac{f_t}{{R_c}^n} \frac{1}{\left(\frac{R_0}{R_c}\right)^2 + 1} \left(\frac{R_c^{n+1} - R_i^{n+1}}{n+1} + \frac{R_c^{n-1} - R_i^{n-1}}{n-1} \right)$$

$$= \frac{27}{8} \cdot 4.3715 \frac{\left(\frac{44}{27}\right)^2 - 1}{\left(\frac{44}{27}\right)^2 + 1} + \frac{1}{8} \times$$

$$\frac{4.3715}{27^{5.153}} \frac{1}{\left(\frac{44}{27}\right)^2 + 1} \left(\frac{27^{5.153+1} - 8_i^{5.153+1}}{5.153 + 1} + \frac{27^{5.153-1} - 8^{5.153-1}}{5.153 - 1} \right)$$

$$= 9.9\ MPa$$

4. Calculate the corresponding radial displacement using Eq. (4-32):

$$u_{R_i} = \frac{f_t}{E_0} \frac{1}{\left(\frac{R_0}{R_c}\right)^2 + 1} \left[(1 + \nu) \frac{R_0^2}{R_i} + (1 - \nu) R_i \right]$$

$$= \frac{4.3715}{29351.5} \times \frac{1}{\left(\frac{44}{27}\right)^2 + 1} \left[(1 + 0.2) \frac{44^2}{8} + (1 - 0.2) \times 8 \right] = 0.012\ mm$$

5. Calculate the corresponding corrosion depth:

$$x = R_i - \sqrt{R_i^2 - \frac{(R_c + R_i) u_{R_i}}{\left(\nu \frac{r}{s} - 1\right)}} = 8 - \sqrt{8^2 - \frac{(27 + 8) \times 0.012}{(3 - 1)}} = 0.013\ mm$$

6. Calculate the corresponding mass loss:

$$ML = \frac{R_i^2 - (R_i - x)^2}{R_i^2} = \frac{8^2 - (8 - 0.013)^2}{8^2} = 0.0033 = 0.33\%$$

The calculation of the corrosion pressure before through cracking is shown in Table A-1.

Table A-1: Calculation of the corrosion pressure before through cracking at different corrosion levels

Mass Loss $\boldsymbol{ML}$	Corrosion Depth $\boldsymbol{x}$ (mm)	Cracking Front $\boldsymbol{R_c}$ (mm)	Corrosion pressure $\boldsymbol{p_{corr}}$ (Mpa)	Radial Displacement at R_i $\boldsymbol{u_{R_i}}$ (mm)
0	0	8	0	0
0.000827008	0.003308716	13	7.414725963	0.00354894
0.001465427	0.005863856	19	9.431756071	0.006947208
0.002297495	0.009195264	23	9.958525663	0.00948643
0.003306378	0.013236461	27	9.901798691	0.012091896
0.004467799	0.017891201	31	9.329972177	0.014663545
0.005754852	0.023052622	35	8.320474963	0.017130722
0.007500722	0.030059361	40	6.562072512	0.020001925
0.008978989	0.035996944	44	4.845788584	0.022102128

Corrosion pressure after through cracking:

The calculation steps are as follows:

1. Assume a penetration depth $x = 0.1$ mm as an example, and calculate the corresponding mass loss percentage:

$$ML = \frac{R_i^2 - (R_i - x)^2}{R_i^2} = \frac{8^2 - (8 - 0.1)^2}{8^2} = 0.0248 = 2.48\%$$

2. Calculate the hoop strain at the outer side of the cylinder (the concrete cover) using Eq. (4-53):

$$\varepsilon_{\theta 0} = 2x \cdot \frac{\left(\nu \frac{r}{s} - 1\right)(2R_i - x)}{\left(\frac{R_0}{R_i} + 1\right)\left(\frac{R_0^2}{R_i^2} + 1\right)} = 2 \times 0.1 \times \frac{(3-1)(2\times 8 - 0.1)}{\left(\frac{44}{8} + 1\right)\left(\frac{44^2}{8^2} + 1\right)} = 0.00049$$

3. Calculate the hoop strain at the rebar surface using Eq. (4-52):

$$\varepsilon_{\theta i} = \varepsilon_{\theta 0} \cdot \frac{1 + (R_0/r)^2}{2} = 0.00049 \times \frac{1 + \left(\frac{44}{8}\right)^2}{2} = 0.0076$$

4. Determine the cases by comparing the values of $\varepsilon_{\theta i}, \varepsilon_{\theta 0}, \varepsilon_u$, and ε_1. In this case, $\varepsilon_1 < \varepsilon_{\theta 0} < \varepsilon_{\theta i} \leq \varepsilon_u$ and lies in the Case 2 (1). Using the integration Equation (21d) in Wang and Liu (2006), the integration I can be calculated:

$$I = \frac{0.15 f_t}{\varepsilon_u - \varepsilon_1} \cdot \left[\varepsilon_u (R_0 - R_i) - \frac{\varepsilon_{\theta 0}}{2} \frac{R_0^2 - R_i^2}{R_i}\right]$$

$$= \frac{0.15 \times 4.3714}{0.002 - 0.0003}\left[0.002(44 - 8) - \frac{0.00049}{2} \times \frac{44^2 - 8^2}{8}\right] = 11.7\ kN/mm$$

5. The corrosion pressure is:

$$p_{corr} = \frac{I}{R_i} = \frac{11.7}{8} = 14.6\ MPa$$

The calculation of the corrosion pressure after through cracking is shown as in Table A-2.

Table A-2: The corrosion pressure after through cracking at different corrosion levels

Mass Loss ML	Corrosion Depth x (mm)	Cracking Front R_c (mm)	hoop strain at R_0 $\varepsilon_{\theta 0}$	Hoop strain at R_i $\varepsilon_{\theta i}$	Integration I (N/mm)	Corrosion pressure p_{corr} (MPa)
0.0248437	0.1	44	0.0004892	0.0076442	11.700912	1.462614
0.049375	0.2	44	0.0009723	0.0151923	4.8239563	0.6029945
0.1210938	0.5	44	0.0023846	0.0372596	0	0

Concrete confining pressure:

Take $R_c = 44\ mm$ as an example. The calculation steps are:

1. The total crack width is calculated using Eq. (4-21):

$$\Sigma w = 2\pi u_{R_i} = 2 \times 3.14 \times 0.0221 = 0.1388\ mm$$

The crack width is

$$w = \frac{\Sigma w}{3} = \frac{0.1388}{3} = 0.046\ mm$$

2. The residual strength of cracked concrete is calculated using Eq. (4-6):

$$\sigma_{rc} = \frac{f_{ct0}}{\kappa \frac{\Phi_p}{\Phi_a} \frac{w}{\Phi_p} + 1} = \frac{1.346}{167 \times \frac{0.046}{10} + 1} = 0.7593\ MPa$$

3. The confining pressure by cracked concrete is calculated using Eq. (4-5):

$$p_{c,c} = \frac{(b - n_p \Phi_p)\Delta z}{A_p^*} \sigma_{rc} = \frac{(88 - 8 \times 2) \times 1}{2 \times 8} 0.7593 = 3.417\ \text{MPa}$$

The calculation of confinement by cracked concrete is shown in Table A-3.

Table A-3: The calculation of confinement by cracked concrete at different corrosion levels

Mass Loss ML	Corrosion Depth x (mm)	Cracking Front R_c (mm)	Crack Width **w** (mm)	Residual Strength of Concrete σ_{rc} (MPa)	Confining Pressure by Concrete $p_{c,c}$ (MPa)
0	0	8	0	4.3714986	19.671744
0.0005822	0.0023293	13	0.0074291	4.137757	18.619907
0.0014654	0.0058639	19	0.0145428	3.7830778	17.02385
0.0022975	0.0091953	23	0.0207874	3.4487807	15.519513
0.0033064	0.0132365	27	0.0253124	3.0432584	13.694663
0.0044678	0.0178912	31	0.0306957	2.5761688	11.59276
0.0057549	0.0230526	35	0.0358603	2.0582353	9.2620591
0.0075007	0.0300594	40	0.0418707	1.3551295	6.098083
0.008979	0.0359969	44	0.0462671	0.7593105	3.4168971
0.0248437	0.1	44	0.1280154	0.4289552	1.9302983
0.049375	0.2	44	0.2544205	0.2564385	1.1539731
0.1210938	0.5	44	0.6239744	0.1178596	0.530368

Stirrups confining pressure:

The steps to calculate the confining pressure by stirrups are as follows:

1. The stress in stirrups is calculated using Eq. (4-11):

$$\sigma_{st} = E_s \sqrt{\frac{a_2}{\left(\alpha \frac{\Phi_{st}}{\Phi_p}\right)^2}\left(\frac{w}{\Phi_p}\right)^2 + \frac{a_1}{\alpha \frac{\Phi_{st}}{\Phi_p}}\frac{w}{\Phi_p} + a_0}$$

$$= 200000 \sqrt{\frac{0.013}{\left(2\frac{6}{16}\right)^2}\left(\frac{0.046}{16}\right)^2 + \frac{0.00009}{2\frac{6}{16}} \cdot \frac{0.046}{16} - 6.75 \times 10^{-8}} = 78.43\ MPa$$

where a_0, a_1, a_2 can be calculated using Eqs. (4-12) to (4-14):

$$a_1 = \frac{8\tau_{02}}{E_s} = \frac{8 \times 2.25}{200000} = 0.00009$$

$$a_2 = \frac{4\tau_{12}\Phi_{st}}{E_s} = \frac{4 \times 1500/14 \times 6}{200000} = 0.013$$

$$a_0 = \frac{a_1^2 \frac{\tau_{12}}{\tau_{11}}}{4a_2\left(\frac{\tau_{12}}{\tau_{11}} - 1\right)} = \frac{0.00009^2 \times 0.3}{4 \times 0.013 \times (0.3 - 1)} = -6.75 \times 10^{-8}$$

2. The confining pressure by stirrups is calculated using Eq. (4-10):

$$p_{c,st} = \frac{A_{st}^*}{A_p^*}\sigma_{st} = \frac{3.14 \times (\frac{6}{2})^2}{40 \times 2 \times 800} \times 78.43 = 2.77\ MPa$$

3. The friction coefficient is determined by Eq. (4-4):

$$\mu(x) = 0.37 - 0.26(x - x_{cr}) = 0.37 - 0.26(0.036 - 0.036) = 0.37$$

4. The bond strength that stirrups contribute is:

$$t_s = p_{c,st} \cdot \mu(x) = 2.77 \times 0.37 = 1.025\ MPa$$

5. The maximum value of the bond force contributed by stirrups is calculated using Eq. (4-15):

$$T_s = K_1 t_r t_d \frac{NA_{tr}}{n} f_c'^p = 31.14 \times 0.952 \times 0.711 \times \frac{10 \times 3.14 \times \left(\frac{6}{2}\right)^2}{2} \times 39^{\frac{1}{2}}$$

$$= 37241\ N$$

where t_r and t_d are calculated using Eqs. (4-16) and (4-17):

$$t_r = 9.6R_r + 0.28 = 9.6 \times 0.07 + 0.28 = 0.952$$

$$t_d = 0.78d_b + 0.22 = 0.78 \times 16 \times 0.039 + 0.22 = 0.711$$

The maximum bond contribution stirrups can provide is:

$$t_{s,max} = \frac{37241}{3.14 \times 16 \times 1000/2} = 1.48\ MPa$$

The calculation of the bond contribution by stirrups is shown in Table A-4.

Table A-4: Calculation of bond contribution by stirrups at different corrosion levels

Mass Loss ML	Cracking Front R_c (mm)	Friction Coefficient $\mu(x)$	Stirrups Stress σ_{st} (mm)	Confinement by Stirrups $p_{c,st}$ (mm)	Bond Contribution by Stirrups $p_{c,st} \cdot \mu(x)$ (MPa)
0.00229	23	0.3769684	25.116486	0.8872399	0.334461
0.00330	27	0.3759177	40.852455	1.443113	0.542491
0.00446	31	0.3747075	52.398717	1.8509847	0.693577
0.00575	35	0.3733655	61.864587	2.1853665	0.815940
0.00750	40	0.3715438	71.735081	2.5340417	0.941507
0.00897	44	0.37	78.430603	2.7705611	1.025107
0.02484	44	0.3533592	176.44941	6.2330756	1.482546
0.04937	44	0.3273592	305.38097	10.787583	1.482546
0.12109	44	0.2493592	662.21199	23.392639	1.482546

Bond strength at different corrosion levels:

Using Eq. (4-3), the bond strength at different corrosion levels can be calculated as in Table A-5. The bond strength is contributed by the confinement of concrete, stirrups and corrosion pressure.

Table A-5: Bond strength at different corrosion levels

Mass Loss ML	Corrosion Depth x (mm)	Friction Coefficient $\mu(x)$	Corrosion pressure p_{corr} (Mpa)	Confining Pressure by Concrete $p_{c,c}$ (MPa)	Bond Contribu-tion by Stirrups $p_{c,st} \cdot \mu(x)$ (MPa)	Bond Strength τ_{bu} (Mpa)
0	0	0.3793592	0	19.67174	0	7.4626
0.000582	0.002329	0.3787535	7.4147259	18.61990	0	9.8457
0.001465	0.005863	0.3778346	9.431756	17.02385	0	10.022
0.002297	0.009195	0.3769684	9.9585256	15.51951	0.334461	9.9546
0.003306	0.013236	0.3759177	9.9017986	13.69466	0.542491	9.6558
0.004467	0.017891	0.3747075	9.3299721	11.59276	0.693577	8.9127
0.005754	0.023052	0.3733655	8.3204749	9.262059	0.81594	7.8575
0.0075	0.030059	0.3715438	6.5620725	6.098083	0.941507	6.5575
0.008979	0.035996	0.37	4.8457885	3.416897	1.025107	5.45561
0.024847	0.1	0.3533592	1.462614	1.930298	1.482546	3.856075
0.049375	0.2	0.3273592	0.6029945	1.153973	1.482546	2.508147
0.121093	0.5	0.2493592	0	0.530368	1.482546	1.948862

After the bond strength is calculated, it can be used in the framework of flexural capacity calculation.

Flexural capacity of the corroded RC beams:

In this example, corrosion depth x = 0.2 mm is considered. Required average bond strength to prevent anchorage failure is calculated using Eq. (5-12):

$$\tau_{avg} = \frac{f_y \cdot d_b}{2l} = \frac{400 \times 16}{2 \times 1000} = 3.2\ MPa$$

The bond strength at corrosion depth 0.2 mm is 2.508147 *MPa* as calculated in Table A-5. For design and conservative purpose, the average bond strength should be calculated using Eq. (5-13):

$$\tau_{bu,avg} = \tau_{bu} \cdot \frac{l_b + \frac{l - l_b}{2}}{l} = \tau_{bu} \cdot \frac{l + l_b}{2l}$$

However, the average bond strength in this example is simply taken as $\tau_{bu}$to better meet the experimental results, because at higher corrosion level, large slip between concrete and steel occurs, the bond stress is more likely to be fully distributed toward to end of the beam. Thus, $\tau_{bu,avg} = \tau_{bu} = 2.508147\ MPa$.

As $\tau_{bu,avg} < \tau_{avg}$, anchorage failure occurs before the yielding of steel. The procedure in Section 5.2 should be used to calculate the flexural capacity of the beam:

1. The flexural tensile force the steel can provide is calculated using Eq. (5-14):

$$T = \tau_{bu,avg} \cdot \pi d_{bx} \cdot l = 2.508 \times 3.14 \times 16 \times 1000 = 122859\ N$$

2. The depth of the compressive stress block is calculated using Eq. (5-19):

$$a = \frac{\tau_{bu,avg} \cdot \pi d_{bx} \cdot l}{\alpha_1 f_c^{'} b} = \frac{1.95 \times 3.14 \times (16 - 0.2) \times 1000}{0.7915 \times 39 \times 156} = 52.33\ mm$$

where α_1 can be calculate using Eq. (5-18):

$$\alpha_1 = 0.85 - 0.0015 f_c^{'} = 0.85 - 0.0015 \times 39 = 0.79$$

3. The flexural capacity is calculated using Eq. (5-15):

$$M_{rx} = T \cdot \left(d - \frac{a}{2}\right) = 122859 \times \frac{\left(133 - \frac{52.33}{2}\right)}{10^6} = 13.125\ kN \cdot m$$

4. Check the strain of tensile steel and strain of compressive concrete:

The strain of tensile steel is calculated using Eq. (5-21):

$$\varepsilon_{sx} = \frac{f_s}{E_s} = \frac{T}{A_{sx} E_s} = \frac{122859}{3.14 \times (8 - 0.2)^2 \times 200000} = 0.0015 < \varepsilon_y = 0.002$$

The strain of compressive concrete can be calculated using Eq. (5-22):

$$\varepsilon_{cx} = \frac{\varepsilon_{sx}}{1 - \left(1 - \frac{\tau_{bu,avg}(x)}{\tau_{bu,avg}(0)}\right) \cdot \left(1 - \frac{9.3 c_x}{l}\right) \cdot \frac{c_x}{d - c_x}}$$

$$= \frac{0.0015}{1 - \left(1 - \frac{1.95}{7.46}\right) \cdot \left(1 - \frac{9.3 \times 52.33}{1000 \times 0.8725}\right) \cdot \frac{\frac{52.33}{0.8725}}{133 - \frac{52.33}{0.8725}}}$$

$$= 0.0016 < \varepsilon_{cu} = 0.0035$$

where

$$c_x = \frac{a}{\beta_1}$$

with

$$\beta_1 = 0.97 - 0.0025 f_c' = 0.97 - 0.0025 \times 39 = 0.8725$$

So the assumption that the beam suffers anchorage failure is satisfied.

The calculation of flexural capacity is shown in Table A-6.

Table A-6: Calculation of flexural capacity at different corrosion levels

Mass Loss ML	Corrosion Depth x (mm)	Bond Strength τ_{bu} (MPa)	Required Bond Strength τ_{avg} (MPa)	Steel Tensile Force **T** (N)	Steel Strain ε_{sx}	Concrete Strain ε_{cx}	Flexural Capacity M_{rx} (kN-m)
0.00000	0	7.463	3.2	134706	0.0020	0.00081	21.82
0.00058	0.00233	9.846	3.2	134577	0.0020	0.00081	21.81
0.00147	0.00586	9.958	3.2	134382	0.0020	0.00081	21.78
0.00331	0.01324	9.328	3.2	133975	0.0020	0.00081	21.74
0.00575	0.02305	7.234	3.2	133434	0.0020	0.00081	21.67
0.00898	0.03006	5.456	3.2	132721	0.0020	0.00081	21.59
0.02484	0.1	3.856	3.2	129214	0.0016	0.00169	18.14
0.04938	0.2	2.508	3.2	122859	0.0015	0.00165	13.13
0.12109	0.5	1.949	3.2	91791	0.0011	0.00122	10.34

As the limitation of the space, only a small amount of corrosion levels are considered here. More calculations were done in excel and the plot of results corresponding to more corrosion levels is shown in Chapter 4 and Chapter 5.

References

ACI Committee 408. (2003). Bond and Development of Straight. Reinforcing Bars in Tension. American Concrete Institute.

Al-Bayati, N. (2009). The Effect of Corrosion on Shear Behaviour of Self-consolidating Concrete Beams. MASc Thesis, Ryerson University, Toronto.

Aldulaymi, Z. (2007). Optimization of the Effect of Corrosion on Bond Behaviour between Steel and Concrete. MASc Thesis, Ryerson University, Toronto.

Almusallam, A. A. (2001). Effect of Degree of Corrosion on the Properties of Reinforcing Steel Bars. Construction and Building Materials, Vol. 15, No. 8, pp. 361-368.

Almusallam, A. A., Al-Gahtani, A. S., Aziz, A., and Rasheeduzzafar. (1996). Effect of Reinforcement Corrosion on Bond Strength. Construction and Building Materials, Vol. 10, No. 2 pp. 123-129.

Al-Sulaimani, G. J., K. M., Basunbul, I. A., and Rasheeduzzafar. (1990). Influence of Corrosion and Cracking on Bond Behaviour and Strength of Reinforced Concrete Members. ACI Structural Journal, Vol. 87, No. 2, pp. 220-231.

Amleh, Lamya. (2005). Class Course Notes CV8306 Civil Engineering: Durability of Structures. Ryerson University, Toronto.

Amleh, L., and Mirza, S. (1999). Corrosion Influence on Bond between Steel and Concrete. ACI Structural Journal, Vol. 96, No. 3, pp. 415-423.

Au, F. T., and Du, J. S. (2004). Prediction of Ultimate Stress in Unbonded Prestressed Tendons. Magazine of Concrete Research, Vol. 56, No. 1, pp. 1-11.

Ballim, Y., and J.C. Reid. (2003) Reinforcement Corrosion and the Deflection of RC Beams: An Experimental Critique of Current Test Methods. Cement and Concrete Composites, Vol. 25, No. 6, pp. 625-632.

Bertolini, L., Elsener, B., Pedeferri, P., and Polder, R. B. (2004). Corrosion of Steel in Concrete: Prevention, diagnosis, repair. Wiley-VCH Verlag GmbH and Co. KGaA, Weinheim.

Bhargava, K., Ghosh, A., Mor, Y., and Ramanujam, S. (2006). Analytical Model for Time to Cover Cracking in RC Structures due to Rebar Corrosion. Nuclear Engineering and Design, Vol. 236, No. 11, pp. 1123-1139.

Bhaskar, S. (2008). Analytical Modeling of the Contact Pressure at the Steel-concrete Interface . MASc Thesis, Ryerson University, Toronto.

Cabrera, J. G., and Ghoddoussi, P. (1992). The Effect of Reinforcement Corrosion on the Strength of the Steel/Concrete Interface. International Conference on Bond in Concrete, Riga, Latvia. pp. 11-24.

Cairns, J., and Abdullah, R. B. (1996). Bond Strength of Black and Epoxy-Coated Reinforcement—A Theoretical Approach. ACI Materials Journal. Vol.93, No.4, pp. 362-369

Cairns, J. (1995) Strength in shear of concrete beams with exposed reinforcement. Proceedings of the Institution of Civil Engineers, Structures and Buildings. Vol .110, No. 2, pp. 176-185.

Cairns, J., and Zhao, Z. (1993). Behavior of Concrete Beams with Exposed Reinforcement. Proceedings of the ICE - Structures and Buildings, Vol. 99, No. 2, pp. 141-154.

Castel, A.; Francois, R., and Arliguie, G. (2000) Mechanical Behaviour of Corroded RC Beams - Part 1: Experimental Study of Corroded Beams. Materials and Structures, Vol. 33, No. 233, pp. 539-544.

Castel, A.; Francois, R.; and Arliguie, G. (2000b) Mechanical Behaviour of Corroded RC Beams - Part 2: Bond and Notch Effects. Materials and Structures, Vol. 33, No. 233, pp. 545-551.

CEB-FIP. (1993). CEB-FIP Model Code 1990. London: Thomas Telford Services Ltd.

Cement Association of Canada. (2006). Concrete Design Handbook: Third Edition. Ottawa: Canadian Standards Association.

Chernin, L., Val, D. V., and Volokh, K. Y. (2010). Analytical Modelling of Concrete Cover Cracking Caused by Corrosion of Reinforcement. Materials and Structures, Vol. 43, No. 4, pp. 543-556.

Chung, L., Cho, S.-H., Kim, J.-H. J., and Yi, S.-T. (2004). Correction Factor Suggestion for ACI Eevelopment Length Provisions Based on Flexural Testing of RC Slabs with Various Levels of Corroded Reinforcing Bars. Engineering Structures, Vol. 26, No. 8, pp. 1013-1026.

Collins, M. P., and Mitchell, D. (1987). Prestressed Concrete Basics. Ottawa: Canadian Prestressed Concrete Institute (CPCI).

Cement Association of Canada. (2006). Concrete Design Handbook (3rd Edition). Canadian Standards Aosociation: Ottawa, Canada.

Coronelli, D. (2002). Corrosion Cracking and Bond Strength Modeling for Corroded Bars in Reinforced Concrete. ACI Structural Journal, Vol. 99, No. 3, pp. 267-276.

CSA. (2004). Design of Concrete Structures. Mississauga: Canadian Stardards Association.

Du, Y. G., A., C. L., and C., C. A. (2005). Effect of Corrosion on Ductility of Reinforcing Bars. Magazine of concrete research, Vol. 57, No. 7, pp. 407-419.

Eyre, J.R., and Nokhasteh, M.-A. (1992) Strength Assessment of Corrosion Damaged Reinforced Concrete Slabs and Beams. Proceedings Institution of Civil Engineers, Structures & Buildings, Vol. 94, pp. 197-203.

Fu, X., and Chung, D. D. (1997). Effect of Corrosion on the Bond Between Concrete and Steel Rebar. Cement and Concrete Research, Vol. 27, No. 12, pp. 1811-1815.

Gere, J. M., and Goodno, B. J. (2011). Mechanics of Materials. Nels: Thomson-Engineering.

Gere, J. M., and Timoshenko, S. P. (1972). Mechanics of Materials. Alton: Pws Pub Co.

Ghosh, A., and Amleh, L. (2006). Modeling the Effect of Corrosion on Bond Strength at the Steel-concrete Interface with Finite-Element Analysis. Canadian Journal of Civil Engineering, Vol. 33, No. 6, pp. 673 -673.

Giuriani, E., Plizzari, G., and Schumm, C. (1991). Role of Stirups and Residual Tensile Strength of Cracked Concrete on Bond. Journal of Structural Engineering, Vol. 117, No. 1, pp. 1-18.

Hassan, A. (2003). Bond of Reinforcement in Concrete with Different Types of Corroded Bars. MASc Thesis, Ryerson University, Toronto.

Highway, F. (1997). The Status of the Nation's Highway Bridges: Highway Bridge Replacement and Rehabilitation Program and National Bridge Inventory. Washington, D. C.: Federal Highway Administration.

Hillerborg, A., Modeer, M., and Peterson, P. E. (1976). Analysis of Crack Formation and Crack Growth In Concrete by means of Fracture Mechanics and Finite Elements. Cement and Concrete Research, Vol. 6, No. 6, pp. 773-781.

Hognestad, E. (1952). Inelastic Behavior in Tests of Eccentrically Loaded Short Reinforced Concrete Columns. ACI Journal Proceedings, Vol. 49, No. 10, pp. 117-139.

Huang, R., and C.C. Yang. (1997) Condition Assessment of RC Beams Relative to Reinforcement Corrosion. Cement and Concrete Composites, Vol. 19, pp. 131-137.

Hussein, L. (2011). Analytical Modeling of Bond Stress at Steel-Concrete Interface due to Corrosion. MASc Thesis, Ryerson University, Toronto.

Jin, W., and Zhao, Y. (2001). Effect of Corrosion on Bond Behavior and Bending Strength of Reinforced Concrete Beams. Journal of Zhejiang University - Science A, Vol.2, No. 3, pp. 298-308.

Joyce, T. A. (2008). The Effects of Steel Reinforcement Corrosion on The Flexural Capacity and Stiffness of Reinforced Concrete Beams. MASc Thesis, Ryerson University, Toronto.

Kim, W., and White, R. N. (1991). Initiation of Shear Cracking in Reinforced Concrete Beams with no Web Reinforcement. ACI Structural Journal, Vol. 88, No. 3, pp. 301-308.

Lan, Y. (2003). Finite Element Analysis of Corrosion and Bond-slip. MASc Thesis, Ryerson University, Toronto.

Lee, H. S., Noguchi, T., and Tomosawa, F. (1998). FEM Analysis for Structural Performance of Deteriorated RC Structures due to Rebar Corrosion. Tromso: Proceedings of the Second International Conference on Concrete under Severe Conditions.

Li, C., Melchers, R. E., and Zheng, J. (2006). Analytical Model for Corrosion-Induced Crack Width in Reinforced Concrete Structures. ACI Structural Journal, Vol. 103, No. 4, pp. 497-487

Lundgren, K. (2002). Modelling the Effect of Corrosion on Bond in Reinforced Concrete. Magazine Of Concrete Research, Vol. 54, No. 3, pp. 165-173.

Maaddawy, T. E., Soudki, K., and Topper, T. (2005). Analytical Model to Predict Nonlinear Flexural Behavior of Corroded Reinforced Concrete Beams. ACI Structural Journal, Vol. 102, No. 4, pp. 550-559.

Macgregor, J. G., and Wight, J. K. (2009). Reinforced Concrete: Mechanics and Design(5th Edition). Upper Saddle River: Pearson Prentice Hall.

Malumbela, G., Moyo, P., and Alexander, M., (2009). Structural behaviour of beams under simultaneous load and steel corrosion. Proceedings Of The 2nd International Conference On Concrete Repair, Rehabilitation And Retrofitting (ICCRRR), Cape Town, South Africa, November 24–26, pp. 645-650.

Mangat, P. S., and Elgarf, M. S. (1999). Flexural Strength of Concrete Beams with Corroding Reinforcement. ACI Structural Journal, Vol. 96, No. 1, pp. 149-158.

Mietz, J., Polder, R., and Elsener, B. (2000). Corrosion of Reinforcement in Concrete: (EFC 31). Aachen: Maney Publishing.

Minkarah, I., and Ringo, B. C. (1981). Behaviour and Repair of Deteriorated Reinforced Concrete Beams. Transportation Research Record Vol. 821, pp. 73-79.

Molina, F. J., Alonso, C., and Andrade, C. (1993). Cover Cracking as a Function of Bar Corrosion: Part 2—Numerical Model. RILEM Materials and Structures, Vol. 26, No. 9, pp. 532-548.

Nielsen, C. (2002). Radial Fictitious Cracking of Thick-Walled Cylinder due to Bar Pull-Out. Magazine Of Concrete Research, Vol. 54, No. 3, pp. 215-221.

Pannell, F.N., and Tam A. (1969). The Ultimate Moment of Resistance of Unbonded Prestressed Concrete Beam. Magazine Concrete Research, Vol. 28, No. 97, pp. 43-54.

Pantazopoulou, S. J., and Papoulia, K. D. (2001). Modeling Cover-Cracking due to Reinforcement Corrosion In RC Structures. Journal of Engineering Mechanics, Vol. 127, No. 4, pp. 342-351.

Raoof, M., and Lin Z. (1996). Structural characteristics of RC beams with exposed main steel. Proceedings Institution of Civil Engineers, Structures & Buildings, Vol. 122, pp. 35-51.

Rodriguez, J., Ortega. L.M., and Casal, J. (1997). Load Carrying Capacity of Concrete Structures with Corroded Reinforcement. Construction and Building Materials, Vol. 11, No. 4, pp. 239-248.

Smith, R. (2007). The Effect of Corrosion on the Performance Of Reinforced Concrete Beams. MASc Thesis, Ryerson University, Toronto.

Stanish, K., Hooton, R. D., and Pantazopoulou, S. J. (1999). Corrosion Effects on Bond Strength in Reinforced Concrete. ACI Structural Journal, Vol. 96, No. 6, pp. 915-921.

Tastani, S. P. (2002). Experimental Evaluation of the Direct Tension-Pullout Bond Test. Bond in Concrete – from research to standards, No. 12.

Tepfers, R. (1979). Cracking of Concrete Cover along Anchored Deformed Reinforcing Bars. Magazine of Concrete Research, Vol. 31, No. 106, pp. 3-12.

Torres-Acost, A. A., Navarro-Gutierrez, S., and Terán-Guillén, J. (2007). Residual flexure capacity of corroded reinforced concrete beams. Engineering Structures, Vol. 29, No. 6, pp. 1145-1152.

Transportation, U. D. (2010). Corrosion Protection. Retrieved July 30, 2010, from Corrosion Protection: http://www.tfhrc.gov/structur/corros/introset.htm

Val, D. V., Chernin, L., and Stewart, M. G. (2009). Experimental and Numerical Investigation of Corrosion-Induced Cover Cracking in Reinforced Concrete Structures. Journal of structural engineering, Vol. 135, No. 4, pp. 376 -385.

Val, L. C. (2011). Numerical Modelling of Bond between Concrete and Corroded Reinforcement - Google Scholar. Retrieved Dec. 3, 2011, from Google Scholar: ftp://ftp.technion.ac.il/pub/supported/kovler/papers/25.doc

Wang, X., and Liu, X. (2004). Modelling Effects of Corrosion on Cover Cracking and Bond in Reinforced Concrete. Magazine of Concrete Research, Vol. 56, No. 4, pp. 191-199.

Wang, X., and Liu, X. (2006). Bond Strength Modeling for Corroded Reinforcements. Construction and Building Materials, Vol. 20, No. 3, pp. 177-186.

Wang, X., and Liu, X. (2008). Modeling the Flexural Carrying Capacity of Corroded RC Beam. Journal of Shanghai Jiaotong University (Science), Vol. 13, No. 2, pp. 129-135.

Wang, X., and Liu, X. (2010). Simplified Methodology for the Evaluation of the Residual Strength of Corroded Reinforced Concrete Beams. Journal of Performance of Constructed Facilities, Vol. 24, No. 2, pp. 108-119.

Xu, G., Wei, J., Zhang, K., and Zhou, X. (2007). A Calculation Model for Corrosion Cracking in RC Structures. Journal of China University of Geosciences, Vol. 18, No. 1, pp. 85-89.

Xu, Y. (1990). Experimental Study of Anchorage Properties for Deformed Bars in Concrete. Ph.D. Thesis, Tsinghua University, Beijing.

Xu, Z. (2002). A Concise Course on Elastic Mechanics. Beijing: Higher Education Press.

Zhao, Y., and Jin, W. (2002). Test Study on Bond Behavior of Corroded Steel Bars and Concrete. Journal of Zhengjiang University (Engineering Science), Vol. 4, No. 1, pp. 352-356.

Zuo, J., Darwin, and D. (1998). Bond strength of High Relative Rib Area Reinforcing Bars. Ph.D. Thesis, University of Kansas Center for Research, Lawrence.

Zuo, J., Darwin, and D. (2000). Splice Strength of Conventional and High Relative Rib Area Bars in Normal and High-Strength Concrete. ACI Structura Journal, Vol. 97, No.4, pp. 630-641.